Arginine Methylation in the E2F1 Pathway

Shunsheng Zheng

Department of Oncology

Linacre College

University of Oxford

Trinity 2013

A thesis submitted in fulfillment of the requirements for the degree of Doctor of Philosophy at the University of Oxford

Arginine Methylation in the E2F1 Pathway

Shunsheng Zheng Department of Oncology

Linacre College University of Oxford

A thesis submitted for the degree of Doctor of Philosophy Trinity 2013

Abstract

The E2F1 pathway plays an important role in coordinating early cell cycle progression. Deregulation of the E2F1 pathway, which may be brought about by somatic mutations in genes such as *INK4A*, *RB1* and *CDK4*, is found in a majority of cancers. The transcription factor E2F1 is able to activate genes involved in proliferation as well as apoptosis, but the mechanisms that govern these opposing biological effects remain poorly understood. In this study, I would describe how E2F1 activity can be regulated by two novel post-translational modifications which result in different functional consequences. It was found that PRMT1 asymmetrically methylates E2F1 at R109, while PRMT5 symmetrically methylates R111 and R113. The symmetric dimethyl marks on E2F1 promoted the recruitment of Skp2, a component of the E3 ubiquitin ligase complex, which coincided with decreased protein stability and transcriptional activity, as well as enhanced cell proliferation and reduced apoptosis. The asymmetric dimethyl marks on E2F1 was found to hinder symmetric dimethylation, leading to reduced cell proliferation and enhanced apoptosis. The competition between PRMT1 and PRMT5 at the E2F1 RG-rich motif was found to be regulated by the adjacent cyclin A binding site. Induction of DNA damage, which resulted in decreased cyclin A level, corresponded to an increase in PRMT1 and decrease in PRMT5 binding. This study uncovers a new mechanism in E2F1 regulation and establishes the importance of arginine methylation in cell proliferation and apoptosis.

Acknowledgements

Curiosity has always been the driving force behind my education and I am fortunate to have parents that not only provided for my upbringing, but also given me the freedom to pursue my passion in science. I am eternally grateful to the teachers in my early education that had to put up with my incessant questions and to my professors during my undergraduate days at Nanyang Technological University, where my friends and I felt like we were expected to become experts in five different fields in a fourteen-week time span. Still, the questions never stopped. As I progressed through the years, I realised that science not just about learning a set of knowledge, but by asking the right questions. Great answers come from great questions.

My initiation into scientific research is credited to A/Prof Yoon Ho Sup, who kindly allowed me to work as an intern in his lab at NTU. There, I received my first set of basic laboratory techniques from Dr Kang Congbao, a PhD student at the time. These skills were developed further during my one-year graduate employment with Dr Yu Qiang's lab at the Genome Institute of Singapore. Dr Wu Zhenlong, my colleague and mentor at GIS, was a pivotal figure whose synergistic partnership allowed us to publish two papers in a year.

Prof Nick La Thangue is a pioneer in E2F biology and an accomplished scientist. It has been a great honour to be his DPhil student and I consider myself fortunate to be able to work under such a distinguished figure. Nick is a supervisor that any student could ever wish for – a rich history of groundbreaking publications, highly resourceful, and a record for producing outstanding DPhil graduates. I was also greatly inspired by Dr Simon Carr, who was my guiding figure, mentor and friend. I will greatly miss the days working with him in the lab. The other colleagues I would like to acknowledge are Dr Er-Chieh Cho, Dr Sarah Loftus, Dr Shonagh Munro, Dr Geng Liu, Dr Jutta Moehlenbrink, Ms Yi-Chien Lu, Dr Lindsay Stimson, Dr Omar Khan, Dr Rebecca Konietzny, Dr Benedikt Kessler and Dr Mark T. Bedford.

I would like to show my deepest appreciation for A*STAR in offering me the overseas PhD scholarship. Special thanks to my friends Audrey Tay and Angeline Liu for their help during the scholarship application process. Finally, I would like to thank my lovely wife Xunxun Liu for all the support and encouragement throughout my studies.

Contents

Chapter 1 Introduction

Chapter 2 Materials and Methods

Chapter 3 Discovery of Arginine Methylation in E2F1

Chapter 4 Molecular properties of Arginine Methylated E2F1

Chapter 5 Phenotypic Effects of E2F1 Arginine Methylation

Chapter 6 Regulators of E2F1 Arginine Methylation

Chapter 7 Discussion

Table of Figures

Abbreviations

°C	Degrees centigrade
53BP1	p53 binding protein 1
ADMA	Asymmetric dimethylarginine
AEBSF	4-(2-Aminoethyl) benzenesulfonyl fluoride hydrochloride
AIDS	Acquired immunodeficiency syndrome
APAF1	Apoptotic protease activating factor
ARF	Alternative reading frame
ATCC	American Type Culture Collection
ATM	Ataxia telangiectasia mutated
ATP	Adenosine triphosphate
ATR	ATM and Rad3-related
AXIN	Axis inhibition protein
β-ME	Beta-mercaptoethanol
Bax	Bcl2-associated X protein
Bcl	B-cell lymphoma 2
bp	Base pair
BSA	Bovine serum albumin
Btg1/Btg2	B-cell translocation gene 1/2
CARM1	Coactivator-associated arginine methyltransferase 1
Caspase	Cysteine aspartic protease
CDC6	Cell division cycle 6
CDK	Cyclin-dependent kinase
CDKN2A	Cyclin-dependent kinase inhibitor 2A
ChIP	Chromatin immunoprecipitation
Chk1	Checkpoint kinase 1
Chk2	Checkpoint kinase 2
CHX	Cycloheximide
COPR5	Co-operator of PRMT5
DBD	DNA-binding domain
DMEM	Dulbecco's modified Eagle's medium
DMSO	Dimethyl sulfoxide
DNA	Deoxyribonucleic acid
Doxo	Doxorubicin
DP	DRTF-associated protein
DPM	Disintegrations per minute
DRTF	Differentiation regulated transcription factor
dsDNA	Double stranded DNA

DTT	Dithiothreitol
E. coli	*Escherichia coli*
E2F	E2 promoter-binding factor
EDTA	Ethylenediaminetetraacetic acid
EMT	Epithelial-mesenchymal transition
ER	Estrogen receptor
Etop	Etoposide
FACS	Fluorescence activated cell sorting
FCS	Foetal calf serum
FOXO1	Forkhead box protein O1
GAPDH	Glyceraldehyde 3-phosphate dehydrogenase
GC	Guanine-Cysteine
GDP	Guanosine diphosphate
GST	Glutathione S-transferase
GTP	Guanosine triphosphate
HA	Haemagglutinin
HAT	Histone acetyl-transferase
HBV	Hepatitis B virus
hCAF	Human chromatin assembly factor
HDAC	Histone deacetylase
HEPES	4-(2-hydroxyethyl)-1-piperazineethanesulfonic acid
HHV8	Human herpesvirus 8
HPV	Human papillomavirus
IGEPAL	Octylphenoxypolyethoxyethanol
INK4A	CDK4 inhibitor A
IPTG	Isopropyl β-D-1-thiogalactopyranoside
IUPAC	International Union of Pure and Applied Chemistry
JAK2	Janus kinase 2
JMY	Junction mediating and regulatory protein
kDa	Kilodalton
LB	Luria-Bertani
LC-MS/MS	Liquid chromatography coupled tandem mass spectometry
LSD1	Lysine-specific demethylase
MAP	Mitogen-activated protein
MDM2	Murine double minute 2 protein
MEP50	Methylosome protein 50
$MgCl_2$	Magnesium chloride
miRNA	MicroRNA
MMA	Monomethylarginine
MRE11	Meiotic recombination 11

mRNA	Messenger RNA
Na_3VO_4	Sodium vanadate
NaCl	Sodium choride
NaF	Sodium fluoride
NES	Nuclear export signal
NFkB	Nuclear factor kappa-light-chain-enhancer of activated B cells
NHS	Nation Health Service
NLS	Nuclear localisation signal
NM23	Non-metastatic 23
NML	Nuclear membrane lysis
NP-40	Nonidet-P40
OGT	N-acetylglucosamine transferase
OHT	4-hydroxytamoxifen
P/CAF	p300/CREB-binding protein associated factor
PAGE	Polyacrylamide gel electrophoresis
PARP	Poly(ADP-ribose) Polymerase
PBS	Phosphate buffered saline
PcG	Polycomb group
PCNA	Proliferating cell nuclear antigen
Pen-Strep	Penicillin-Streptomycin
PHD	Pleckstrin homology domain
PI	Propidium iodide
PML	Plasma membrane lysis
pRb	Retinoblastoma protein
PRMT	Protein arginine methyltransferase
PSBT	Protein buffered saline with Tween
PTM	Post-translational modification
PUMA	p53 upregulated modulator of apoptosis
PVDF	Polyvinylidene fluoride
RNA	Ribonucleic acid
ROS	Reactive oxygen species
rpm	Revolutions per minute
SAM	s-adenosyl-methionine
Sam68	Src-associated substrate of mitosis of 68 kDa
SCF	Skp-Cullin-F-box
SDS	Sodium dodecyl sulphate
siRNA	Small interfering RNA
Skp2	S-phase kinase-associated protein 2
SmD1	Small nuclear ribonucleoprotein D1
SMN	Survival motor neuron

SOB	Super Optimal Broth
ssDNA	Single stranded DNA
ST7	Suppression of tumorigenicity 7
SWI/SNF	Switch/Sucrose non-fermentable
TA	Transactivation domain
TBP	TATA-binding protein
TDRD	Tudor domain-containing protein
Tet.	Tetracycline
TopBP1	Topoisomerase IIβ binding protein 1
TP53	Tumor protein p53
TP53INP1	Tumor protein p53 inducible nuclear protein 1
TR3	Testicular receptor 3
Tris-HCl	Tris(hydroxymethyl)aminomethane-hydrochloric acid
TSS	Transcription start site
UV	Ultraviolet light
v/v	Volume per volume
w/v	Weight per volume
WHO	World Health Organisation

1. Introduction

1.1 Impact of cancer on people and society

Cancer is a disease class characterised by uncontrolled proliferation of cells which at advanced stages, may spread throughout the body and result in pain, disability or death. In addition to suffering from physical symptoms, cancer patients and their families also experience high levels of emotional distress, which often associates with psychological consequences such as depression or suicide (Williams and Dale, 2006). In 2008, 12.7 million new cancer cases were diagnosed and 7.6 million cancer-related deaths were reported worldwide, equivalent to 13% of total global mortality (Jemal et al., 2011). Due to increasing life expectancies and an expanding world population, the number of cancer incidences is expected to rise. According to World Health Organization (WHO) estimates, by 2030, the global annual cancer-related deaths may increase up to 11.8 million.

The detrimental impact of cancer on the economy is significant. Depending on the stage and severity of the cancer, patients suffer considerable reduction in work productivity. In 2008, the global economic loss due to premature death or disability from cancer cost up to £561 billion, equivalent to 1.5% of the world's gross domestic product (Rijo M. John, 2012). In the United Kingdom alone, the National Health Service (NHS) spent approximately £4.35 billion on the diagnosis and treatment of cancer, which equated to 5.2% of the 2007 healthcare budget (DH, 2007).

In light of the negative impact cancer brings about to individuals and society, intensive research has been carried out to better understand this class of disease. Hopefully, the knowledge generated from cancer research will help us design more effective tools and drugs in the diagnosis and treatment of cancer, extending lives and reducing human suffering. This study adds to that knowledge by unravelling a new mechanism in regulated cell growth and programmed cell death, as well as providing greater insight to a decade-old enigma regarding the self-conflicting behaviour of the transcription factor E2F1.

1.2 Cancer cell biology

The human body is made up of cells which grow and die in a tightly-controlled fashion. Each cell serves specific functions that contributes to the overall well-being of the body, and its growth is kept in check by physical and chemical signals from its surrounding cells (Raff, 1992). All cells in the human body originate from a single zygote and thus contain the same genetic material. As these cells are clones of one another, it is in their evolutionary interest to communicate and work together to ensure the health and survival of the whole body, so that they can ensure the propagation of their genes to the next generation through the gametes.

Human cells replicate by going through a process known as the cell cycle, which is marked by four distinct phases: G1 (gap 1), S (synthesis), G2 (gap 2) and M (mitosis), followed by cytokinesis, which divides a parent cell into two daughter cells. The cell cycle contains checkpoints that prevent the cell from going into the

next phase if it does not fulfill certain prerequisites, such as successfully completing DNA replication. Despite this, DNA replication is not perfect and one error is estimated to occur in the synthesis of every 30 million base pairs (Roberts and Kunkel, 1988). Reactive oxygen species (ROS) formed from normal metabolic processes and external environmental insults, such as exposure to oncoviruses, mutagens or radiation, can cause further DNA damage and lead to higher mutation rates (Grivennikov et al., 2010).

When a cell detects DNA damage, it arrests the cell cycle and activates a group of specialised proteins functionally known as the DNA repair machinery, which ensures that any DNA damage is repaired before the cell cycle is allowed to progress (Friedberg et al., 2006). If the DNA damage is extensive, the cell exits the cell cycle and either goes into a dormant state known as senescence, or a type of programmed cell death known as apoptosis (Thompson, 1995). Unlike necrosis – which involves cell death caused by traumatic injury that ruptures the cell membrane, spills cellular contents into the surrounding environment, and results in regional tissue damage – cells which undergo apoptosis form cell fragments which phagocytic cells can easily recognise and engulf, thereby limiting any damage to the body (Farber, 1994).

Given that there are approximately one hundred trillion cells in the body, it is unsurprising that every once in a while a mutation could be missed by the DNA repair machinery and passed onto daughter cells. This accidental change in the genomic sequence is known as an acquired somatic mutation (Evan and Vousden, 2001). Most of these mutations do not cause any change in phenotype and are

known as silent mutations. Sometimes, a mutation may result in a phenotypic change that is detrimental to the cell. Cells which acquire such deleterious traits are likely to lose out in growth competition with its healthier neighbouring cells and are quickly removed from the population, rendering them harmless.

The problem arises when the phenotypic changes allow a cell to gain selective advantages over its neighbouring cells, such as the ability to replicate an unlimited number of times (immortality), self-sustain its own proliferative signals, be insensitive to growth suppressors, evade apoptosis, or avoid elimination by the immune system (Hanahan and Weinberg, 2011). Over time, a colony of these abnormal cells may grow into a neoplasia, more commonly known as a tumour. If the tumour is localised and non-invasive, it is termed a “benign tumour” and is rarely life-threatening. Cancer or a “malignant tumour” occurs when tumour cells gain the ability to expand into the surrounding tissue (invasion), spread through the blood or lymphatic system (dissemination), implant into other organs (colonisation), and form secondary tumours (metastasis) (Chiang and Massague, 2008).

1.3 Darwinian microevolution

A key concept in molecular oncology is that a cell becomes cancerous through the deregulation of molecular pathways which usually have normal roles in cellular function. These aberrations must fulfill two criteria for Darwinian microevolution to occur. First, the lesion must confer selective advantages to the individual cell, that is, by acquiring tumourigenic traits. Second, the traits must be

heritable – both somatic mutations and epigenetic changes fulfill these criteria. Unlike somatic mutations, which change the underlying DNA sequence, epigenetic changes involve chromatin remodelling, DNA methylation, or histone modifications, which not only adulterates genetic expression, but can also be passed on to successive generations (Berdasco and Esteller, 2010).

1.4 Cancer genes

Any genetic change that leads to cancer occurs either on a proto-oncogene or a tumour suppressor. A proto-oncogene is a normal gene with the potential to become a cancer-causing gene (i.e. oncogene) when mutated or overexpressed. These genes are usually involved in signal transduction, cell cycle regulation, proliferation or migration (Croce, 2008). An example of a frequently upregulated oncogene is *RAS*, which is activated in up to 25% of all human tumours (Malumbres and Barbacid, 2003). Ras proteins are small GTPases – enzymes that hydrolyse guanosine triphosphate (GTP) to guanosine diphosphate (GDP) and inorganic phosphate – which transmit proliferative signals to the cell (Downward, 2003).

A tumour suppressor gene naturally protects a cell from tumour formation. These genes are often engaged in cell cycle regulation, DNA repair, apoptosis, or are simply the negative regulators of oncogenes (Sherr, 2004). Switching off a tumour suppressor gene usually requires both copies of the gene to be deactivated for loss of function to occur due to the diploid nature of human somatic cells

(Knudson, 1971). The exception to this is a dominant negative mutation, which results in a mutant protein with the ability to quench the activity of a normal protein through homo-complex formation (May and May, 1999). An example of a tumour suppressor gene is *TP53*, which is mutated or deleted in more than 50% of all human tumours (Hollstein et al., 1991). The p53 protein is a transcription factor – a DNA binding protein that controls the expression of genes and the synthesis of RNA – which induces cell cycle arrest and activates DNA repair or apoptosis when cells detect DNA damage (Guo et al., 2000).

1.5 Knudson's two-hit hypothesis

The activation of a single oncogene or the deactivation of a tumour suppressor gene alone is usually insufficient to cause cancer. Due to the diploid nature of autosomal chromosomes in somatic cells, the chances of phenotypic defects arising from mutation of a single allele copy is reduced. Even if both copies of the gene are mutated, a change in a single trait is unlikely to cause cancer. This theory, first proposed by Carl O. Nordling in 1953, suggested that traits leading to cancer required multiple genes to be deregulated over time through accumulated mutations, which partially accounted for the correlation between cancer incidences and longevity (Nordling, 1953). This theory was further developed through a systematic investigation of retinoblastoma by Alfred G. Knudson in 1971 (Knudson, 1971). Knudson observed that unilateral retinoblastoma (cancer in one eye) occurred sporadically, whereas bilateral retinoblastoma (cancer in both eyes)

was often hereditary and had earlier onset. He postulated a two-hit model, whereby two mutational events were required for tumour formation. Thus, if an individual carried two healthy copies of the RB gene, two mutational events were required for tumour formation. Whereas, if the individual inherited one copy of defective RB and one copy of wild type RB, only one mutational event was required for tumour formation. This accounted for the earlier tumour onset in these high-risk individuals (Rushlow et al., 2009).

Carcinogenesis may also be accelerated through prolonged exposure to mutagens or radiation, which causes extensive DNA damage and increase the incidence of genetic defects. Certain viruses, such as the hepatitis B virus (HBV) (Buendia, 1992) and the human papillomavirus (HPV) (Walboomers et al., 1999)also increase the likelihood of cancer through expression of viral oncogenes. Precancerous cells, which express tumour antigens, are usually removed by the immune system in healthy individuals. As such, patients suffering from acquired immunodeficiency syndrome (AIDS) are predisposed to cancers that are rare in immunocompetent individuals, such as Kaposi's sarcoma, caused by human herpesvirus 8 (HHV8) (Antman and Chang, 2000). This highlights the importance of the immune system in cancer prevention.

1.6 Early studies on E2F1

E2F1, the first member of the E2F family to be discovered, was initially described as a cellular factor required for the adenovirus E1A protein to activate its E2 promoter – hence the name **E2** Promoter-Binding **F**actor (Kovesdi et al., 1986). In a separate independent experiment, a newly discovered protein bearing functional resemblance to the adenovirus E1A protein was found to decrease DNA binding activity during the differentiation of F9 embryonic cancer stem cells, and was hence given the name **d**ifferentiation **r**egulated **t**ranscription **f**actor (DRTF) (La Thangue and Rigby, 1987). Further research found that both factors bound to the same DNA consensus sequence and were functionally indistinguishable (Helin et al., 1992; Kaelin et al., 1992), so for a period of time the transcription factor was referred to as DRTF/E2F (Nevins, 1992; La Thangue, 1994). We now know that these two factors are the same (Trimarchi and Lees, 2002).

Eventually, other proteins with similar functional domains were discovered and grouped into the E2F family (Adams and Kaelin, 1995), which comprises eight members to date. The initially discovered member was thus renamed E2F-1, or more recently, E2F1. Later on, through affinity purification and microsequencing, an essential cofactor of E2F1 was discovered and was given the name **D**RTF-associated **p**rotein (DP) (Girling et al., 1993). Three members of the DP family have been identified to date. The first two, DP-1 (Helin et al., 1993) and DP-2 (Zhang and Chellappan, 1995) act as E2F1 co-activators, whereas DP-3 acts as a transcriptional co-repressor (Qiao et al., 2007).

1.7 Structural properties of E2F1

The E2F1 protein is made up of 437 amino acids. It is found predominantly in the cell nucleus due to the presence of a nuclear localisation signal (NLS) between amino acid (a.a.) residues 85-91 (Ivanova et al., 2007) (Fig 1.1). The NLS is flanked by a Cyclin A binding domain (a.a. 87-95). Recruitment of active CyclinA-CDK2 to E2F1 during the late S phase of the cell cycle results in phosphorylation of S375, which increases E2F1's affinity to its inhibitor pRb, thereby winding down its transcriptional activity (Peeper et al., 1995).

The DNA binding domain (DBD) of E2F1 (a.a. 120-191) contains a helix-loop-helix structure which recognises the consensus sequence TTTCGCGC on target gene promoters (Nevins, 1992). It is the only domain that is conserved among all members of the E2F family and is the primary criteria for inclusion into the group. The DP binding domain (DP) (a.a. 201-317) contains a leucine-repeat sequence and a marked-box motif, which allows E2F1 to form a heterodimer with its transcriptional cofactor DP-1 (Hallstrom and Nevins, 2003). The E2F and DP family proteins share conserved DNA binding and dimerisation domains, and it is shown that E2F1/DP-1 interaction increases DNA binding affinity (Magae et al., 1996).

The transactivation domain (TA) of E2F1 (a.a. 368-437) interacts with proteins that initiate transcription, such as TATA-binding protein (TBP), a component of the transcription factor II D (TFIID). (Lee and Young, 2000). The interaction between E2F1 and TBP confers specificity to the TFIID complex, allowing it to recognise and bind to the TATA box, a specific DNA sequence

approximately thirty base-pairs upstream of the transcription start site (TSS) of a gene promoter (Emili and Ingles, 1995). Within the TA domain of E2F1 lies a pRb-binding domain (a.a. 409-426), which binds to hypo-phosphorylated pRb. The relationship between pRb and E2F1 will be elaborated in a later section.

1.8 The E2F family

The E2F family comprises eight members E2F1–E2F8 which share conserved DNA-binding domains (DeGregori and Johnson, 2006) (Fig 1.1). E2F1–6 and members of the DP family, DP-1 and DP-2, also contain conserved dimerisation domains, allowing complex formation and increased transcriptional activity (La Thangue, 1994). E2F1–3 contains a nuclear localisation signal (NLS) within the Cyclin A-binding domain, which directs them to the nucleus; while E2F4–5 contain nuclear export signals (NES), which primarily localises them to the cytoplasm (Magae et al., 1996). E2F1–3 binds primarily to pRb; E2F4 binds to all three members of the pocket protein family (pRb, p107 and p130); while E2F5 interacts preferentially with p107 and p130 only. E2F6–8 contains neither the transactivation nor the pocket protein binding domains, and E2F7–8 contains double copies of DBD (Trimarchi and Lees, 2002).

The E2F family is functionally subdivided into activators and repressors. E2F1–2 and the longer spliced variant of E2F3 (known as E2F3a), promote transcription and drive cell cycle progression, and thus are described as “activator E2Fs”. The combined mutation of E2F1, E2F1 and E2F3a has been shown to

completely abolish cell proliferation (Wu et al., 2001). The shorter spliced variant of E2F3 (E2F3b) and E2F4–8 participate in gene repression, and are therefore termed “repressor E2F”. This theory of sibling rivalry within the E2F family is supported by studies in the fruit fly *Drosophila melanogaster*, which contains only two E2F members: *dE2F1* and *dE2F2* (Dynlacht et al., 1994) . It was observed that the phenotypic effects caused by *dE2F1* depletion could be rescued by the co-depletion of *dE2F2*, thereby suggesting the presence of antagonistic forces within the E2F family (Frolov et al., 2001). Interestingly, it was found that although all activating E2Fs were able to induce S-phase entry, only E2F1 was able to promote apoptosis (DeGregori et al., 1997). Subsequent studies performed by other groups showed a modest transcriptional activation of apoptotic genes by E2F2 and E2F3a overexpression (Nahle et al., 2002; Vigo et al., 1999), but the effects were later demonstrated to be dependent on E2F1 accumulation (Lazzerini Denchi and Helin, 2005).

Instead of the nuclear localisation signals present in the activators E2F1–3a, the repressors E2F4 and E2F5 possess nuclear export signals (NES) which shuttle them into the cytoplasm with the help of the nuclear export factor CRM1 (Gaubatz et al., 2001). Nonetheless, the cytoplasmic localisation of E2F4/5 can be reversed through interaction with the pocket proteins pRb or p130, which allows them to cross the nuclear membrane, associate with histone deacetylases (HDACs) and attenuate transcription (Iavarone and Massague, 1999). The repressive nature of E2F4/5 is supported by the fact that they are highly expressed in quiescent (G0)

cells, while E2F1–3a is found in actively dividing cells (Ikeda et al., 1996; Moberg et al., 1996).

E2F6 lacks the transactivation and pocket protein binding domain present in E2F1–5, but forms heterodimers with DP proteins, allowing it to compete for E2F target promoters (Gaubatz et al., 1998). It is shown to be a component of the Bmi1-containing polycomb complex which represses transcription through epigenetic silencing (Trimarchi et al., 2001).

E2F7/8 has two distinct DNA-binding domains which recognise E2F target promoters and inhibit their transcription (de Bruin et al., 2003; Logan et al., 2004; Logan et al., 2005). They have been implicated in the DNA damage response (Zalmas et al., 2008), embryonic development (Li et al., 2008) and angiogenesis (Weijts et al., 2012). The mechanism of how they achieve transcriptional repression has not been confirmed, but they are known to be act independently of pocket proteins and members of the DP family (Di Stefano et al., 2003; Maiti et al., 2005).

Figure 1.1 Structural properties of the E2F family

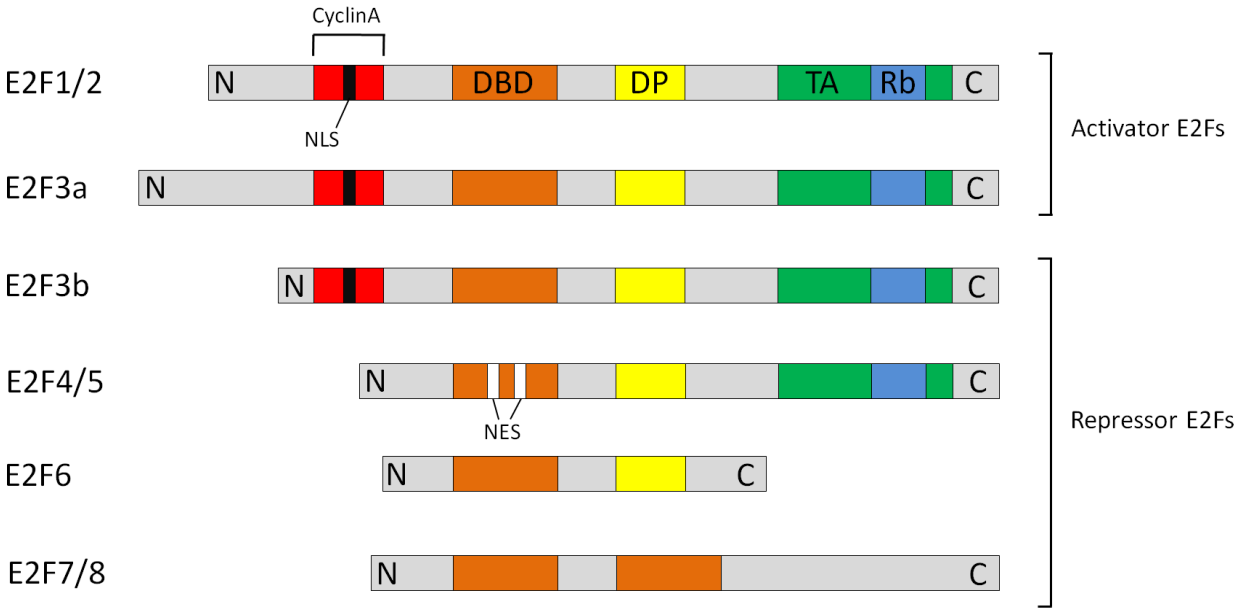

The E2F family consists of members which share conserved structural and sequence similarities. They are grouped into activators and repressors of transcription. N – NH3 terminus; NLS – nuclear localisation signal; DBD – DNA binding domain; DP – DP binding domain; TA – transactivation domain; Rb – pocket protein binding domain; C – COOH terminus.

1.9 E2F1 and cell cycle regulation

As mentioned earlier, the cell cycle is divided into four distinct phases: G1, S, G2 and M. The boundary between the G1 and S phase contains a restriction point. A cell which transgresses this boundary becomes committed to DNA replication without the need for further proliferative stimulation, and will ineluctably progress through the remaining cell cycle phases (Sherr, 1996). The restriction point and the phases of the cell cycle are regulated by the activity of cyclin-CDK complexes. A cyclin-dependent kinase (CDK), as its name suggests, is an inactive enzyme (apoenzyme) which is dependent on its specific cofactor cyclin for the formation of an active enzyme complex (holoenzyme). CDK levels remain relatively constant at all phases of the cell cycle, but the temporal synthesis and degradation of cyclins result in oscillating levels of cyclin-CDK enzymatic activity (Kastan and Bartek, 2004). These include the interphase CDKs (CDK2, 4 and 6) and the mitotic CDK1. Recent studies have shown that mouse embryos develop normally until mid gestation without all three interphase CDKs, but not without CDK1, highlighting its essential role in mammalian cell division (Santamaria et al, 2007). The ten mammalian cyclins discovered to date are divided into four different classes (A, B, D and E types). (Malumbres et al., 2013). Two families of CDK inhibitors regulate CDK activity: INK4 (INK4A, INK4B, INK4C and INK4D) and Cip/Kip proteins (p21, p27 and p57) (Malumbres et al., 2005). In the ‘classical’ model of the mammalian cell cycle, progression through the restriction point at the G1/S phase boundary is preceded by the accumulation of D-type cyclins and their association with CDK4/6,

which triggers the phosphorylation of pRb and activation of the transcription factor E2F1 (Harbour et al., 1999)

The retinoblastoma protein, a direct repressor of E2F1, belongs to a family known as the “pocket proteins”, which includes members such as p107 and p130 (Wang, 1997). These proteins are named for their homologous “pocket regions” that envelop their target motif sequences, such as those within the C-terminus of E2F1. The pRb protein contains multiple phosphorylation sites which affect its binding affinity to E2F1 (Lees et al., 1993).

Before entering G1 phase, cells are kept in a quiescent state through CDK inhibitors such as $p16^{INK4A}$, which bind tightly to CDK4/CDK6 and inhibit their kinase activity (McConnell et al., 1999). The hypophosphorylated pRb remains tightly bound to E2F1 and prevents it from activating its transcriptional targets (Mittnacht, 1998) (Fig 1.2A).

When cells receive mitotic signals, they stimulate the degradation of CDK inhibitors such as $p16^{INK4A}$ and release CDK4/CDK6, allowing them to interact with the D-type cyclins (Benassi et al., 1999). The resulting cyclin D-CDK4/6 complex phosphorylates pRb, which alters its conformation and binding affinity to E2F1 (Kato et al., 1993). The released E2F1 transcriptionally activates a number of genes important for cell cycle progression, such as cyclin D1 and E2F1 which auto-upregulate themselves, as well as cyclins E and A which complexes with CDK2/6 to phosphorylate other important targets (Fig 1.2B). This process sets in

motion a positive feedback loop which ensures natural progression of cells past the G1/S boundary (Lundberg and Weinberg, 1998).

During S phase progression, cyclin A-CDK2 binds to E2F1 and phosphorylates DP-1, which decreases their DNA-binding affinity and transcriptional activity (Benassi et al., 1999; Xu et al., 1994). At the S/G2 transition, E2F1 activity is abolished through polyubiquitination by the SCF complex and degradation by the proteasome. The F-box protein responsible for recognizing E2F1 is Skp2 (Marti et al., 1999). Like cyclins, Skp2 expression fluctuates during the cell cycle, and its levels peak at the S/G2 transition. This coincides with a sharp drop in E2F1 activity during G2 phase entry.

Figure 1.2 E2F1 and cell cycle regulation

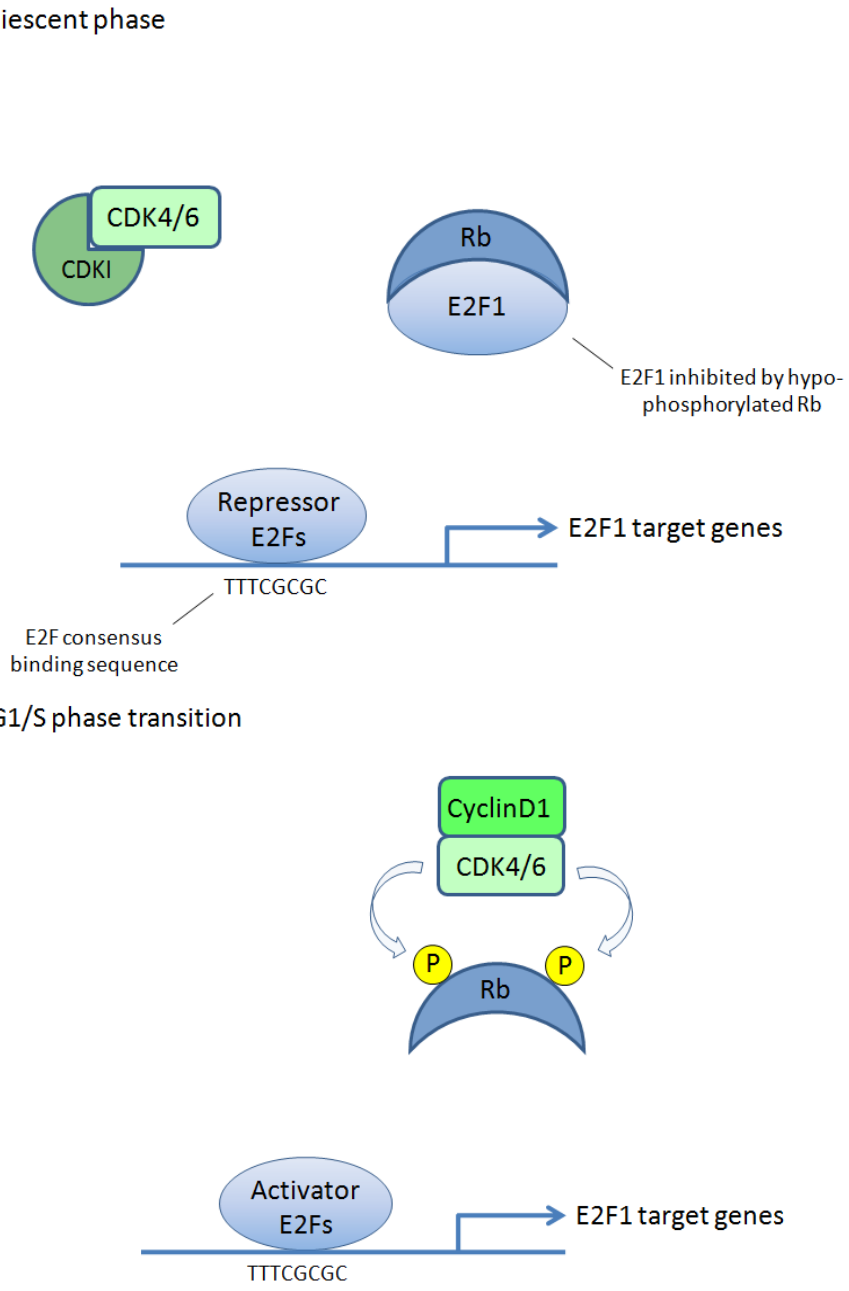

(**A**) In quiescent cells, CDK4/6 activity is kept in check by CDK inhibitors such as $p16^{INK4A}$. Hypo-phosphorylated pocket proteins, such as pRb, bind tightly to activator E2Fs, such as E2F1, preventing the activation of E2F target genes.
(**B**) During G1/S phase transition, degradation of CDK inhibitors and the accumulation of D-type cyclins allow formation of active cyclin-CDK complexes. This in turn allows phosphorylation of pocket proteins, which release activator E2Fs and promote the transcription of E2F target genes.

1.10 E2F1 pathway in carcinogenesis

Given the central role that E2F1 plays in cell cycle progression and proliferation, it is easy to see why deregulation of the E2F1 pathway is associated with up to ninety percent of all cancers (Sherr and McCormick, 2002). It is important to note that multiple mutations are not usually found within the E2F1 pathway, emphasizing that disruption of the pathway can be achieved by simply targeting any one of its regulatory components.

The involvement of E2F1 in carcinogenesis is intimately linked to *RB1,* a gene named after the pediatric eye tumour, retinoblastoma (Friend et al., 1986). The *RB1* gene is found to be absent or mutated in up to one-third of all human cancers (Hatakeyama and Weinberg, 1995). Some cancer-causing viruses, such as the adenovirus and human papillomavirus (HPV) – the main cause of cervical cancer – transform healthy cells into pre-cancerous ones by hijacking pRb and disrupting the pRb/E2F1 interaction (Bandara and La Thangue, 1991). Oncoproteins of these viruses, such as adenovirus E1A, or HPV E7, contain an LXCXE motif which binds to the small pocket region of protein Rb, causing conformational changes to its protein structure which decreases its binding affinity with E2F1. The untimely activation of E2F1 activity in this manner allows cells to artificially bypass the G1/S phase checkpoint, leading to an increased proliferation rate (Mulligan and Jacks, 1998).

The second most frequent mutation after *RB1* is *CDKN2A*, a gene that encodes multiple distinct proteins through alternative splicing, such as $p16^{INK4A}$, which functions as a CDK inhibitor (CDKI). Downregulation of $p16^{INK4A}$ promotes

CDK4 activity, leading to hyper-phosphorylation of pRb and increased activity of E2F1. The result is an enhancement of cell growth which brings them one step towards cancer. In addition, mutations resulting in overactive Cyclin D1 and CDK4 have also been found in many cancers, highlighting the relevance of E2F1 activity deregulation in carcinogenesis (Sherr, 1996).

Direct mutations on the *E2F1* gene itself are uncommon – only recently has a somatic mutation (R166H) been discovered in a rare variant of human epithelial mesothelioma (Yu et al., 2011). The dearth of somatic mutations on the *E2F1* gene suggests that disruption of E2F1 activity at the protein level, rather than the gene level, is the preferred route for tumorigenesis. In support of this hypothesis, ectopic expression of E2F1 protein was shown to cause oncogenic transformation of normal cells (Xu et al., 1995) and the overexpression of E2F1 protein in transgenic mice was linked to higher incidences of tumour formation (Kasahara et al., 2000).

1.11 Apoptotic nature of E2F1

So far, it is evident that E2F1 plays an important role in cell cycle progression and acts as a growth promoter. However, it has also been observed that E2F1 knockout mice demonstrate an increase in thymocyte apoptosis (Field et al., 1996) and greater susceptibility to tumour formation compared to wild type (Yamasaki et al., 1996), suggesting a role for E2F1 in apoptosis. In another study, Rb-deficient mice, having elevated levels of E2F1, displayed increased apoptosis and embryonic lethality, which could be rescued by the concurrent suppression of

E2F1 (Tsai et al., 1998). These and other accumulating evidence support the hypothesis that E2F1 could be, at least in some situations, a tumor suppressor.

Although a couple of early reports suggested a transcription-independent role of E2F1 in apoptosis, based on observations that only the DNA-binding domain, but not the transactivation domain, was essential for apoptosis (Hsieh et al., 1997; Phillips et al., 1997), this postulation was quickly overturned by the discovery of a growing number of E2F1-transcribed genes involved in apoptosis. Some of these genes act through the p53 pathway (Vousden and Lu, 2002), while others function in a p53-independent fashion (Irwin et al., 2000).

One of these E2F1 targets is $p14^{ARF}$, the product of an alternative reading frame of *CDKN2A*, which also encodes the CDK inhibitor $p16^{INK4A}$. ARF is an inhibitor of mdm2, an E3 ligase responsible for the ubiquitination and degradation of p53 (Sherr and Weber, 2000). E2F1 overexpression results in the upregulation of ARF and the consequent accumulation of p53, triggering the transcription of p53-dependent apoptotic genes (Pomerantz et al., 1998). E2F1 also promotes the transcription of p53 cofactors such as JMY, which upregulates Bax, a strongly pro-apoptotic protein of the Bcl-2 family (Hershko et al., 2005). Upon DNA damage, E2F1 has also been reported to transcriptionally upregulate ATM (Berkovich and Ginsberg, 2003), CHK2 (Stevens et al., 2003) and TP53INP1 (Hershko et al., 2005), which leads to the phosphorylation and accumulation of p53.

APAF1, the transcriptional target of both E2F1 and p53, encodes apoptotic protease activating factor 1, a key component of the apoptosome (Moroni et al.,

2001). An active apoptosome, assembled from the oligomerisation of Apaf-1, cytochrome c and dATP, is responsible for the cleavage and activation of caspase 9, which in turn triggers a cascade of caspase cleavages that commits the cell to apoptosis (Li et al., 1997). Overexpression of E2F1 activity has been shown to increase mRNA and protein levels of Apaf-1, resulting in cleavage and activation of caspases 3, 6 and 9 (Moroni et al., 2001). On the contrary, depletion of Apaf-1 had been shown to significantly reduce E2F1-triggered apoptosis (Furukawa et al., 2002).

Tumours which carry inactivating mutations in both *TP53* and *RB1* often show an elevated level of p73 expression (Tophkhane et al., 2012). As a member of the p53 family, activation of p73 allows transcription of p53-responsive apoptotic genes in situations where p53 is absent. It was demonstrated that p73 depletion (Irwin et al., 2000) or expression of dominant negative p73 mutants (Stiewe and Putzer, 2000) was able to rescue E2F1-triggered apoptosis. An example of p73-dependent cell death occurs in cycling peripheral T cells, where activation of the T-cell receptor results in E2F1-induced, p53-independent apoptosis (Lissy et al., 2000). Histone deacetylase (HDAC) inhibitors have also been shown to eliminate HPV-positive cells through the E2F1-p73 pathway (Finzer et al., 2004). The flowchart in Fig 1.3 provides an overview of some examples of E2F1 target genes and the roles they play in cell function.

Figure 1.3 E2F1 target genes and their roles in cellular function

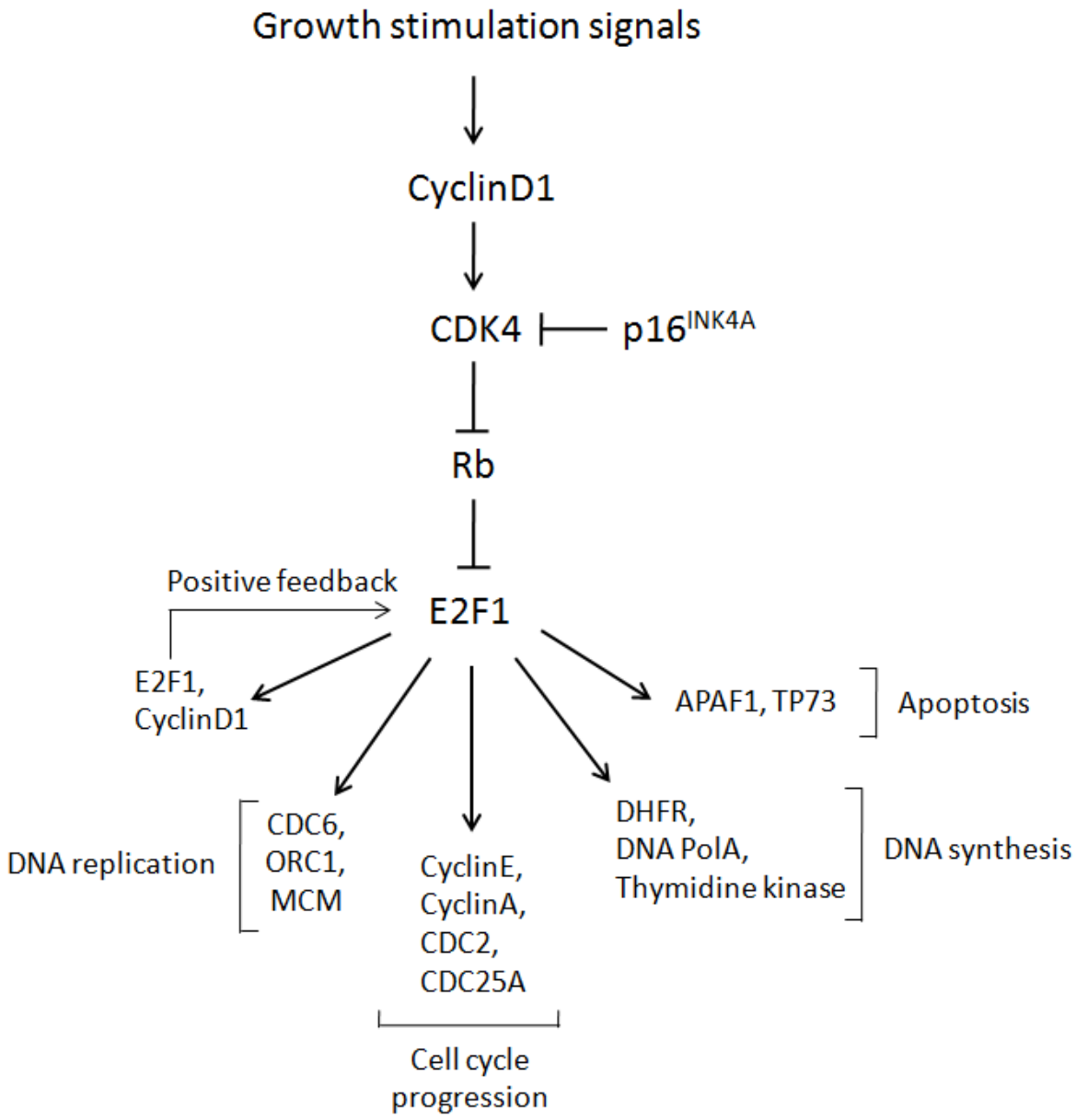

The flowchart shows one of the many signaling pathways that regulate the cell cycle and highlights a few examples of genes activated by E2F1. Targets such as E2F1 and Cyclin D1 result in a positive feedback loop, which ensures forward progression of the cell cycle. Some targets promote DNA synthesis and replication, such as thymidine kinase. Under certain conditions, such as DNA damage, E2F1 may promote the transcription of apoptotic genes, such as p73 and APAF1.

1.12 Regulation of E2F1

Due to its importance in cellular function, the activity of E2F1 is tightly controlled through multiple degrees of regulation. DP-1, the most important binding partner of E2F1, is absolutely essential for its activity (Bandara et al., 1994; Girling et al., 1993). Depletion of the DP-1 gene in mice leads to embryonic lethality, highlighting its importance in growth and development (Kohn et al., 2003). DP-1 is regulated by cyclin A/CDK2 phosphorylation which decreases its DNA binding affinity (Krek et al., 1995).

The predominant inhibitor of E2F1 activity is pRb, a tumour suppressor that is absent or functionally inactive in one-third of all human tumours (Hatakeyama and Weinberg, 1995). Various studies have shown that interaction between E2F1 and pRb not only masks the E2F1 transactivation domain (Dimova and Dyson, 2005), but also help recruit repressive complexes, such as histone deacetylases (HDAC) (Kachhap et al., 2010), chromatin remodeling complex (SWI/SNF) (Gunawardena et al., 2004) or polycomb group proteins (PcG) (Ji et al., 2012) to suppress E2F1 targets at the epigenetic level.

MicroRNAs, such as miR-449 and miR34, are induced by both E2F1 and p53 (Lize et al., 2010). Although they are pro-apoptotic in nature, they have also been shown to repress E2F1 at the mRNA level, providing a negative feedback loop (Feng and Yu, 2010). It is postulated that these microRNAs act as a safety mechanism to prevent excessive E2F1-induced proliferation (Yan et al., 2012).

Post-translation modifications (PTMs), such as phosphorylation, acetylation and methylation have also been shown to occur on E2F1, which provide fine tuning of its binding and transcriptional activity (Fig 1.4). For example, phosphorylation of E2F1 S332 and S337 prevents its interaction with pRb (Sahin and Sladek, 2010), and phosphorylation of S403 and S433 by p38 MAP kinase mediates E2F1 export and protein degradation (Ivanova et al., 2009).

Several studies have shown that E2F1 protein levels are upregulated upon DNA damage (Blattner et al., 1999). Under these conditions, ataxia telangiectasia mutated/ ataxia telangiectasia and Rad3-related (ATM/ATR) kinases are recruited to E2F1 and phosphorylate S31 (Lin et al., 2001). The phosphorylation of S31 increases the association of E2F1 to DNA topoisomerase IIβ binding protein 1 (TopBP1) (Liu et al., 2003), and is believed to recruit Brg1/Brm, an important component of the SWI/SNF chromatin-remodelling complex (Liu et al., 2004). It is also demonstrated that 14-3-3τ specifically binds to phosphorylated S31 and inhibits its ubiquitination, which partially accounts for the increase in E2F1 stability (Wang et al., 2004). Induction of DNA damage by etoposide or UV treatment activates Chk2 kinase, which phosphorylates E2F1 at S364 leading to increased protein stability and apoptosis (Stevens et al., 2003).

Acetylation of K117, K120 and K125 by histone acetyltransferases p300 and P/CAF has been shown to increase E2F1 protein stability, DNA binding ability, transcriptional activity (Martinez-Balbas et al., 2000). These lysine residues are situated near the DNA binding domain of E2F1 and their acetylation is believed to alter protein structure, leading to increased DNA affinity. Treatment with

chemotherapeutic agents such as doxorubicin has been reported to trigger E2F1 acetylation and promote specific binding to the p73 promoter, thereby promoting cell death (Pediconi et al., 2003).

The histone methyltransferase Set7/9 was shown methylate E2F1 at K185 and prevent E2F1 accumulation. It appears that E2F1 lysine methylation antagonizes other post-translational modifications, such as acetylation and phosphorylation, but promotes ubiquitination and protein degradation. The methyl-lysine mark can be removed by the histone demethylase LSD1, which is activated under DNA damage conditions (Kontaki and Talianidis, 2010).

Figure 1.4 Post-translational modifications on E2F1

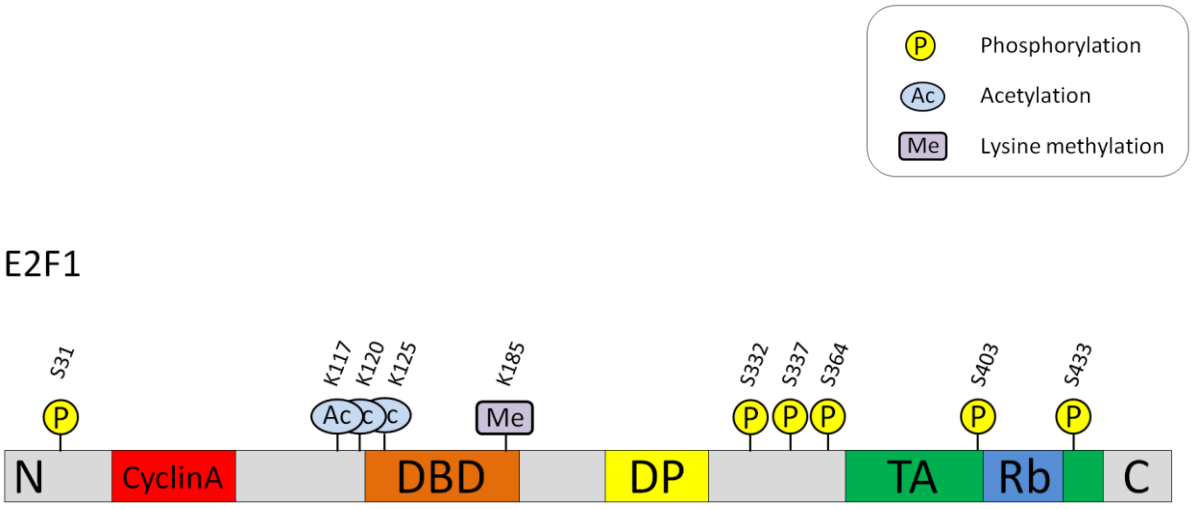

The schematic shows the positions of E2F1 post-transcriptional modifications that are described in scientific literature. The functional domains are included for reference. N – NH3 terminus; CyclinA – cyclin A binding domain; DBD – DNA binding domain; DP – DP binding domain; TA – transactivation domain; Rb – pocket protein binding domain; C – COOH terminus; S – serine; K – lysine.

1.13 Arginine methylation

Arginine is one of the twenty naturally occurring amino acids found in the human body. The arginine side chain contains a guanidino group which contains five hydrogen bond donors that can potentially form interactions with hydrogen bond acceptors. Covalent modifications on arginine, such as methylation, remove these potential hydrogen bond donors from the guanidino group and alter the shape of its electrostatic cloud. Under physiological conditions, the arginine guanidino group exists in a cationic state and methylation does not remove this positive charge present on the arginine side chain (Tripsianes et al., 2011). Instead, addition of methyl groups confers additional mass, volume and hydrophobicity which cause changes to protein-protein interactions through structural and steric effects. Such disruptions can be seen in the example of Sam68, where arginine methylation of its proline-rich motifs inhibits its binding to SH3 domains, while sparing WW domains (Bedford et al., 2000). In addition, arginine methylation has been found to increase protein affinity to aromatic rings through cation-pi interactions (Hughes and Waters, 2006), as exemplified by the interaction between the arginine methylated tail of SmD1 and the aromatic ring of the SMN tudor domain (Sprangers et al., 2003).

Methylation of the arginine side chain occurs on its terminal nitrogen atoms, each of which is given the symbols ω and ω' by IUPAC nomenclature (IUPAC, 1984). Monomethylation occurs when either one of these nitrogen atoms is methylated and is usually regarded as an intermediary step towards the creation of dimethylarginines. An asymmetric dimethylarginine (ADMA) is generated from a

monomethylarginine (MMA) by the subsequent addition of another methyl group on the same terminal guanidine nitrogen atom, whereas a symmetric dimethylarginine (SDMA) is created by the methylation of two different terminal guanidine nitrogen atoms (Fig 1.5) (Bedford and Clarke, 2009). Of these, ADMAs are reported to the most prevalent, while SDMAs and MMAs together form half of that or less (Bedford and Clarke, 2009).

Methylation of guanidino groups on the arginine side chain under physiological conditions is extensive. It has been reported that up to two percent of arginine residues were found methylated in nuclear extracts from rat hepatocytes (Boffa et al., 1977), suggesting that arginine methylation in biological context is anything but rare. Methylated arginine sites are usually flanked by one or more glycine residues (Gary and Clarke, 1998), although exceptions do exist. Although this post-translational modification is not currently as well characterised as phosphorylation, protein arginine methylation has since been implicated in transcriptional control, signal transduction, DNA repair and protein transduction (Bedford and Clarke, 2009).

Arginine methylated substrates include histones and non-histone proteins. Like other post-translational modifications, arginine methylation on histones epigenetically alters gene expression. Effector proteins that recognise methyl-specific marks usually contain PHD, Chromo or Tudor domains, such as WDR5 (Migliori et al., 2012). Examples of arginine methylated non-histone proteins include FOXO1 (Yamagata et al., 2008), Axin (Cha et al., 2011) and CRAF (Andreu-Perez et al., 2011).

Figure 1.5 Types of arginine methylation

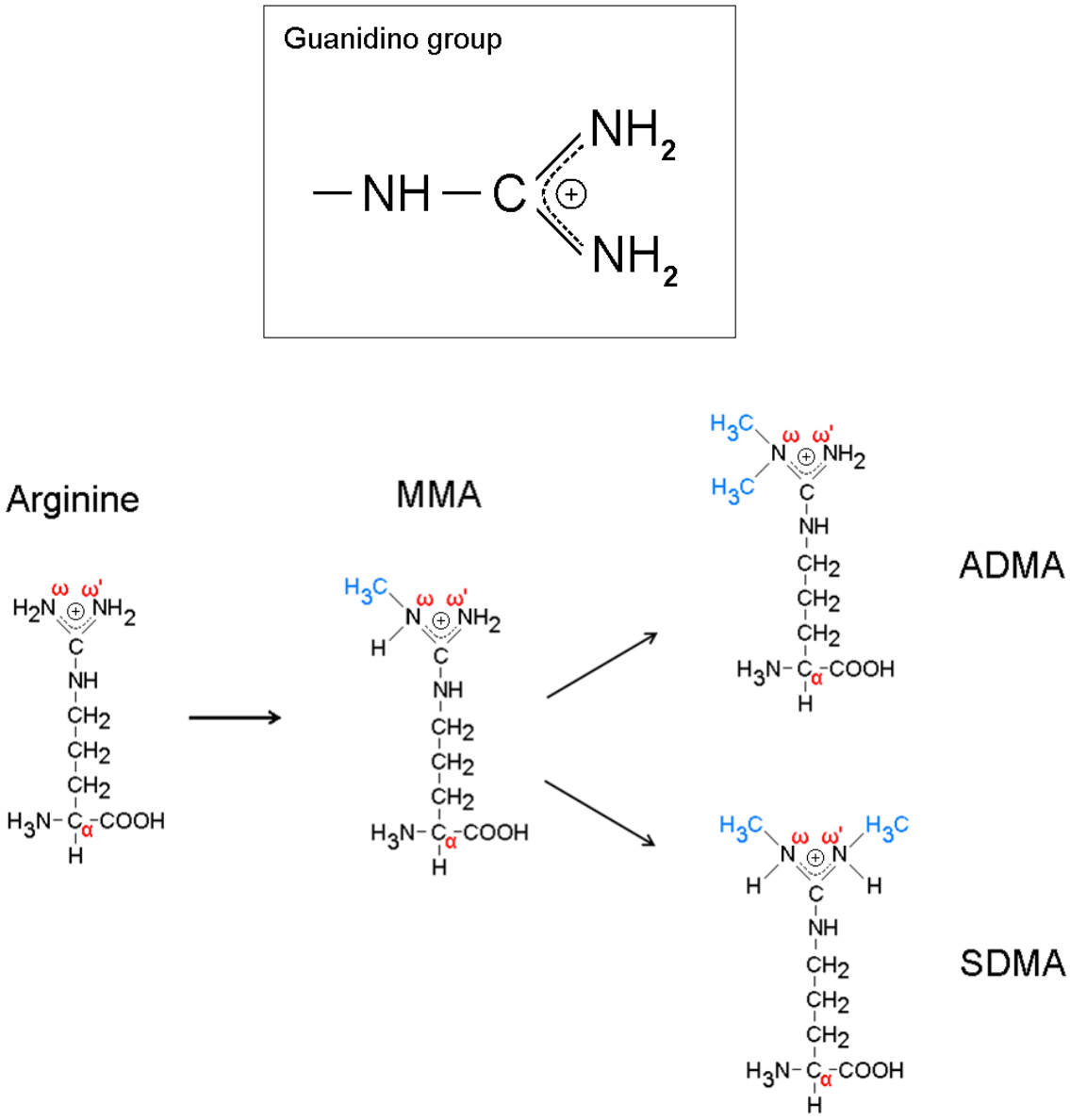

Methylation occurs on the terminal nitrogens of the guanidino group on the arginine side chain. Three types of methylation are possible under physiological conditions. A monomethylarginine (MMA) is regarded as an intermediary step towards dimethylarginines. An asymmetric dimethylarginine (ADMA) is generated by a double methylation on the same terminal guanidine nitrogen atom (ω), whereas a symmetric dimethylarginine is created by the methylation of two different terminal guanidine nitrogen atoms (ω and ω').

1.14 Protein arginine methyltransferases

The methylation of arginine residues is catalysed by a family of enzymes known as the protein arginine methyltransferases (PRMTs), of which nine have been discovered to date in mammals. All members of the PRMT family use S-adenosyl-L-methionine (SAM/AdoMet) as their cosubstrate and methyl group donor. In addition to their enzymatic activity, members of the PRMT family also share similar structural characteristics, such as a common seven-beta strand, “double E” and “THW” sequence motifs. Most PRMTs described to date tend to target glycine and arginine (GAR)-rich motifs (Yang and Bedford, 2013), with the possible exception of PRMT4 (also known as CARM1), which targets proline/glycine/methionine (PGM)-rich motifs (Cheng et al., 2007)

The PRMT family is categorised into four classes. Type I PRMTs (PRMTs 1, 3, 4, 6 and 8) catalyse asymmetric dimethylation of arginines, while type II PRMTs (PRMTs 5 and 7) catalyse symmetric dimethylation. Both type I and II PRMTs monomethylate arginine as an intermediary step towards dimethylation. However in some cases, PRMT7 catalyses arginine monomethylation as an endpoint in itself (Zurita-Lopez et al., 2012), distinguishing it as a type III PRMT. Type IV PRMT (RMT2) catalyses the formation of MMA in the internal guanidino nitrogen (denoted δ-N) of the arginine side chain. However, this has only been described in yeast where RMT2 was shown to methylate the ribosomal protein L12 in Saccharomyces cerevisiae (Chern et al., 2002). In contrast, type I and II PRMTs have been described in mammals, fish (Hung and Li, 2004), flies (Boulanger et al., 2004).

The predominant types of PRMTs in their respective subclasses are PRMT1 and PRMT5. Both are ubiquitously expressed and regulate cellular processes such as cell growth, proliferation and differentiation. Complete knockout of either PRMT1 (Yu et al., 2009) or PRMT5 (Tee et al., 2010) in mice resulted in embryonic lethality, while PRMT4/CARM1 knockout mice died at birth (O'Brien et al., 2010) highlighting the importance of these enzymes in cell survival. In contrast, mice with PRMT2 (Yoshimoto et al., 2006), PRMT3 (Swiercz et al., 2007) and PRMT6 (Neault et al., 2012) knockouts are viable. These PRMTs target a smaller repertoire of substrates and are expressed in fewer types of cells.

Regulation of PRMT activity may be achieved through post-translational modifications, regulatory proteins, subcellular compartmentalisation and miRNA. For example, phosphorylation of CARM1 at S217 during mitosis by an unknown kinase prevents it from binding to S-adenosyl-L-methionine (SAM/AdoMet), thereby inhibiting its methyltransferase activity (Higashimoto et al., 2007). Interestingly, glycosylation by N-acetylglucosamine transferase (OGT) was shown to prevent CARM1 phosphorylation and its correct cellular localisation during mitosis (Sakabe and Hart, 2010).

PRMTs confer methylarginine marks on substrates which can be recognised by Tudor domain-containing proteins (TDRDs) (Chen et al., 2011). The aromatic cages of methylarginine-binding Tudor domains are structurally narrower than their methyl-lysine-binding counterparts, which favour interaction with the planar methyl-guanidinium group. The increased bulk and hydrophobicity of methylarginine promotes non-electrostatic interaction with the aromatic cage of the Tudor domain.

1.15 PRMT1

PRMT1, the first discovered member of the PRMT family, has wide substrate specificity and accounts for a great majority of arginine methylation in mammalian cells. It is reported that up to 85% of all arginine methyltransferase activity in cultured RAT1 fibroblasts or primary mouse hepatocytes could be attributed to PRMT1 (Tang et al., 2000). Structural studies have identified three distinct peptide-binding channels on the PRMT1 catalytic domain, which allows a diverse set of substrates to be exposed to its active site (Zhang and Cheng, 2003). Mutations in any one of these channels were shown by surface-scanning analysis to inhibit binding of specific substrates (Lee et al., 2007). The three-dimensional structure of PRMT1 shows that it exists as a homodimer (Zhang and Cheng, 2003). However, a host of other interacting partners have been described, such as NFkB, Sam68, Btg1/Btg2 and hCAF (Bedford and Clarke, 2009).

Although PRMT1 is required for early mouse development, it was reported that cells deficient in this enzyme are actually viable *in vitro* (Pawlak et al., 2000). Overexpression of aberrant isoforms (Goulet et al., 2007) of PRMT1 have been associated with cancer of the breast (Mathioudaki et al., 2011), prostate (Seligson et al., 2005), lung (Yoshimatsu et al., 2011), colon (Mathioudaki et al., 2008) and bladder (Cheung et al., 2007), as well as leukemia (Zou et al., 2012).

PRMT1 is known to play a role in epigenetic regulation by asymmetrically dimethylating the third arginine of histone H4 (H4R3me2a) (Wang et al., 2001). While this mark is linked to transcriptional activation, the underlying mechanism remains unclear. What is known is that the methylation status of H4R3 and the

binding of its reader protein TDRD3 are both correlated with higher prostate cancer recurrence and poorer prognosis for breast cancer patient survival (Nagahata et al., 2004). PRMT1 has also been implicated in the methylation of DNA repair proteins such as MRE11 and the p53 binding protein 1 (53BP1). MRE11 is involved in homologous recombination repair of DNA double-strand breaks (Yu et al., 2012) while 53BP1 is responsible for the detection, signalling and repair of damaged DNA through non-homologous end joining (Boisvert et al., 2005). Inhibition of arginine methylation in these proteins by PRMT inhibitors was shown to promote the accumulation of DNA damage.

Arginine methylation by PRMT1 has also been shown to affect protein stability. In the example of forkhead box protein O1 (FOXO1), methylation of R248 and R250 by PRMT1 prevents AKT from phosphorylating S253. As phospho-S253 is a necessary signal for FOXO1 nuclear export and proteasome-mediated degradation, PRMT1 inadvertently stabilises FOXO1, promoting the transcriptional activation of target genes (Yamagata et al., 2008). In another example, PRMT1-mediated arginine methylation stabilises Axin and directly prevents it from being degraded by the proteasome, resulting in an attenuation of the Wnt-signalling pathway (Cha et al., 2011).

PRMT1 activity can be negatively regulated by the orphan receptor TR3 (Lei et al., 2009) and by the chromatin assembly factor 1 (hCAF1) (Robin-Lespinasse et al., 2007). Interaction with BTG1 (Lin et al., 1996) or PRMT2 (Pak et al., 2011) has been reported to increase PRMT1 activity towards some of its substrates.

1.16 PRMT5

PRMT5 is the most well-characterised type II arginine methyltransferase. In contrast to PRMT1, the biological roles of PRMT5 have been linked to transcriptional repression (Fabbrizio et al., 2002), especially of tumour suppressor genes such as ST7 and NM23 (Pal et al., 2004). PRMT5 is also responsible for symmetric dimethylation of histones H3R8 and H4R3, both which are key epigenetic markers of transcriptional repression. The depletion of PRMT5 has been shown to reduce cell growth (Wang et al., 2008) while overexpression leads to increased proliferation (Pal et al., 2007). Overexpression of PRMT5 or an increase in its enzymatic activity has been found in gastric (Kim et al., 2005), colorectal (Cho et al., 2012) and lung cancers (Wei et al., 2012), as well as in lymphoma (Pal et al., 2007) and leukemia (Wang et al., 2008). PRMT5 can be phosphorylated by a constitutively active janus kinase 2 mutant ($JAK2^{V617F}$), which disrupts its interaction with methylosome protein 50 (MEP50) and represses its enzymatic activity. The $JAK2^{V617F}$ mutant is found in a majority of patients suffering from myeloproliferative neoplasms (Liu et al., 2011).

Interaction with binding partners appears to exert great influence over PRMT5 specificity. For example, complex formation of PRMT5 with co-operator of PRMT5 (COPR5) in the nucleus results in the preferential methylation of H4R3 over H3R8 (Lacroix et al., 2008). In addition, phosphorylation of MEP50 by cyclin D1-CDK4 was shown to enhance its interaction with PRMT5 and promote neoplastic growth (Aggarwal et al., 2010). The SWI/SNF chromatin remodelling complex is also known to enhance PRMT5 activity in histone substrates (Pal et al.,

2004). Non-coding RNAs play a major role in PRMT5 regulation and more than 50 miRNAs have been predicted to anneal to its 3'-untranslated region (3'-UTR) (Wang et al., 2008). For example, low levels of miR-92b and miR-96 in mantle cell lymphoma (MLL) was shown to induce PRMT5 and symmetric dimethylation of H3R8 and H4R3, leading to epigenetic repression of ST7 (Pal et al., 2007) . Other microRNAs discovered in lymphoid cancer that specifically inhibit PRMT5 include miR-19a, miR-25, miR-32 and miR-92 (Wang et al., 2008).

Chromatin immunoprecipitation (ChIP) experiments showed that PRMT5 is associated with the transcription start site of the cyclin E1 promoter and may be linked to its transcriptional repression. Ectopic expression of PRMT5 negatively affects cyclin E1 promoter activity, though the mechanism remains unclear (Fabbrizio et al., 2002). PRMT5 also plays a role in epithelial-mesenchymal transition (EMT). Depletion of PRMT5 resulted in an increase in E-cadherin levels (Hou et al., 2008), whereas overexpression of PRMT5 promoted anchorage-dependent cell growth (Pal et al., 2004), supporting the notion that PRMT5 may promote cancer cell migration and invasion. Another important target of PRMT5 is the transcription factor p53, encoded by the tumour suppressor gene *TP53*. The p53 transcription factor is a key regulator that plays a major role in the coordination of cell cycle arrest, DNA repair and apoptosis. When subjected to DNA damage, p53 is methylated at R333, R335 and R337, whereas PRMT5 depletion resulted in a p53-dependent apoptosis (Jansson et al., 2008). This not only highlights the oncogenic nature of PRMT5, but also offers a strategy to sensitise cancer cells to chemotherapy.

1.17 Research Objectives

E2F1, a master regulator of cell growth, is deregulated in most cancers, but the mechanisms that govern its activity are not completely understood. While the Rb/E2F1 pathway is deregulated in up to ninety percent of cancers, somatic mutations on the E2F1 gene itself are rare, which makes it likely that disruption of E2F1 activity occurs at the non-genetic level. These regulatory factors may include histone modifiers, chromatin remodelling complexes, non-coding RNAs, protein inhibitors/cofactors, or post-translational modifications.

A number of post-translational modifications (PTMs) have been reported on E2F1. These modifications can be influenced by external stimuli such as exposure to ultraviolet (UV) radiation or addition of DNA damaging agents. Recent studies suggest the presence of crosstalk between PTMs that occur on E2F1, drawing parallels with covalent modifications on histone tails that characterise the “histone code”. While histone modifications modify chromatin structure and DNA availability, E2F1 modifications cause changes in protein stability, DNA/protein binding affinity and transcriptional activity. These changes often translate to visibly clear phenotypes, such as changes to proliferation, differentiation or apoptosis, depending on the cell type and context.

While the impact of methylation in molecular regulation has been extensively investigated in DNA and histones, methylation of non-histone proteins has not been as well-characterised. Recent discoveries have shown that methylation of transcription factors and other non-histone proteins can play a major role in cell regulation. In particular, the discovery of lysine methylation in E2F1 and

arginine methylation in p53 evokes the question of whether arginine methylation may play a role in E2F1 regulation.

This study describes the discovery and characterization of arginine dimethylation in E2F1. PRMT1, a methyltransferase with wide substrate specificity, was found to asymmetrically dimethylate E2F1 at R109. PRMT5, which require interaction with MEP50 for catalytic activation, was found to symmetrically dimethylate E2F1 at R111 and R113. These representative type I and type II PRMTs are likely to compete for binding and methylation of closely positioned arginines in an RG-rich motif on E2F1 through steric repulsion. It was observed that inhibition of SDMA marks on R111 and 113 could lead to E2F1-dependent cell growth inhibition and apoptotic induction. This could be achieved by PRMT5 depletion or promotion of ADMA on R109. It was also observed that addition of DNA damaging agents, such as doxorubicin or etoposide, resulted in decreased cyclin A levels, which correlated to increased ADMA and decreased SDMA marks on E2F1. Together, this study reveals a new regulatory mechanism of E2F1 activity through arginine methylation.

.

2. Materials and Methods

2.1 Cell culture

U2OS and SAOS2 cell lines were obtained from the American Type Culture Collection (ATCC). They were maintained in Dulbecco's Modified Eagle Medium (DMEM) (GIBCO®) supplemented with 10% (v/v) Foetal Calf Serum (FCS) (Biosera) and 1% (v/v) Penicillin-Streptomycin (Pen-Strep) (Gibco®). Stable Tet-On cell lines expressing inducible PRMT5 were prepared as previously described (Jansson et al., 2008). They were maintained in DMEM supplemented with 5% (v/v) Tet-negative FCS, 100µg/ml G418 (Clontech), 0.3% (v/v) hygromycin (Clontech) and 1% (v/v) Pen-Strep. 1 µg/ml doxycline was used to induce PRMT5 expression. Stable cell lines expressing ER-E2F1 fusion protein were prepared as previously described (Vigo et al., 1999). They were maintained in DMEM with 10% (v/v) FBS, 1% Pen/Strep (v/v) and 2 µg/ml puromycin (Clontech). 300 nM 4-hydroxytamoxifen (OHT) (Clontech) was used to induce nuclear translocation of ER-E2F1. Cells were passaged every 3–5 days to maintain 40–60% confluency. During passage, waste medium was removed from the culture flask, briefly rinsed with phosphate-buffered saline (PBS) (Oxoid), and Trypsin-EDTA (Lonza) was added to detach the cells from their flasks. After incubating at 37°C for 5–10 minutes, fresh medium containing FBS was added to neutralise trypsin activity and 5–10% of the cells were transferred into a new flask containing fresh tissue culture medium. For long-term storage in liquid nitrogen, cells were transferred to freezing

media comprising 90% (v/v) FCS and 10% (v/v) DMSO (Sigma) before being frozen down.

2.2 Antibodies

Cleaved PARP, PRMT1 and PRMT5 antibodies were from Cell Signaling. p73 antibody was from Abcam. PARP-1 antibody was from BD Pharmingen. HA antibody was from Covance. Acetyl-lysine, asymmetric dimethyl-arginine, symmetric dimethyl-arginine antibodies were from Merck Millipore. Apaf-1, Cdc6, Chk1, Chk2, Cyclin A, Cyclin E, DHFR, E2F1, GAPDH, and PCNA antibodies were from Santa Cruz. Flag and β-actin antibodies were from Sigma. Mouse and rabbit secondary antibodies were from GE Healthcare. Trueblot® secondary antibodies were from eBioscience. HA or Flag antibody-coupled agarose beads were from Sigma.

2.3 DNA plasmid transfection

GeneJuice® Transfection Reagent (Invitrogen) was added to OPTI-MEM® I Reduced Serum Media (Gibco®) and incubated at room temperature for 5 minutes. Plasmids were added to the mix and incubated for another 15 minutes before addition to mammalian cells in a drop-wise fashion. The cells were incubated at 37°C for 48 – 72 hours before harvest. Protein expression was confirmed by immunoblotting. Where appropriate, pBB14-GFP or pCMV-β-gal plasmids were co-

transfected to assess relative transfection efficiency. In experiments involving transfection of more than one plasmid, control vector was included to ensure equal amounts of transfected DNA across all samples. A list of plasmids used in this study is shown below. All mutant plasmids were generated by site directed mutagenesis.

Plasmid	Tag	Expression	Description
pBB14	GFP	Bacteria	Used as transfection control
pcDNA3.1-HA-E2F1(WT)	HA	Mammalian	Wild type E2F1
pcDNA3.1-HA-E2F1(109)	HA	Mammalian	Arg to Lys point mutation at residue 109
pcDNA3.1-HA-E2F1(111)	HA	Mammalian	Arg to Lys point mutation at residue 111
pcDNA3.1-HA-E2F1(113)	HA	Mammalian	Arg to Lys point mutation at residue 113
pcDNA3.1-HA-E2F1(111/113)	HA	Mammalian	Arg to Lys point mutations at residues 111 and 113
pcDNA3.1-HA-E2F1(KKK)	HA	Mammalian	Arg to Lys point mutations at residue 109, 111 and 113
pcDNA3.1-HA-E2F1Δ87-95	HA	Mammalian	Deletion of cyclin A binding domain
pcDNA3.1-FL-HA-PRMT1	HA	Mammalian	Expresses enzymatically active PRMT1
pcDNA3.1 Vector	-	Mammalian	Vector template
pFlag PRMT5	Flag	Mammalian	Expresses enzymatically active PRMT5
pFlag Vector	Flag	Mammalian	Vector template

pGEX-E2F1(WT)	GST	Bacteria	Wild type E2F1
pGEX-E2F1(R109K)	GST	Bacteria	Arg to Lys point mutation at residue 109
pGEX-E2F1(R111K)	GST	Bacteria	Arg to Lys point mutation at residue 111
pGEX-E2F1(R113K)	GST	Bacteria	Arg to Lys point mutation at residue 113
pGEX-E2F1(R111/113K)	GST	Bacteria	Arg to Lys point mutations at residues 111 and 113
pGEX-E2F1(KKK)	GST	Bacteria	Arg to Lys point mutations at residue 109, 111 and 113
pGEX-PRMT1	GST	Bacteria	Expresses enzymatically active PRMT1
pGEX-Vector	GST	Bacteria	Vector template
pTRE-HA-PRMT5(WT)	HA	Mammalian	Induced by 1μg/ml doxycycline
pTRE-HA-PRMT5(Δ360-372)	HA	Mammalian	Induced by 1μg/ml doxycycline
pTRE Vector	HA	Mammalian	Induced by 1μg/ml doxycycline
pFlag-PRMT5(Δ360-372)	Flag	Mammalian	Deletion of catalytic domain
β-gal	-	Mammalian	Used as transfection control
p73-luciferase	-	Mammalian	For luciferase reporter assay
Apaf1-luciferase	-	Mammalian	For luciferase reporter assay
Cdc6-luciferase	-	Mammalian	For luciferase reporter assay
Cyclin E-luciferase	-	Mammalian	For luciferase reporter assay
E2F1-luciferase	-	Mammalian	For luciferase reporter assay
DHFR-luciferase	-	Mammalian	For luciferase reporter assay

2.4 Small interfering RNA (siRNA)

Oligofectamine reagent (Invitrogen) and siRNA were incubated separately with OPTI-MEM® I Reduced Serum Media (Gibco®) for 5 minutes at room temperature. The two mixtures were combined and incubated for a further 20 minutes. Waste medium from the cells were removed and replaced with serum-free DMEM before adding the siRNA transfection mix in a dropwise fashion. The cells were incubated at 37°C for 6 hours, after which fresh medium containing 10% FCS was re-introduced. Commercial non-targeting siRNA control was from Dharmacon. In experiments involving treatment of more than one siRNA, non-targeting siRNA was included to ensure equal amounts of transfected siRNA across all samples. The siRNA sequences used in this study are as shown.

siRNA	**Sequence**
Non-targeting control (NC)	5'- UUC UCC GAA CGU GUC ACG -3'
PRMT1	5’- GGA CAU GAC AUC CAA AGA -3’
PRMT5	5’- CCG CUA UUG CAC CUU GGA A -3’
E2F1	5’- AAC UCC UCG CAG AUC GUC AUC -3’
Cyclin A	5’ -CCA UUG GUC CCU CUU GAU U -3’

2.5 Immunoblotting

Cells were harvested by treatment with trypsin and lysed by adding NP-40 Lysis Buffer (50 mM Tris-HCl (pH 7.4), 150 mM NaCl, 1% Igepal CA-630/NP-40, 1 mM EDTA, 1 mM NaF, 1 mM Na_3VO_3, protease inhibitor cocktail, 1 mM AEBSF). The cell suspension was incubated on ice for 1 hour and vortexed at 10 minute intervals to release the cell contents. The lysate was centrifuged at 13,000 rpm for 15 minutes to remove cell debris and the supernatant was transferred into clean 1.5 ml microcentrifuge tubes.

Protein concentrations of the extracts were measured by Bradford protein assay (BioRad). Cell extracts were mixed with SDS loading dye (62.5mM Tris-HCl (pH 6.8), 25% (v/v) glycerol, 2% (w/v) SDS, 5% (v/v) β-ME, 0.0625% (w/v) Bromophenol blue), heated at 95°C for 5 minutes, loaded into SDS-polyacrylamide gels and subjected to gel electrophoresis (SDS-PAGE). Proteins were transferred to a polyvinylidene fluoride (PVDF) membrane and a reversible Ponceau stain was used to determine transfer efficiency. The membrane was blocked with 5% (w/v) milk and incubated with primary antibody at room temperature for 1 hour or at 4°C overnight. After primary antibody incubation, the membrane was washed three times with PBST (PBS + 0.1% Tween) and incubated with secondary antibody for an hour. Excess secondary antibody was then rinsed off by washing the membrane three times with PBST. The membrane was incubated with SuperSignal West Dura Extended Duration substrate (ThermoScientific) for 5 minutes and luminescence from the membrane was detected using Fuji Medical X-ray film (Fujifilm).

2.6 Bradford assay

To create a calibration curve, 1 ml of Bradford assay solution was dispensed into 6 disposable plastic cuvettes. 0 µl, 1 µl, 2 µl, 3 µl, 4 µl, and 5 µl of 2 mg/ml BSA standard were added to each and OD_{595} was recorded with a spectrophotometer. To measure protein concentration, 2 µl of the purified protein sample was added to 1 ml Bradford assay solution and the measured OD_{595} was compared against the calibration curve.

2.7 Cell fractionation

Cells were harvested by treatment with trypsin and suspended with plasma membrane lysis (PML) buffer (10 mM HEPES (pH 7.5), 2 mM $MgCl_2$, 1 mM EDTA, 10 mM KCl, 1 mM DTT, 10 mM NaF, 0.1 mM Na_3VO_4, protease inhibitor cocktail). The cell suspensions were incubated on ice for 15 minutes and gently tapped at 5 minute intervals to ensure proper mixing. 10% (v/v) Igepal CA-630 was added to the cell suspensions to a final concentration of 0.6% and incubated on ice for 5 minutes. They were then vortexed at maximum intensity for 10 seconds and incubated on ice for another 5 minutes. This step was repeated again to rupture the plasma membranes. The cell suspensions were centrifuged at 13,000 rpm for 30 seconds to pellet down the nuclei. The supernatant, containing the cytosolic fraction, were transferred to new 1.5 ml microcentrifuge tubes. Nuclear membrane lysis (NML) buffer (25 mM HEPES (pH 7.5), 500 mM NaCl, 1 mM DTT, 10 mM NaF, 10% (v/v) glycerol, 0.1% (v/v) Igepal CA-630, 5 mM $MgCl_2$, protease inhibitor

cocktail) were added to the nuclear pellets and mixed vigorously by vortex. The nuclear suspensions were incubated on ice for 1 hour and transferred to -20°C overnight to rupture the nuclear membranes. The nuclear extracts were sonicated at 23% amplitude to shear DNA and release nuclear binding proteins. They were then centrifuged at 13,000 rpm and the supernatant, containing the nuclear fraction, were transferred to new 1.5 ml microcentrifuge tubes. The extraction purity was assessed by immunoblotting, with GAPDH as control protein for cytosolic fraction and PCNA as control protein for nuclear fraction.

2.8 Co-Immunoprecipitation (Co-IP)

Antibodies were added to protein extracts in 15 ml Falcon tubes and incubated at 4°C for 1 hour with gentle rotation to allow specific protein-antibody interaction. IgA- or IgG-agarose beads (Sigma) were added to the extracts and incubated at 4°C overnight with gentle rotation for antibody-bead coupling. On the following day, the beads were washed thrice with IP wash buffer (50 mM Tris-HCl (pH 7.4), 150 mM NaCl, 0.1% Igepal CA-630/NP-40, 1 mM EDTA, 1 mM NaF, 1 mM Na_3VO_3, protease inhibitor cocktail) to remove unbound proteins. Protein complexes bound to the antibody-agarose beads were eluted by adding SDS loading dye and heating at 95°C for 5 minutes. Eluted proteins were detected by immunoblot. Trueblot® secondary antibodies (eBioscience) were used to minimise background luminescence caused by non-specific immunoglobin 55 kDa heavy and 23 kDa light chains.

2.9 Purification of active enzymes

Flag or HA antibody-conjugated beads (Sigma) were used to immunoprecipitate ectopically expressed proteins containing Flag or HA tag respectively. The beads were washed 4 times with IP wash buffer and eluted with 0.2 mg/ml 3x-Flag peptide (Sigma) or HA peptide (Sigma) dissolved in methylation buffer (50 mM Tris-HCl (pH 8.0), 20 mM KCl, 5 mM DTT, 1 mM EDTA). Enzyme activity was determined by ^{3}H-SAM methylation assay using histones as positive substrate control.

2.10 DNA transformation

1 µl DNA plasmid was added to 50 µl competent *Escherichia coli* (*E. coli)* cells in a 1.5 ml microcentrifuge tube and incubated on ice for 30 minutes. Cells were heat-shocked in a 42°C waterbath for 45 seconds, which temporarily disrupted plasma membrane integrity and allowed uptake of introduced DNA plasmids. The cells were immediately transferred to ice and incubated for 5 minutes to restore membrane integrity. 200 µl Super Optimal Broth (SOB) media was added to the newly transformed cells and incubated at 37°C for 30 minutes for metabolic recovery and expression of antibiotic resistance genes. The cells were plated onto an agar plate containing suitable antibiotics and incubated at 37°C overnight.

2.11 Purification of GST-tagged recombinant proteins

E. coli BL21 (DE3) strain was transformed with relevant plasmids and inoculated into Luria-Bertani (LB) media containing suitable antibiotics. The flasks were shaken at 37°C with an Orbital shaker incubator until OD_{600} 0.6 – 0.8 and 1 mM IPTG was added to induce protein expression. The cell cultures were shaken for a further 2 hours at its optimum expression temperature before pelleting at 8000 rpm for 15 minutes. The supernatant was removed and the cells resuspended in PBS. Triton X-100 was added to a final concentration of 1% (v/v) and the cells were incubated at 4°C for an hour, followed by sonication at 23% amplitude to break down the peptidoglycan cell wall and to shear bacterial DNA. The lysate was centrifuged at 13,000 rpm for 30 minutes to remove cell debris and the supernatant was transferred into a clean 15 ml tubes containing glutathione sepharose beads (GE healthcare). The GST-tagged proteins were bound to the sepharose beads by incubation at 4°C for 2 hours and then eluted using 20 mM reduced glutathione dissolved in 50 mM Tris-HCl (pH 8.0). Excess glutathione was removed via dialysis using Slide-A-Lyzer Dialysis Cassette (ThermoScientific) with a 10 kDa molecular weight cut-off. The dialysis buffer (50 mM Tris-HCl (pH 8.0), 100 mM NaCl, 1 mM EDTA, 10% (v/v) glycerol) was kept cold at 4°C throughout the dialysis process. Purified recombinant proteins were either used for experiments on the same day or stored at -80°C.

2.12 ^{3}H-SAM methylation Assay

Purified enzyme, protein or peptide substrate, ^{3}H-SAM and methylation buffer (50 mM Tris-HCl (pH 8.0), 20 mM KCl, 5 mM DTT, 1 mM EDTA) were mixed and incubated at 30°C for 1 hour. The reactions were then spotted onto 2.1 cm P81 filter paper (Whatman®) and allowed to air dry. The filter paper was washed with washing buffer (46 mM $NaHCO_3$, 4mM Na_2CO_3, pH 9.2) and briefly rinsed with acetone.

After air-drying for 15 minutes, the filter paper was transferred to scintillation vials containing Ready Protein^{+}™ Liquid Scintillation cocktail (Beckman Coulter®). The disintegrations per minute (dpm) were detected using a scintillation counter. Autoradiography was performed by subjecting the reaction mix to SDS-PAGE gel electrophoresis and transferring to PVDF membrane. The membranes were briefly stained with Ponceau to determine transfer efficiency as well as a loading control. After air-drying, the membranes were sprayed with EN3HANCE® Spray (PerkinElmer), placed in an intensifying screen (Kodak) and exposed to Fuji medical X-ray film (Fujifilm) at -80°C for one week.

2.13 Reverse transcription polymerase chain reaction (RT-PCR)

RNA from cells was extracted using RNeasy Mini Kit (Qiagen) according to the manufacturer's instructions. The reverse transcription and PCR amplification was performed using a Titanium® One-Step RT-PCR kit (Clontech). The primer sequences used are as shown.

Primer	Sequence
18S forward	5'-GATACCGAACGAGACTCTGGC-3'
18S reverse	5'-CCATCCAATCGGTAGTAGCG
Apaf-1 forward	5'-TCCGGCGGGATTTGACTGCT-3'
Apaf-1 reverse	5'-CCTCTGGTTCTATCCCTTTTGCCCG-3'
Cdc6 forward	5'-CGCTTTACCCAGAGTCGCCCT-3'
Cdc6 reverse	5'-GTCGCTGTGAGGCCACGACC-3'
Cyclin E forward	5'-GGAAGGCAAACGTGACCGTTGA-3'
Cyclin E reverse	5'-ACTGCATTATTGTCCCAAGGCTGGC-3'
DHRF forward	5'-TAAACTGCATCGTCGCTGTGT-3'
DHRF reverse	5'-AGGTTGTGGTCATTCTCTGGAAA-3'
E2F1 forward	5'-CCGTGGACTCTTCGGAGAAC-3'
E2F1 reverse	5'-GGGACAACAGCGGTTCTTGC-3'
GAPDH forward	5'-CGGAGTCAACGGATTTGGTCGTAT-3'
GAPDH reverse	5'-AGCCTTCTCCATGGTGGTGAAGAC-3'
p73 forward	5'-GGATTCCAGCATGGACGTCTT-3'
p73 reverse	5'-GCGCGGCTGCTCATCT-3'

PRMT1 forward	5’-CAGCCCCGAGTCCCCGTACA-3’
PRMT1 reverse	5’-GCGCATCCGGTAGTCGGTGG-3’
PRMT5 forward	5’-AGTACAGAAGGGCTCAAGCCACC-3’
PRMT5 reverse	5’-GGAGTTCTTGAGGCTGAGTGCGT-3’

2.14 E2F1-derived peptides

E2F1 peptides were synthesised by Alta Bioscience and the purity was confirmed by mass spectrometry. The peptide sequences are as shown.

Peptide	**Sequence**
E2F1 peptide	AESSGPARGRGRHPGKG
109 peptide	AESSGPA(R)GRGRHPGKG, where (R) is asymmetrically dimethylated
111/113 peptide	AESSGPARG(R)G(R)HPGKG, where (R) is symmetrically dimethylated
KKK peptide	AESSGPAKGKGKHPGKG

2.15 Chromatin immunoprecipitation (ChIP)

Cells were seeded in 150 cm^2 dishes and transfected with DNA plasmids or siRNA as described previously. Formaldehyde was added to a final concentration of 1% and incubated at room temperature with gentle shaking for 10 minutes to form DNA-protein cross-links. Glycine was added to a final concentration of 125 mM and incubated with gentle shaking for 5 minutes to neutralise the formaldehyde and cross-linking activity.

The cells were then collected by aspirating the culture media, rinsing twice with ice cold PBS, scraping the dishes in 5 ml PBS, and transferring the cells to new 15 ml Falcon tubes. The dishes were further rinsed with 3 ml PBS and the remaining cells were transferred to 15 ml Falcon tubes. The cells were centrifuged at 1500 rpm for 10 minutes and the supernatant removed. The pellets were re-suspended in 500 µl SDS lysis buffer (1% SDS, 5 mM EDTA, 50 mM Tris-HCl, pH 8.0, protease inhibitor) and transferred to new 1.5 ml Eppendorf tubes. The cell suspensions were sonicated at 4°C for 8–15 minutes to generate sheared, soluble chromatin with fragment sizes between 200–1000 bp.

They were then centrifuged at 13,000 rpm for 10 minutes to pellet down cell debris. The DNA sizes were analysed by diluting 5 µl of the supernatant with 5 µl of TE buffer (1 mM EDTA, 10 mM Tris-HCl, pH 8.0), adding 2 µl of Pronase (Merck), incubating at 42°C for 2 hours, and visualising on a 1% agarose gel. 30 µl of the supernatant were transferred to new 1.5 ml screw cap tubes to be used as “ChIP Input” controls, while the rest of the supernatant were transferred to new 1.5 ml Falcon tubes and topped up with 2500 µl dilution buffer (1% Triton-X100, 2 mM

EDTA, 20 mM Tris-HCl, pH 8.0, 150 mM NaCl, protease inhibitor). 240 µl of protein A/G beads, blocked with BSA for 4 hours, were added to the Falcon tubes and rotated at 4°C for 4 hours to pre-clear the mixtures. They were then centrifuged at 800 rpm for 2 minutes and the supernatant was transferred to new 15 ml Falcon tubes. 80 µl of blocked protein A/G beads and 1–10 µg of control or specific antibodies were added. The tubes were rotated at 4°C overnight.

On the following day, the beads were each washed once with buffer TSE-I (0.1% NP40, 1% Triton-X100, 2 mM EDTA, 20 mM Tris-HCl, pH 8.0, 150 mM NaCl), buffer TSE-II (0.1% NP40, 1% Triton-X100, 2 mM EDTA, 20 mM Tris-HCl, pH 8.0, 500 mM NaCl), buffer III (0.25 M LiCl, 1% NP40, 1% sodium deoxycholate, 1 mM EDTA, 10 mM Tris-HCl, pH 8.0) and TE-wash buffer (2 mM EDTA, 10 mM Tris-HCl, pH 8.0). 120 µl of elution buffer (1% SDS, 10 mM EDTA, 50 mM Tris-HCl, pH 8.0, 0.5 mg/ml RNase A) were added to the beads and transferred to new 1.5 ml screw cap tubes. The Falcon tubes were further rinsed with 120 µl elution buffer and the remaining beads were transferred to the screw cap tubes. 210 µl of elution buffer were also added to the input samples.

The samples were incubated at 65°C overnight to reverse cross-linkage. DNA was purified from the samples using a PCR purification kit (Qiagen) according to the manufacturer's instructions. The purified DNA was prepared for quantitative real-time PCR (qPCR) using KAPA™ SYBR® FAST qPCR Kit (Kapa Biosystems). Triplicates were performed for each reaction condition. The equipment used was a 7500 Fast Real-Time PCR System (Applied Biosystems). The primer sequences used in the qPCR are as shown.

Primer	Sequence
Albumin forward	5’-TGGGGTTGACAGAAGAGAAAAGC-3’
Albumin reverse	5’-TACATTGACAAGGTCTTGTGGAG-3’
Apaf-1 forward	5’-CTTGGCCAGGCTGGTCTTGAAT-3’
Apaf-1 reverse	5’-GCAGCCATTCAAAATTATGACACAT-3’
Cdc6 forward	5’-GGCCTCACAGCGACTCTAAGA-3’
Cdc6 reverse	5’-CTCGGACTCACCACAAGC-3’
Cyclin E forward	5’-GGCCTCACAGCGACTCTAAGA-3’
Cyclin E reverse	5’-CCGACGGCGAGCGGGAAGCAG-3’
DHFR forward	5’-TTCTGCTGTAACGAGCGGGCT-3’
DHFR reverse	5’-CTACAAGTTAGAGAAACAGCGTTACTCGAA-3’
E2F1 forward	5’-AGGAACCGCCGCCGTTGTTCCCGT-3’
E2F1 reverse	5’-GCTGCCTGCAAAGTCCCGGCCACT-3’
P73 forward	5’-TGAGCCATGAAGATGTGCGAG-3’
P73 reverse	5’-GCTGCTTATGGTCTGATGCTTATG-3’

2.16 Luciferase reporter assay

E2F1 gene promoter-luciferase constructs were co-transfected with E2F1 and β-gal plasmids and harvested after 48 hours. The cells were lysed with 120 µl reporter lysis buffer (Promega) and 50 µl was transferred to 96-well plates. Luciferase reporter readings were read and normalised against β-gal assay values, which was used as an internal control for transfection efficiency. All experiments were performed in triplicate.

2.17 Colony formation assay

1000 cells per well were seeded in a 6-well plate and transfection of DNA plasmids or siRNA was performed as described previously. Cell confluencies were visually monitored daily via light microscopy over a period of 7 – 10 days before ending the experiment. The culturing media was gently aspirated to avoid physically damaging the cells and the plates were briefly rinsed with cold PBS. Crystal violet stain was applied to the cells for 2 minutes, followed by rinsing with copious amount of autoclaved deionised water and left to air dry. Scanning was done with a Gelcount™ Colony Counter (Oxford Optronics).

2.18 ATP assay and manual cell counting

ATP assays were performed using CellTitre-Glo® luminescent cell viability assay kit from Promega as instructed in the manufacturer's protocol. The luminescent signals were detected using a Berthold Technologies MicroLumat Plus LB96V reader. Manual counting of viable cells was performed by staining them with Trypan Blue dye for 5 minutes, transferring them to a hemocytometer and visualising under a light microscope. Cells not stained by the Trypan Blue dye were taken to be viable.

2.19 Flow cytometry

pBB14-GFP was co-transfected with expression vectors in cells subjected to FACS to monitor transfection efficiency. Harvested cells were washed with PBS and fixed with 70% ethanol for at least one hour. After fixation, the cells were washed again with PBS and 30 µl RNase (Qiagen) was added. 0.1 mg/ml propidium iodide (Sigma) was added to the cell and incubated in the dark at room temperature for 30 minutes before analysis by BD FACS Calibur 4 flow cytometer.

2.20 Cycloheximide protein half-life assay

Cells were transfected with the relevant E2F1 plasmids for 48 hours before adding 100µg/ml cycloheximide (CHX) (Fluka). They were then harvested at the indicated time points and subjected to immunoblotting. Band intensity was quantified using Image J software (Novell) and plotted. The half-life was calculated from the plot by taking ln 2/x, where x is the decay constant.

2.21 DNA damage agents

Doxorubicin and etoposide were from Sigma. For all experiments involving the addition of drugs, an equivalent volume of DMSO was used in the negative control.

2.22 Statistical analysis

All quantitative data are presented as mean ± SD unless otherwise indicated. Differences between experimental groups were evaluated for statistical significance using Student's *t*-test for unpaired two group comparison or one-way ANOVA where appropriate. *P* values less than 0.05 were considered to be statistically significant.

3. Discovery of arginine methylation in E2F1

Against the backdrop of other post-translational modifications, such as phosphorylation, acetylation, ubiquitination and neddylation, it was possible that methylation may also play a role in regulating E2F1 activity. A recent publication showing lysine methylation on E2F1 (Kontaki and Talianidis, 2010) not only supports this view, but also raises the possibility that other PTMs have been left undiscovered. The protein arginine methyltransferase 5 (PRMT5) have been shown to symmetrically dimethylate R333, R335 and R337 of p53 under DNA damage (Jansson et al., 2008), and depletion of PRMT5 led to p53-dependent apoptosis. Given the similarity to p53 as a DNA damage-responsive transcription factor, I was curious to see if arginine methylation was also present in E2F1.

3.1 Two types of arginine dimethylation found in E2F1

The most direct way to determine whether arginine methylation was present in E2F1 was by purifying it from cells. Endogenous E2F1 was immunoprecipitated from p53-deficient osteosarcoma cells (SAOS2) and probed for arginine methylation signals using methyl-specific antibodies. Two types of arginine dimethylation, symmetric (SDMA) and asymmetric (ADMA), were found on E2F1 (Fig 3.1A). When E2F1 was depleted, both ADMA and SDMA signals disappeared, which increases the likelihood that these marks occurred on E2F1 (Fig 3.1B).

The discovery of arginine dimethylations on E2F1 led to an investigation to determine which enzymes were responsible for the catalysis. Since PRMT1 and PRMT5 were responsible for the majority of arginine dimethylation in cells, they were included in the pool of potential candidates. A preliminary screen showed that E2F1 interacted with PRMT1 and PRMT5 (Fig 3.2A, lane 3). However, the immunoprecipitation of PRMT1 (lane 4) and PRMT5 (lane 5) suggests that these two enzymes do not complex with each other and may not bind to the same E2F1 molecule. The siRNA-mediated depletion of PRMT1 and PRMT5 abolished ADMA and SDMA signals on E2F1 respectively (Fig 3.2B, lanes 9 and 10), implying that these enzymes were responsible for the arginine methylation of E2F1. It is worth noting that when PRMT1 was depleted, there was an increase in E2F1-PRMT5 immunoprecipitation. On the other hand, when PRMT5 was depleted, an increase in E2F1-PRMT1 immunoprecipitation occurred. This provides a clue there may be competition between PRMT1 and PRMT5 for E2F1 interaction. Interestingly, siRNA-mediated depletion of PRMT5 appeared to increase E2F1 (Fig 3.2B, lane 3), which suggests that symmetric dimethylation of arginine may inhibit E2F1 stability. The mechanism behind this phenomenon will be investigated further in the next chapter.

Figure 3.1 Arginine methylation in endogenous E2F1

A

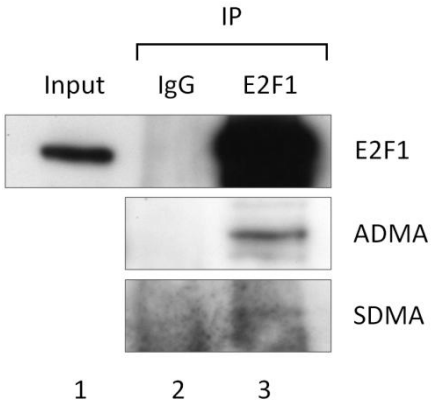

B

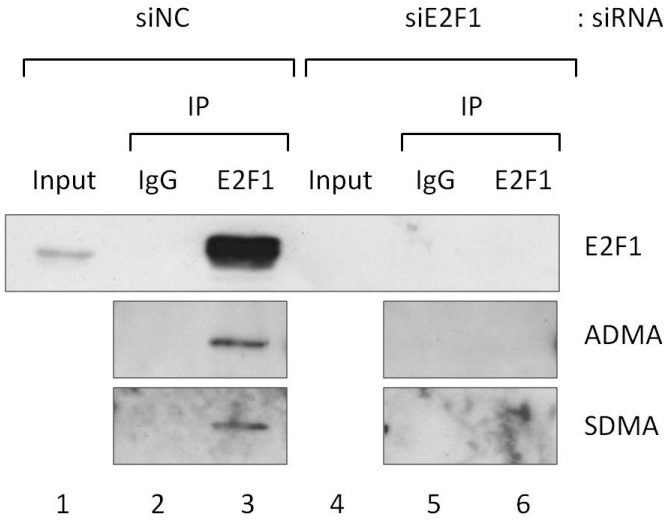

(**A**) ADMA and SDMA signals detected in endogenous E2F1. Cells lysate from SAOS2 cells were immunoprecipitated with control IgG or E2F1 antibodies, and subsequently immunoblotted with the indicated antibodies. Input levels of E2F1 protein are as shown.

(**B**) E2F1 depletion abolished ADMA and SDMA signals. SAOS2 cells were transfected with 50nM non-targeting control (siNC) or E2F1 (siE2F1) siRNA. The corresponding cell lysates were subjected to immunoprecipitation with control IgG or E2F1 antibodies, and immunoblotted with the indicated antibodies. Input levels of E2F1 protein are shown.

Figure 3.2 Binding and methylation by PRMT1 and PRMT5

A

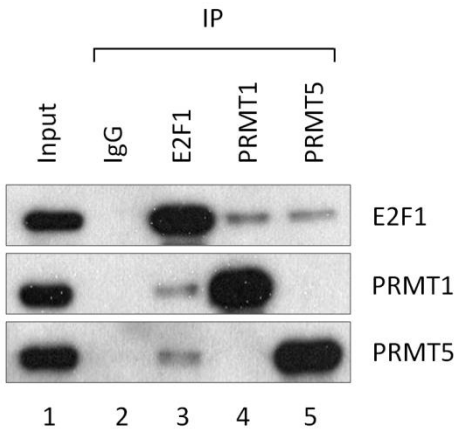

B

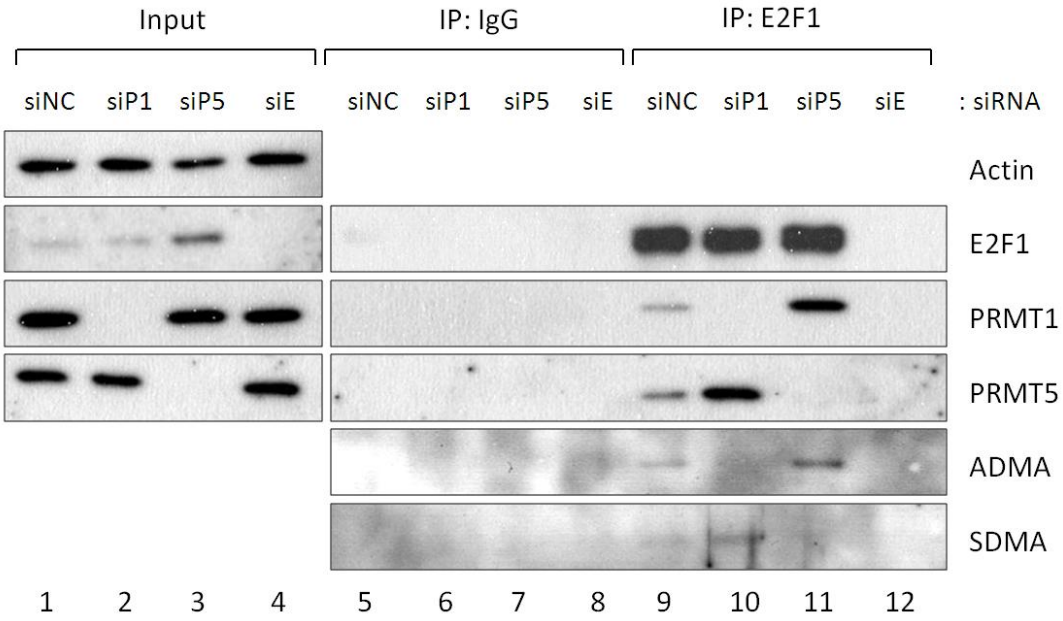

(**A**) E2F1 co-precipitated with PRMT1 or PRMT5 in cells. Lysate from SAOS2 cells was immunoprecipitated with control IgG, E2F1, PRMT1 or PRMT5 antibodies, and subsequently immunoblotted with the indicated antibodies. Input levels of the respective proteins are shown.

(**B**) PRMT1 or PRMT5 depletion coincided with loss of ADMA or SDMA respectively. SAOS2 cells were transfected with 50nM non-targeting control (siNC), PRMT1 (siP1), PRMT5 (siP5) or E2F1 (siE) siRNA. The corresponding cell lysates were immunoprecipitated with control IgG or E2F1 antibodies, and subsequently immunoblotted with the indicated antibodies. Input levels of the respective proteins are shown.

3.2 E2F1 is methylated by PRMT1 and PRMT5

Although PRMT1 and PRMT5 depletion coincided with the respective loss of ADMA and SDMA, further evidence was needed to confirm that these enzymes directly catalyse E2F1 arginine methylation. To recreate the methylation reactions *in vitro*, GST-tagged PRMT1, PRMT5 and E2F1 were expressed and purified from bacterial (*E.coli*) and used in an *in vitro* methylation assay. A tritium-labelled SAM was used as a cofactor and ^{3}H-methyl-group donor.

When E2F1 was incubated with GST-PRMT1, there was a significant increase in tritium labeling compared to GST control (Fig 3.3), implying that PRMT1 was catalysing the covalent addition of ^{3}H-methyl groups to E2F1. However, when E2F1 was incubated with GST-PRMT5, no significant difference was observed compared to GST control. To investigate, a control experiment using histones as substrate revealed that the bacterially expressed GST-PRMT5 was enzymatically inactive. Some groups have proposed that PRMT5 may require cofactors such as MEP50 to form a holoenzyme (Antonysamy et al., 2012). It was possible that the bacterial expression system did not provide such co-factors. Therefore, a decision was made to purify PRMT5 from mammalian cells.

As E2F1 was shown to be methylated by PRMT1 purified from bacteria, it was used as a positive control for methylation experiments involving enzymes purified from mammalian cells. HA-tagged PRMT1 was expressed in osteosarcoma cells (U2OS) and purified using the same principles as the previous immunoprecipitation experiments. An excess amount of HA peptides was used to

elute HA-PRMT1 from agarose beads instead of the usual SDS denaturant, which preserved protein structure and minimised loss of enzyme activity. Part of the elution was immunoblotted with PRMT1 or HA antibodies to determine protein yield (Fig 3.4A). A probe for PRMT5 was performed to rule out the possibility of any non-specific immunoprecipitation of competing enzyme. Both GST-E2F1 and histones were methylated by HA-PRMT1 purified in this manner, providing repeatable observations from two different systems, as well as promoting the feasibility of this protocol (Fig 3.4B).

Using similar principles, Flag-tagged PRMT5 was expressed, purified and subjected to a methylation assay (Fig 3.5) The purified FL-PRMT5 was able to methylate both GST-E2F1 and histones (Fig 3.5B). A PRMT5 mutant with a deletion in the catalytic domain (Δ360-372) did not show any methylation activity, which implied that the enzymatic reaction was catalysed by PRMT5 instead its binding partners.

Figure 3.3 E2F1 methylation by recombinant PRMTs

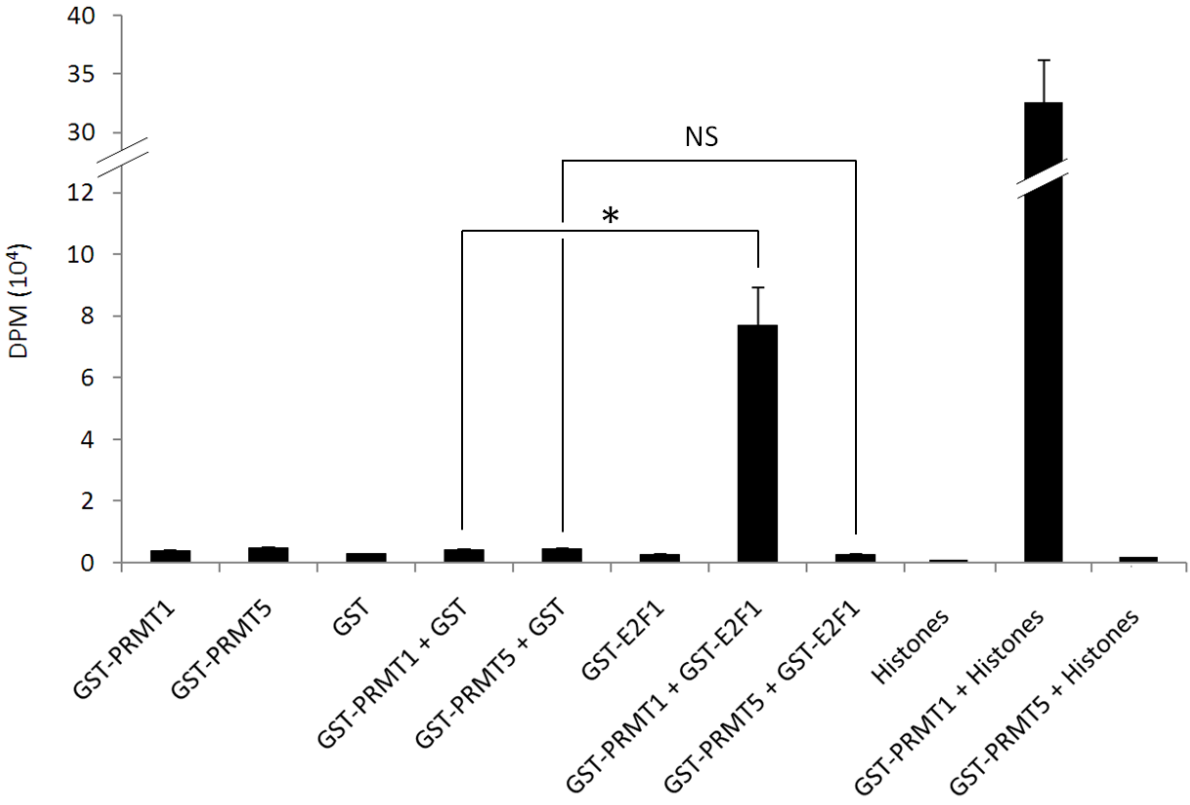

Recombinant GST-PRMT1 or PRMT5 was incubated with 1µg GST-E2F1 in methylation assays with tritium-labelled SAM as co-substrate. Incorporation of ^{3}H-methyl groups was detected by a scintillation counter and measured in disintegrations per minute (DPM). Histones were used as positive control substrate. The GST tag, enzyme or substrates alone were used as negative controls. Data shown are means of 3 independent experiments with error bars representing standard deviation; * $p < 0.05$; NS – no statistically significant difference.

Figure 3.4 E2F1 methylation by PRMT1 purified from human cells

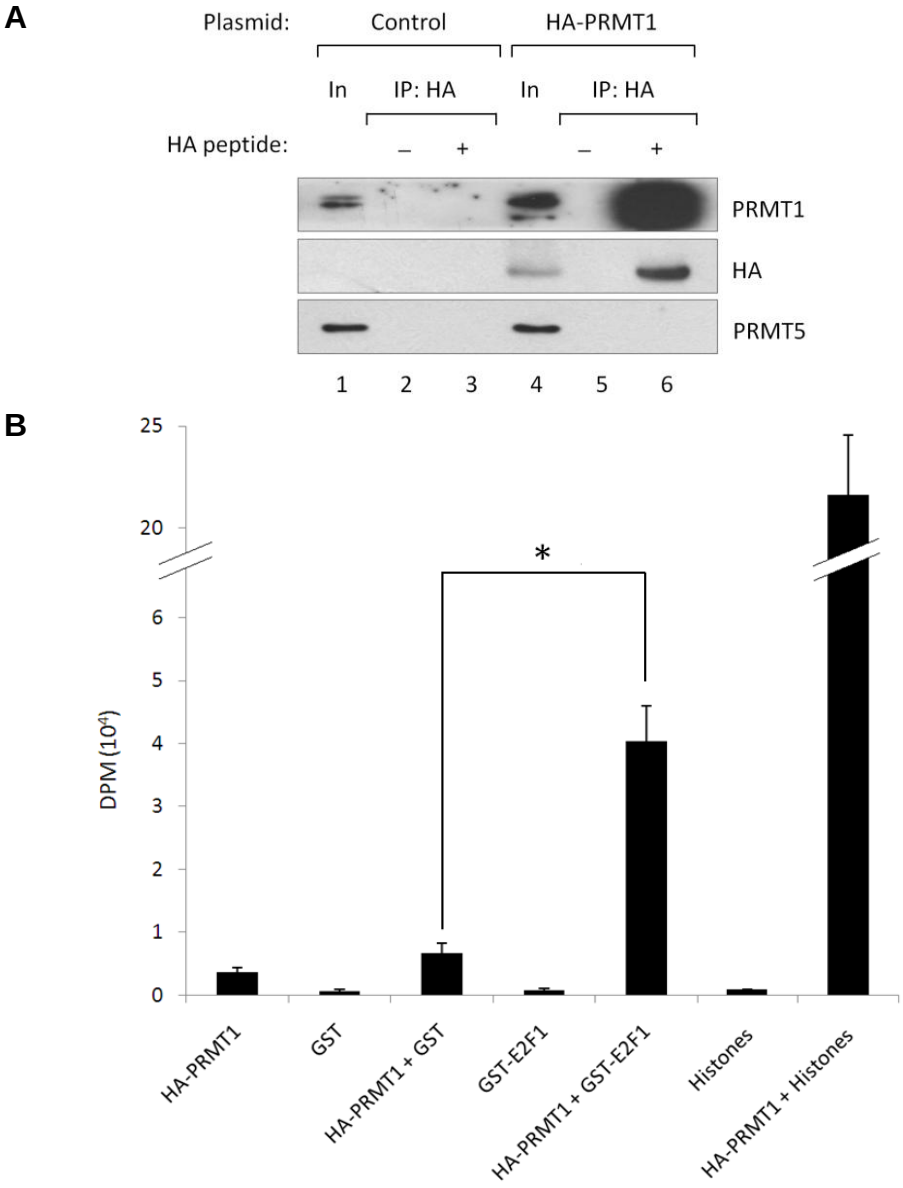

(**A**) Purification of transfected HA-PRMT1 from cells. U2OS cells were transfected with 4 µg control or HA-PRMT1 plasmid. The corresponding cell lysates were subjected to immunoprecipitation using HA antibody-conjugated beads and the bound HA-PRMT1 enzyme was eluted with excess HA peptide. Immunoblotting was performed with the indicated antibodies. Protein input levels (In) are shown.

(**B**) Activity of purified HA-PRMT1 on E2F1. HA-PRMT1 was incubated with 1µg GST-E2F1 in methylation assays with ^{3}H-SAM as co-substrate. Incorporation of ^{3}H-methyl groups was detected by a scintillation counter and measured in disintegrations per minute (DPM). Histones were used as the positive control substrate. The GST tag, enzyme or substrates alone were used as negative controls. Data shown are means of 3 independent experiments with error bars representing standard deviation; * $p < 0.05$.

Figure 3.5 E2F1 methylation by PRMT5 purified from human cells

A

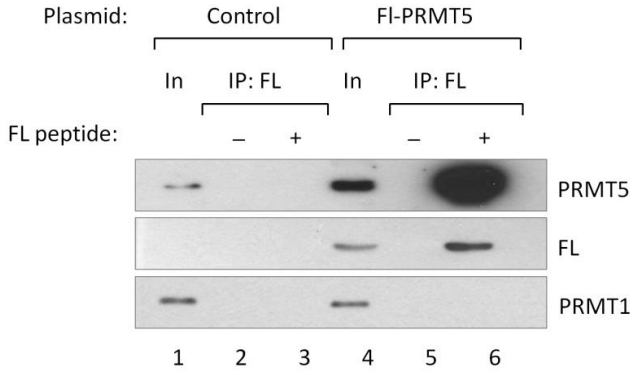

B

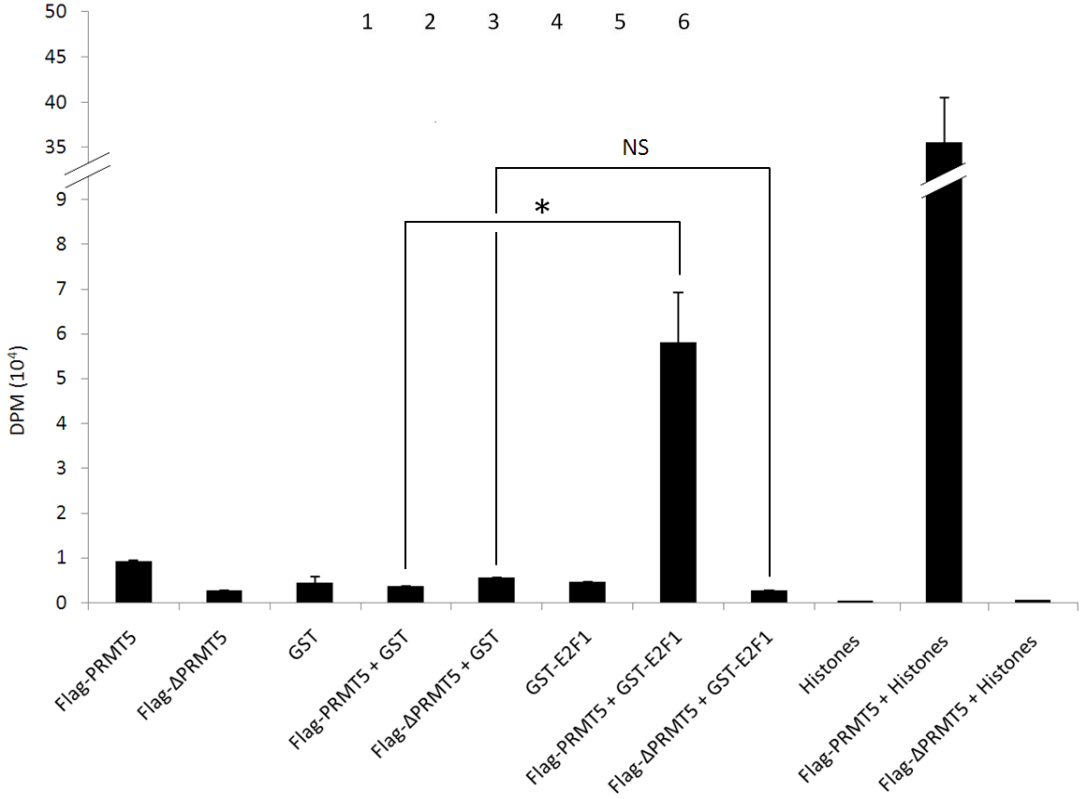

(**A**) Purification of transfected FL-PRMT5 from cells. U2OS cells were transfected with 4 µg control or FL-PRMT5 plasmid. The corresponding cell lysates were subjected to immunoprecipitation using FLAG antibody-conjugated beads and the bound FL-PRMT5 enzyme was eluted with excess FLAG peptide. Immunoblotting was performed with the indicated antibodies. Protein input levels (In) are shown.

(**B**) Activity of purified FL-PRMT5 on E2F1. FL-PRMT5 or catalytically inactive FL-ΔPRMT5 was incubated with 1µg GST-E2F1 in methylation assays with ^{3}H-SAM as co-substrate. Incorporation of ^{3}H-methyl groups was detected by a scintillation counter and measured in disintegrations per minute (DPM). Histones were used as the positive control substrate. The GST tag, enzymes or substrates alone were used as negative controls. Data shown are means of 3 independent experiments with error bars representing standard deviation; * $p < 0.05$; NS – no statistically significant difference.

3.3 Identification of methylated E2F1 arginine residues

To identify the positions of methylated E2F1 arginine residues, a sequence alignment was performed against the methylation region on p53. This revealed a conserved RG-rich motif that may be targeted by PRMTs (Fig 3.6A). Site-directed mutagenesis was used to substitute the arginines with lysines, which preserved the positive charge on the side chain but prevented methylation by arginine methyltransferases. The E2F1 mutant derivatives were purified from *E.Coli* in a similar manner as before (Fig 3.6B) and used in ^{3}H-SAM methylation assays.

The results were visualized by autoradiography (Fig 3.7A) and quantified by scintillation counting (Fig 3.7B). Incubation with PRMT1 allowed methylation of all E2F1 mutants except R109K and KKK, implying that the methylation by PRMT1 occurred on R109. In contrast, incubation with PRMT5 allowed methylation of only wild-type E2F1 and R109K, implying that methylation by PRMT5 occurred on R111 and R113.

Figure 3.6 Mutagenesis of potential E2F1 methylation sites

A

331 QIRGRERFE 339 p53
107 PARGRGRHP 115 E2F1

107 PAKGRGRHP 115 E2F1(R109K)
107 PARGKGRHP 115 E2F1(R111K)
107 PARGRGKHP 115 E2F1(R113K)
107 PARGKGKHP 115 E2F1(R111/113K)
107 PAKGKGKHP 115 E2F1(KKK)

B

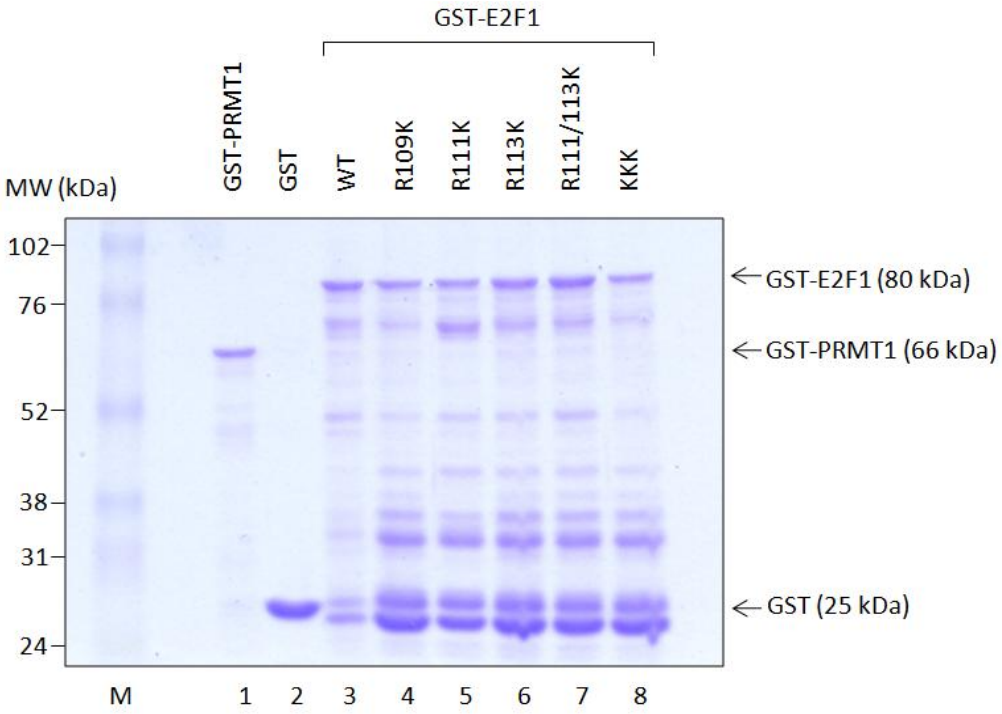

(**A**) Conserved arginine residues in E2F1 corresponding to p53 methylation sites are highlighted in yellow. Arginine to lysine substitutions were created on E2F1 at R109, R111 and R113, which are highlighted in cyan.

(**B**) Purification of recombinant E2F1 mutant derivatives. BL21(DE3) strain of *E. coli* was transformed with plasmids encoding GST-E2F1 protein derivatives and the corresponding cell lysates were incubated with glutathione-conjugated beads. The bound GST-E2F1 protein derivatives were eluted with excess reduced glutathione and subjected to dialysis. Recombinant GST-tagged E2F1 proteins were visualised with Coomassie Brilliant Blue stain. GST-PRMT1 and GST tag are shown for comparison.

Figure 3.7 Methylation of recombinant E2F1 mutant derivatives *in vitro*

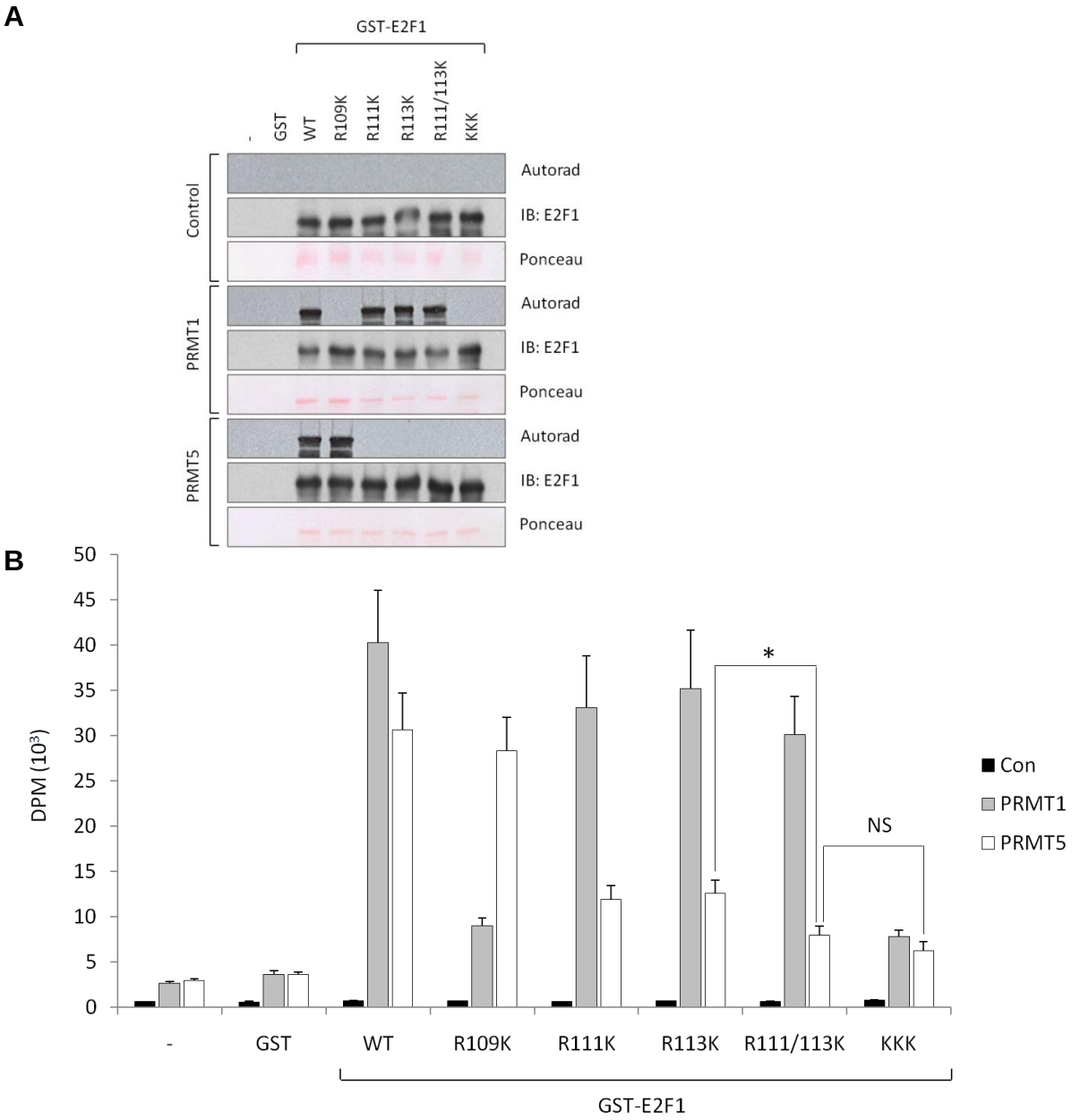

(**A**) ^{3}H methyl group incorporation as visualised on an autoradiograph. Active recombinant enzymes HA-PRMT1 or FL-PRMT5 was incubated with 1µg GST-E2F1 protein derivatives in methylation assays with ^{3}H-SAM as co-substrate. Incorporation of ^{3}H-methyl groups was detected by autoradiography. The identity of methylated protein was confirmed by immunoblotting with E2F1 antibodies. Ponceau staining was used as a loading control.

(**B**) Incorporation of ^{3}H methyl groups measured in disintegrations per minute (DPM). Negative control is shown in black; HA-PRMT1 is shown in grey; and FL-PRMT5 is shown in white. The GST tag, enzymes or substrates alone were used as negative controls; where (–) represents absence of substrate. Data shown are means of 3 independent experiments with error bars representing standard deviation; * $p < 0.05$; NS – no statistically significant difference.

3.4 Methylation of modified E2F1-derived peptides

To differentiate whether the arginine residues in the E2F1 RG-rich motif were indeed methylated by PRMTs, or were simply the docking sites for these enzymes, allowing for methylation of distal arginines, E2F1-derived peptides corresponding to the RG-motif and its flanking regions were chemically synthesized and subjected to a similar methylation assay (Fig 3.8A). The E2F1 peptide, which contained no arginine residues other than the ones in the conserved motif, was methylated by PRMT1 and PRMT5, confirming that the arginines in this motif were indeed methylated by these enzymes (Fig 3.8B).

Due to the proximity of the arginine residues on the RG-rich motif, it was possible that steric hindrance could result in competition between the methylation of R109, R111 and R113. To test the hypothesis, two other peptides were synthesized to mimic arginine dimethylated E2F1 in cells. The first had an asymmetrically dimethylated arginine at residue 109, while the second had symmetrically dimethylated arginines at residues 111 and 113. These were subjected a ^{3}H-SAM methylation assay as described previously.

The results showed that peptide R109 (ADMA) was methylated by PRMT5 but not PRMT1, implying that the prior methylation of R109 had prevented PRMT1 from adding more methyl groups to the residue. The methylation by PRMT5 was sub-optimal compared to E2F1 peptide, which was consistent with the hypothesis that steric hindrance by the neighbouring ADMA on R109 was partially inhibiting methylation of R111 and R113 by PRMT5.

The peptide R111/113 (SDMA) was methylated by PRMT1 but not PRMT5, which implied that prior methylation of R111 and R113, had prevented PRMT5 from further methylating these residues. Methylation by PRMT1 was also sub-optimal compared to E2F1 peptide, again consistent with the hypothesis of steric hindrance between neighbouring arginine residues.

A control experiment using an E2F1-derived peptide with all its arginines replaced with lysines (peptide KKK) was unable to be methylated by either PRMT1 or PRMT5, further eliminating any possibility that the enzymes were methylating arginine residues outside the RG-rich motif.

Figure 3.8 Methylation of modified E2F1-derived peptides

A

E2F1 : AESSGPA **R** G **R** G **R** HPGKG
R109 (ADMA) : AESSGPA **(R)**G **R** G **R** HPGKG, where **(R)** is asymmetrically dimethylated
R111/113 (SDMA) : AESSGPA **R** G**(R)**G**(R)** HPGKG, where **(R)** symmetrically dimethylated
KKK : AESSGPA **K** G **K** G **K** HPGKG

B

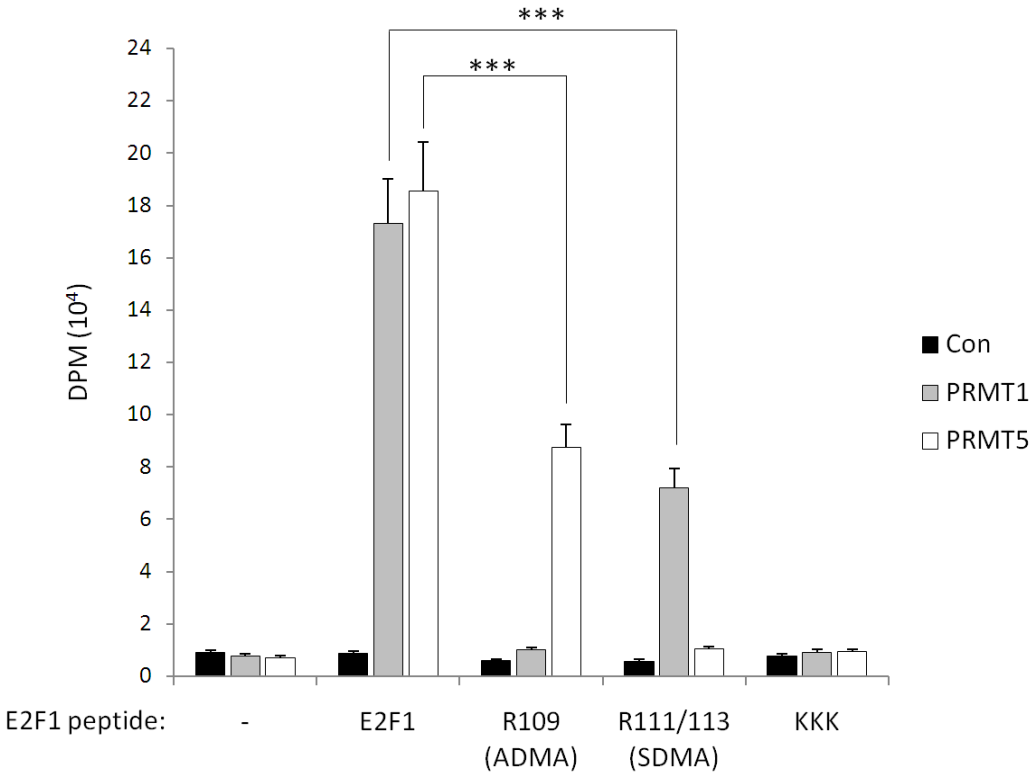

(**A**) 17-residue peptides corresponding to the putative E2F1 arginine methylation region were chemically synthesized. *E2F1* represents unmethylated E2F1; *R109 (ADMA)* represents E2F1 asymmetrically dimethylated at R109; *R111/113 (SDMA)* represents E2F1 symmetrically dimethylated at R111 and R113; *KKK peptide* represents mutant E2F1 with arginine to lysine substitutions at R109, R111 and R113.

(**B**) Incorporation of ^{3}H methyl groups measured in disintegrations per minute (DPM). Active recombinant enzymes HA-PRMT1 or FL-PRMT5 were incubated with the above peptides in methylation assays with ^{3}H-SAM as co-substrate. Negative control is shown in black; HA-PRMT1 is shown in grey; and FL-PRMT5 is shown in white. The enzymes or substrates alone were used as negative controls; where (–) represents absence of peptide. Data shown are means of 3 independent experiments with error bars representing standard deviation; *** $p < 0.001$.

3.5 Confirmation of methylated E2F1 arginine residues in cells

To confirm the positions of methylated arginine residues in cells, another set of E2F1 mutants were created which could be expressed in mammalian cells. These protein derivatives were fused with HA-tag to allow distinction from endogenous E2F1. A fractionation experiment was performed to determine whether these amino acid substitutions affected intracellular localisation of E2F1 (Fig 3.9). GAPDH was used as the marker for the cytosolic fraction (Mazzola and Sirover, 2003), while PCNA was used as the marker for the nuclear fraction (Connolly and Bogdanffy, 1993) . The results indicate that arginine to lysine substitutions had no effect on nuclear localisation of E2F1, excluding the possibility of attributing any changes to methylation, transcriptional activity or phenotype to differences in cellular localisation.

These E2F1 mutants were then immunoprecipitated in cells and probed for arginine dimethylation (Fig 3.10). Wild-type E2F1, which acted as the positive control, displayed both ADMA and SDMA signals (Fig 3.10B, lane 6). The absence of ADMA signals in R109K and KKK implied that asymmetrical dimethylation occurred at E2F1 arginine residue 109 (Fig 3.10B, lanes 9 and 21). SDMA signals were absent in the R111/113K and KKK mutants (Fig 3.10B, lanes 18 and 21) but not R111K and R113K mutants (lanes 12 and 15), implying that symmetric dimethylation occurred on both arginine residues in the E2F1 RG-rich motif. These results were consistent with the methylation assays performed *in vitro* (Fig 3.7).

Figure 3.9 Cellular localisation of E2F1 mutants

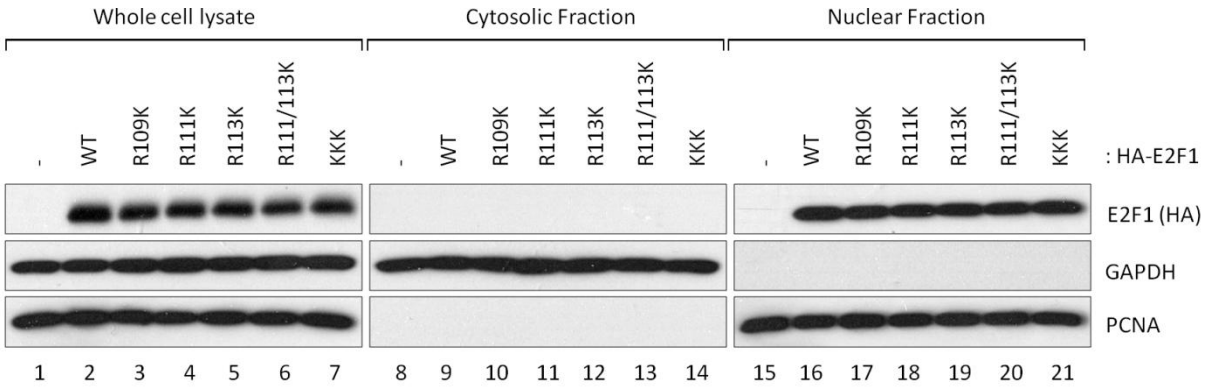

Cell fractionation showing relative protein levels in the cytoplasm and nucleoplasm. SAOS2 cells were transfected with 1 µg empty vector control (–) or HA-E2F1 plasmids as indicated. The plasma membrane was gently lysed using a mild detergent while sparing the nuclear membrane. Fractionation was performed by centrifugation and removal of the cytosolic fraction. The nuclear membrane was subsequently disrupted using a slightly harsher detergent. Immunoblotting was performed with the indicated antibodies. GAPDH was used as the loading control for cytosolic fraction while PCNA served as the loading control for nuclear fraction.

Figure 3.10 Arginine dimethylation of E2F1 mutants in cells

A

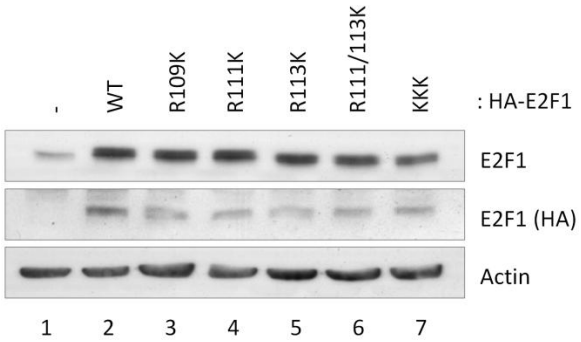

B

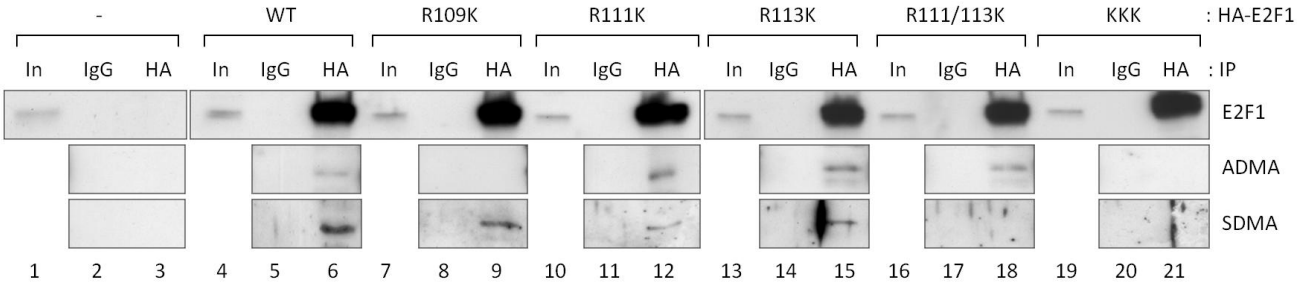

(**A**) Relative expression of transfected E2F1 mutant derivatives. SAOS2 cells were transfected with ~1 µg empty vector control (–) or HA-E2F1 plasmids as indicated and the corresponding lysates were immunoblotted with HA or E2F1 antibodies. Actin was used as loading control.

(**B**) Arginine methylation signals in different E2F1 mutant derivatives. Cell lysates from (A) were subjected to immunoprecipitation using control IgG or HA antibodies, followed by immunoblotting with E2F1, ADMA or SDMA antibodies as indicated. E2F1 protein input levels (In) are shown.

3.6 Chapter summary

Studies have shown that PRMT1 and PRMT5 are the major methyltransferases that target glycine and arginine (GAR)-rich motifs (Yang and Bedford, 2013). The results in this chapter show that a conserved E2F1 RGRGR motif is also a target of these two PRMTs, but distinction lies in the location of the residues and type of dimethylation. From the evidence gathered, PRMT1 asymmetrically dimethylates R109, while PRMT5 symmetrically dimethylates R111 and R113. The results also suggest competition between PRMT1 and PRMT5 for methylation in the E2F1 RG-rich motif, most likely as a result of steric effects between the closely situated arginine residues (Fig 3.11).

Figure 3.11 Competitive binding and methylation by PRMT1 and PRMT5

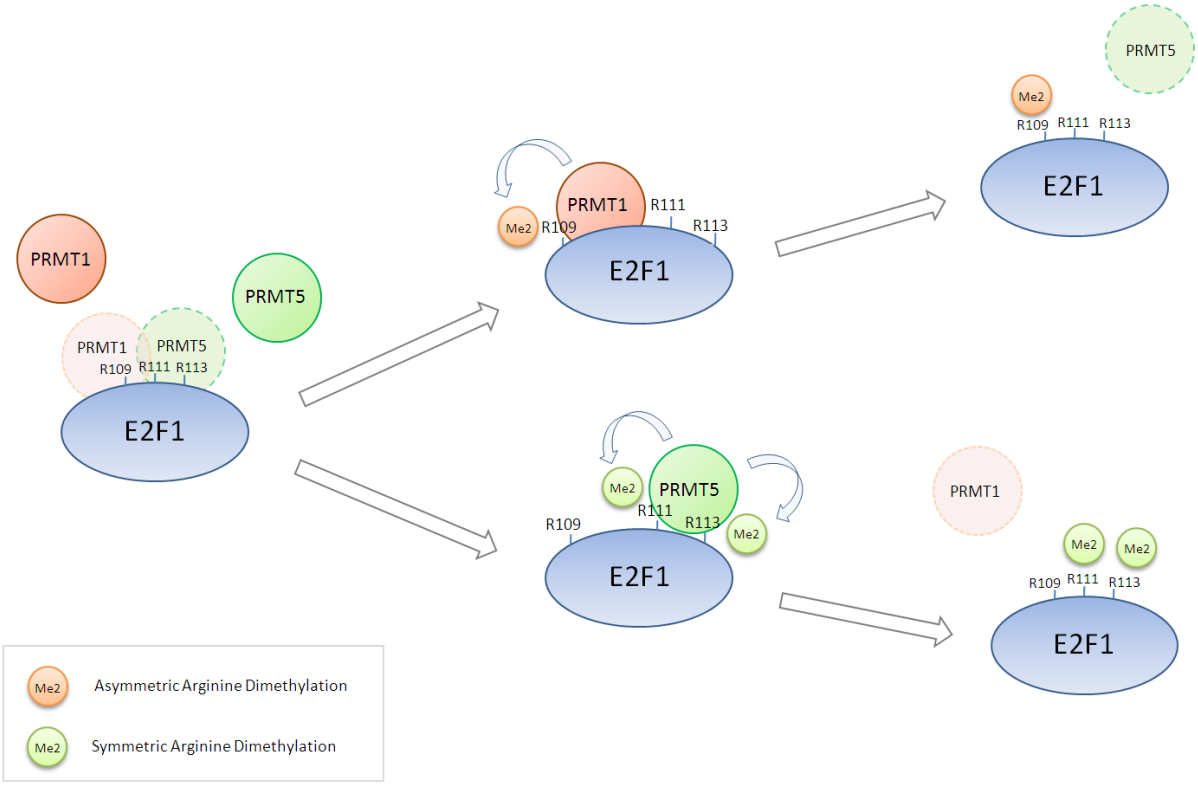

Due to the close proximity of R109, R111 and R113 (the putative sites for E2F1 methylation), PRMT1 and PRMT5 might encounter steric competition when they try to interact with E2F1. In addition, the presence of dimethylated arginines on neighbouring residues could also bring about some degree of spatial constrain, which may reduce binding between E2F1 and PRMT1 or PRMT5.

4. Molecular properties of arginine methylated E2F1

Post-translational modifications such as methylation often result in changes to protein properties. The addition of dimethyl groups to arginine confers additional bulk and hydrophobicity, which may affect the molecular properties of E2F1. The transcriptional activity of E2F1 is mainly regulated by its protein levels and DNA binding. In this chapter, I shall describe how E2F1 arginine methylation by PRMT1 and PRMT5 could influence protein stability and promoter affinity, leading to changes in its transcriptional activity.

4.1 Changes in E2F1 protein stability due to arginine methylation

E2F1, it was possible that the methyl groups affected E2F1 protein stability. To investigate, cycloheximide was used to inhibit protein synthesis and rate of protein degradation was visualised by immunoblot.

Following the depletion of PRMT1 and/or PRMT5 (Fig 4.1A) and the addition of cycloheximide, endogenous E2F1 protein levels were traced for 8 hours (Fig 4.1B). The percentage change of E2F1 relative to pre-addition of cycloheximide was plotted (Fig 4.1C) and the half-life was calculated (Fig 4.1D). The results show that PRMT1 depletion decreased the half-life of E2F1, implying that ADMA marks protect E2F1 from protein degradation. In contrast, PRMT5 depletion increased E2F1 half-life, implying SDMA marks promotes E2F1

degradation. Surprisingly, co-depletion of PRMT1 and PRMT5 led to the greatest increase in E2F1 stability, suggesting that the complete lack of arginine methylation prevents E2F1 from recognition by the protein degradation complex.

To confirm the involvement of the E2F1 RG-rich motif in regulating protein stability, HA-tagged E2F1 mutant plasmids were transfected into cells and treated with cycloheximide. The expressed E2F1 mutants were visualised by immunoblot with antibodies against HA to prevent cross-reaction with endogenous E2F1 (Fig 4.2A). Relative changes in E2F1 protein levels were plotted (Fig 4.2B) and the half-lives calculated (Fig 4.2C). The results show that on average, ectopically expressed E2F1 tend to have shorter half-lives compared to endogenous E2F1. This may be caused by the natural tendency of cells to increase the degradation rate of exogenous or highly over-expressed proteins. The R109K mutant had a shorter half-life compared to wild-type E2F1, implying that methylation of that residue was important for increasing E2F1 stability. In contrast, the R111/113K had a longer half-life than wild-type E2F1, implying that methylation of R111 and R113 increased E2F1 degradation. The KKK mutant had the longest half-life of all, implying that the complete absence of methylation in the E2F1 RG-rich motif gave E2F1 protection from the protein degradation machinery. These findings were consistent with the experimental observations in endogenous E2F1 (Fig 4.1), again supporting a model in which methylation within the RGRGR motif by PRMT1 and PRMT5 can impact on E2F1 stability and turnover in cells.

Figure 4.1 Endogenous E2F1 stability upon PRMT depletion

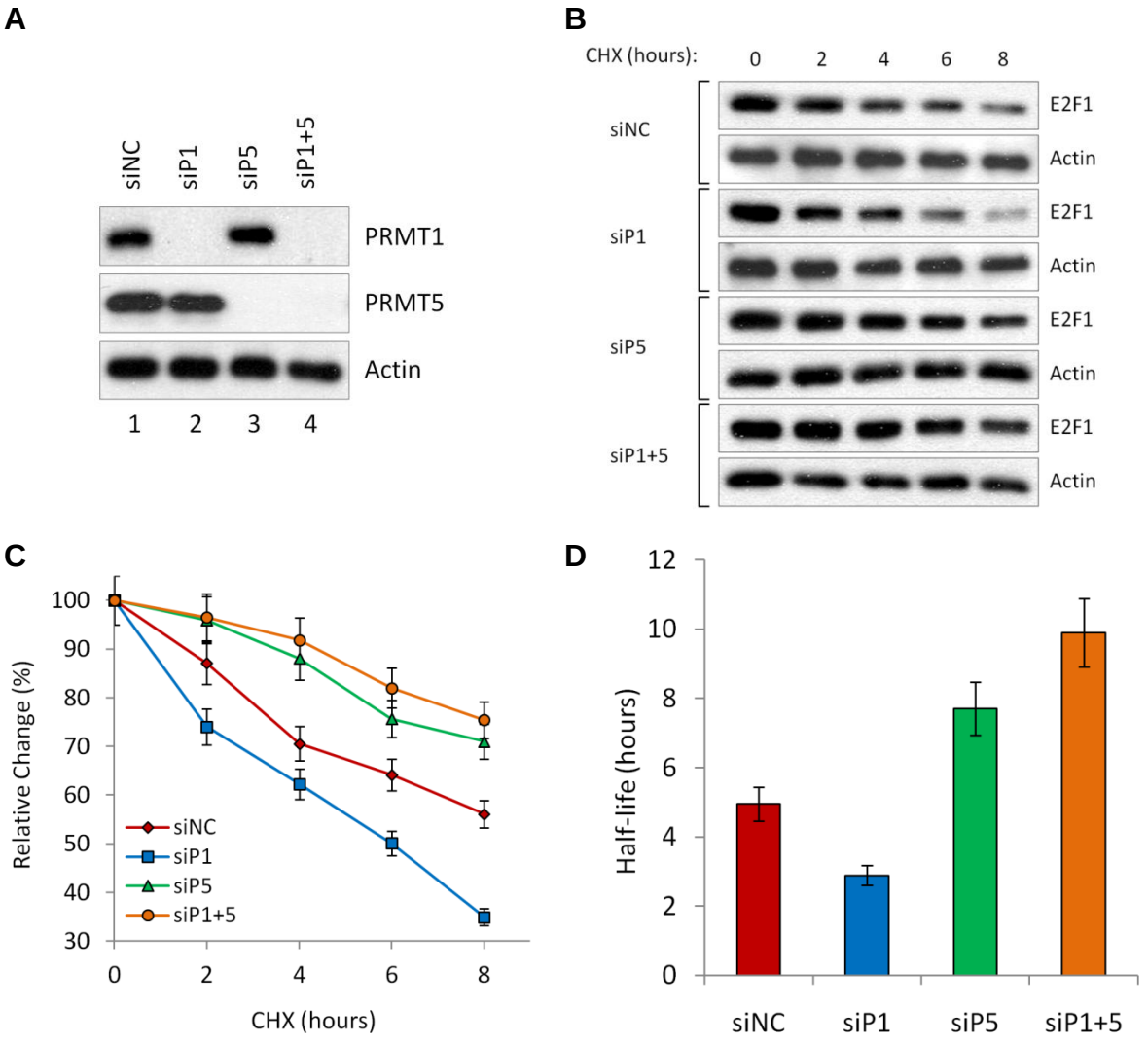

(**A**) PRMT1 and PRMT5 protein levels upon siRNA-mediated depletion. SAOS2 cells were treated with 50 nM non-targeting control (siNC), PRMT1 (siP1) and/or PRMT5 (siP5) and harvested after 48 hours. The corresponding cell lysates were immunoblotted with the indicated antibodies to assess relative protein levels. Actin was used as loading control.

(**B**) Endogenous E2F1 levels upon inhibition of protein synthesis. 100 µg/ml of cycloheximide was added to cells 48 hours after siRNA treatment as in (A). The cells were harvested at 0, 2, 4, 6 and 8 hours post-cycloheximide addition. The corresponding lysates were immunoblotted with antibodies against E2F1. Actin was used as loading control.

(**C**) Quantitation of E2F1 protein levels shown as percentage change relative to cycloheximide pre-treatment.

(**D**) E2F1 protein half-life calculated from data plotted in (C). Data shown are means of 3 independent experiments with error bars representing standard deviation.

Figure 4.2 Protein stability in E2F1 mutants

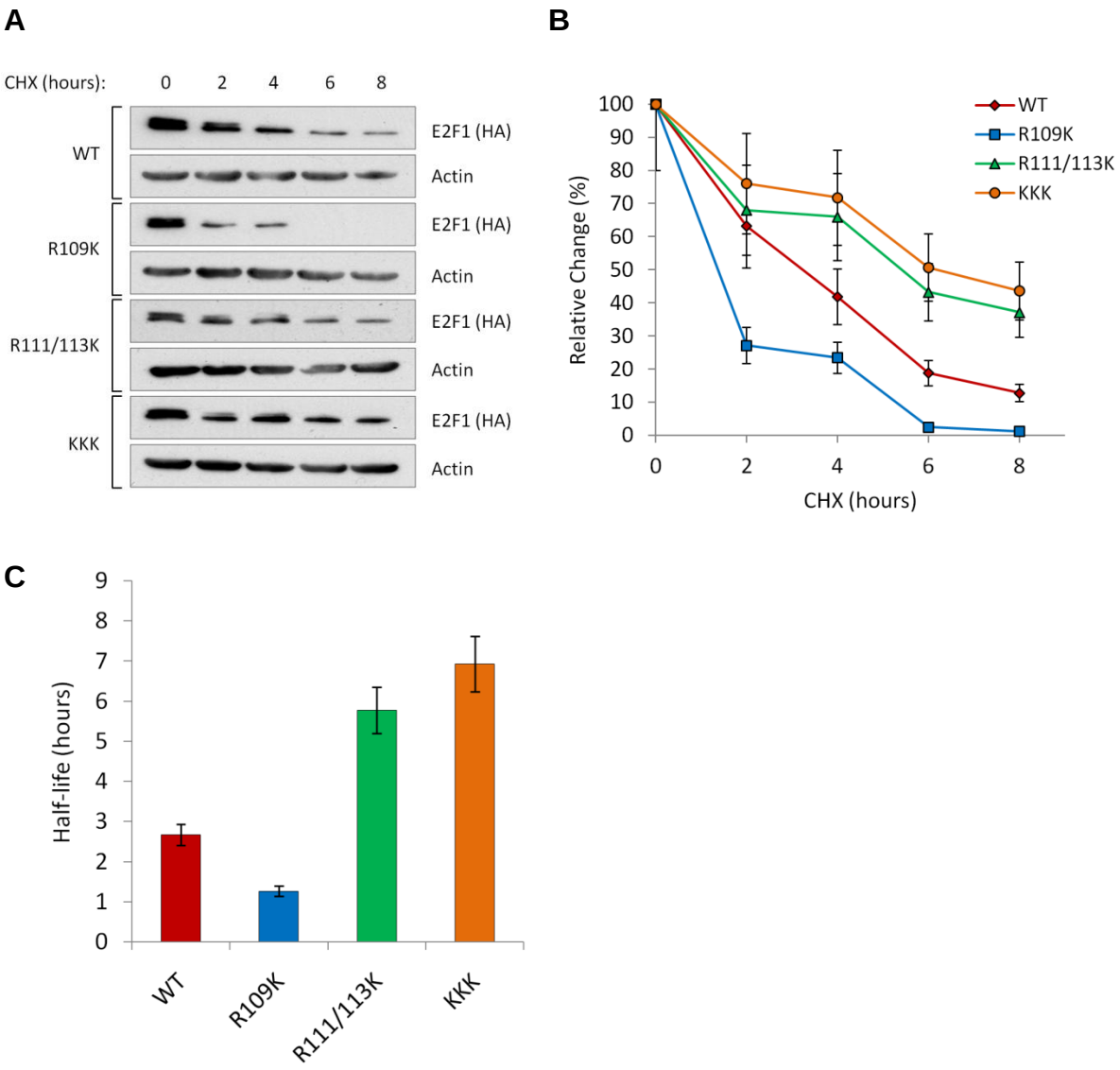

(**A**) Levels of E2F1 mutant derivatives upon inhibition of protein synthesis. SAOS2 cells were transfected with ~ 1 µg of HA-E2F1 plasmids for 72 hours. 100 µg/ml of cycloheximide was then added and cells were harvested at 0, 2, 4, 6 and 8 hours post-treatment time points. The corresponding lysates were immunoblotted with antibodies against HA. Actin was used as loading control.

(**B**) Quantitation of E2F1 protein levels shown as percentage change relative to cycloheximide pre-treatment.

(**C**) HA-E2F1 protein half-life calculated from data plotted in (B). Data shown are means of 3 independent experiments with error bars representing standard deviation.

4.2 Arginine methylation affects E2F1 recruitment to ubiquitin ligase complex

In the natural course of the cell cycle, E2F1 is degraded by the proteasome complex during the S/G2 transition. To be targeted for degradation, it is necessary for E2F1 protein to be polyubiquitinated. This is carried out by an ubiquination system comprising three enzymes, E1, E2 and E3 (Fig 4.3A). The ubiquitin-activating enzyme (E1) activates free ubiquitin in an energy-dependent process through the hydroxylation of adenosine triphosphate (ATP). The protein-bound ubiquitin is then transferred to an ubiquitin-conjugating enzyme (E2). The ubiquitin ligase (E3) subsequently catalyses the ubiquitin transfer from E2 to substrate. The E3 ligase is an enzyme complex comprising Skp1, CUL1 and F-box protein; with Skp1 and CUL1 providing structural scaffolding, while the F-box protein conferring substrate specificity. It has been reported that Skp2 is the F-box protein that specifically targets E2F1 protein for ubiquitination and degradation (Marti et al., 1999). As E2F1 degradation was linked to Skp2 binding, it was possible that changes in arginine methylation could affect the interaction of these two proteins.

To test this hypothesis, E2F1 mutants were expressed in cells and immunoprecipitated with HA antibodies. The immunoblot results showed that Skp2 had an increased interaction with R109K compared to wild-type E2F1. This coincided with an increase in SDMA and depletion of ADMA signals. In contrast, Skp2 bound less strongly to R111K, R113K and R111/113K, which correlated with stronger ADMA and weaker SDMA signals. Interestingly, the Skp2 interaction was almost abolished in the KKK mutant, which did not contain any ADMA or SDMA

marks. These results indicate that E2F1-Skp2 binding had a positive correlation with SDMA, but a negative correlation with ADMA. It is likely that SDMA marks on the RG-rich motif help recruit E3 ligase to E2F1, thus promoting its ubiquinination and degradation. The ADMA marks may exert their influence by inhibiting SDMA through steric competition. This deduction is made because when ADMA was absent in both R109K and KKK, the removal of SDMA made a difference to Skp2 binding (Fig 4.3B, lanes 17 and 21); but when SDMAs were absent in both R111/113K and KKK, the depletion of ADMA did not cause significant changes to Skp2 binding (Fig 4.3B, lanes 20 and 21). This model is further supported by an experiment done by a fellow colleague, Dr Geng Liu, which showed that PRMT5 depletion led to a decrease in ubiquination marks on wild-type E2F1 but not the KKK mutant (Cho et al., 2012, Fig 3D). Together with the results in the previous section, these observations provide a mechanistic insight of how dimethylarginine marks on E2F1 could influence the recruitment of E3 ubiquitin ligase and cause changes to its protein stability and half-life.

Figure 4.3 Interaction between Skp2 and E2F1 mutants

A

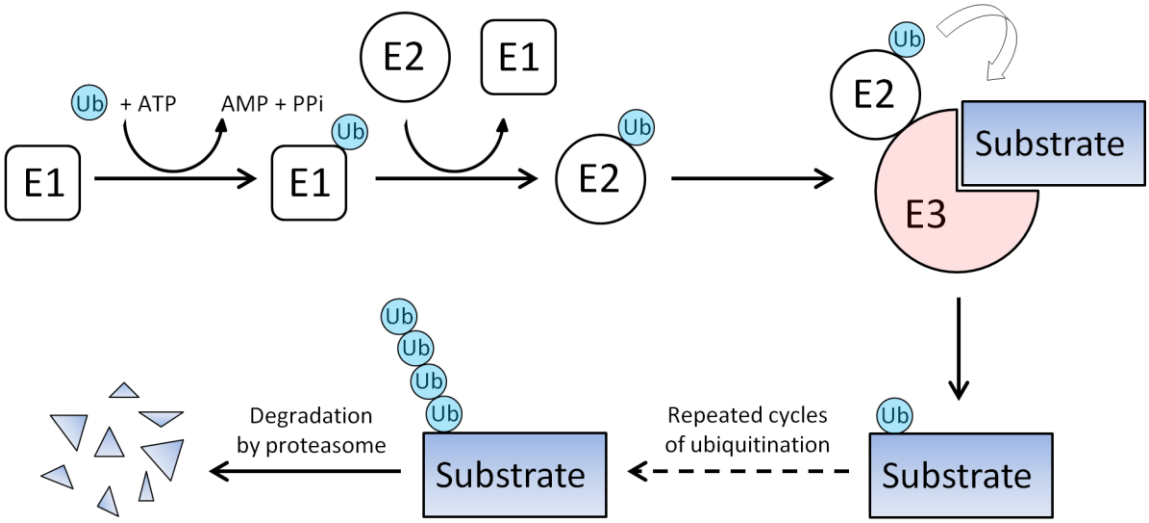

B

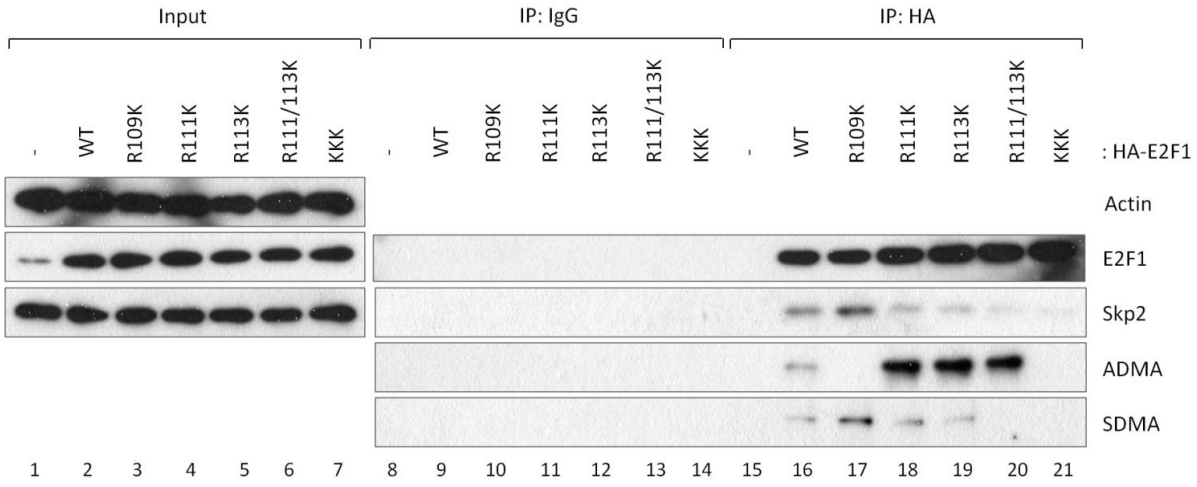

(**A**) The polyubiquitination process involves ubiquitin-activating enzyme (E1), ubiquitin-conjugating enzyme (E2) and ubiquitin ligase (E3). Ubiquitin ligase is a multi-protein complex composing Skp1, CUL1 and F-box protein. Skp2 is an F-box protein that confers binding specificity to E2F1.

(**B**) SAOS2 cells were transfected with ~1 µg empty vector control (–) or HA-E2F1 plasmids and the corresponding lysates were subjected to immunoprecipitation using control IgG or HA antibodies, followed by immunoblotting with the indicated antibodies. Input levels of the respective proteins are shown. Actin was used as loading control.

4.3 Depletion of PRMTs affects transcription of E2F1 target genes

To understand how arginine methylation could impact E2F1 target genes, immunoblotting was used to visualise their protein levels upon siRNA-mediated PRMT depletion (Fig 4.4A). PRMT1 depletion caused a slight decrease in E2F1 and apoptosis-related proteins Apaf-1 and p73, without major changes to cyclin E, CDC6 and DHFR (Fig 4.4A, lane 2). PRMT5 depletion led to upregulation of E2F1 and almost all E2F1 targets except CDC6 (Fig 4.4A, lane 3). Co-depletion of both PRMTs resulted in a similar effect as PRMT5 depletion alone (Fig 4.4A, lane 4).

Reverse-transcription polymerase chain reaction (RT-PCR) was used to visualise the mRNA levels of E2F1 target genes (Fig 4.4B) and quantitative RT-PCR (QPCR) was used to numerate the results (Fig 4.4C and D). The results show that PRMT1 depletion led to an overall downregulation in mRNA levels of E2F1 target genes, with pro-apoptotic targets such as Apaf-1 and p73 having a greater decrease than proliferative targets Cyclin E, CDC6 and DHFR. In contrast, PRMT5 depletion led to an overall upregulation in mRNA levels of E2F1 target genes, with pro-apoptotic targets having a greater increase compared to proliferative genes. Co-depletion of both PRMTs resulted in an overall increase in mRNA levels in a similar manner as PRMT5 depletion alone, but the magnitude was slightly smaller.

Together the results show that PRMT1 depletion, which prevents ADMA and promotes SDMA on E2F1, has a negative effect on the transcription of its target genes, including itself. PRMT5 depletion, which prevents SDMA and promotes ADMA on E2F1, has a positive effect on self-transcription and

transcription of its target genes. Since co-depletion of both PRMTs led to effects similar to PRMT5 depletion alone, it is possible that the removal of SDMAs from E2F1 is directly responsible for these transcriptional differences.

Figure 4.4 Transcription of E2F1 target genes upon PRMT depletion

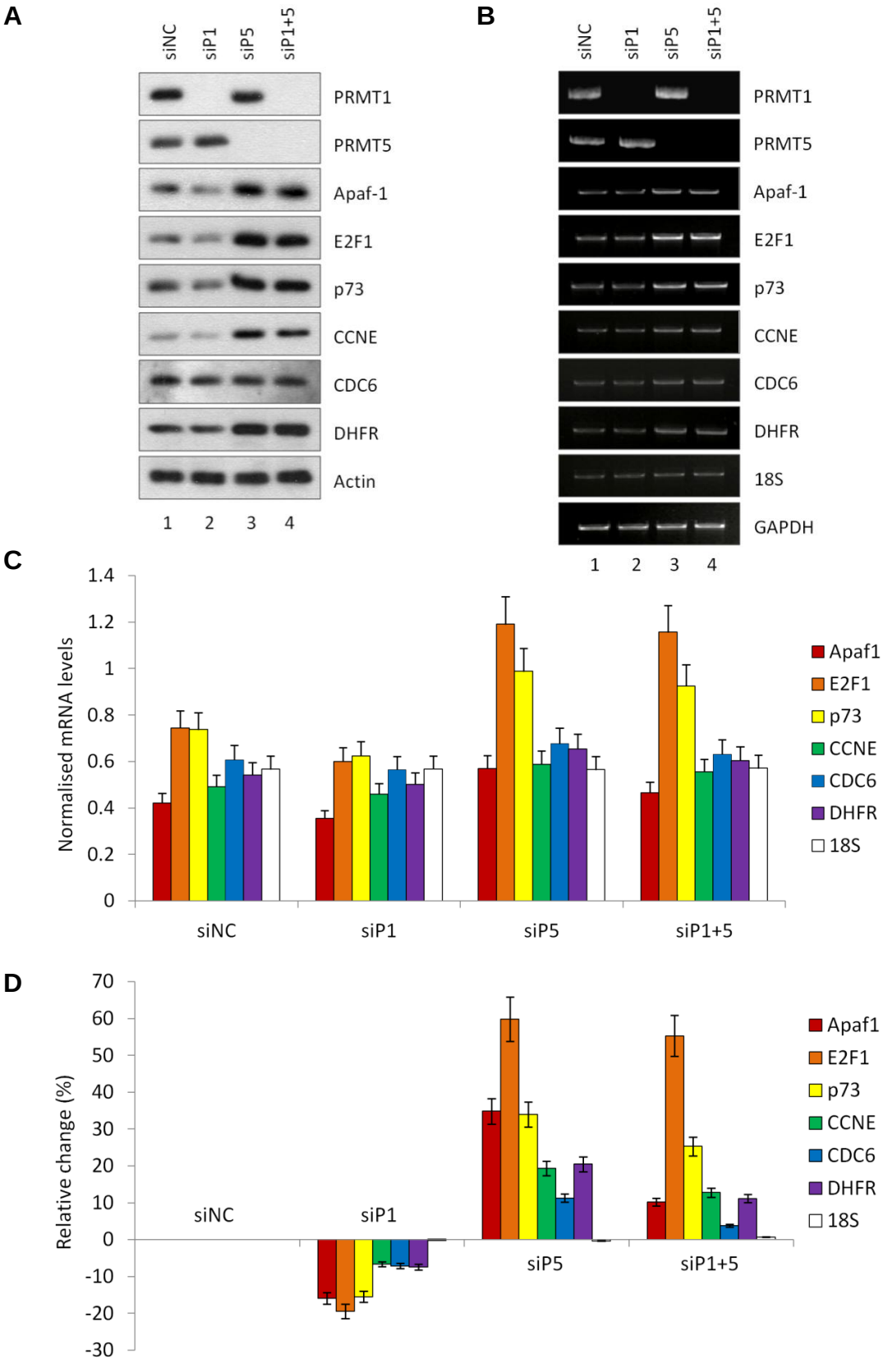

(**A**) Protein levels of E2F1 target genes upon PRMT1 and/or PRMT5 depletion. SAOS2 cells were treated with 50 nM non-targeting control (siNC), PRMT1 (siP1) and/or PRMT5 (siP5) and harvested after 48 hours. The corresponding cell lysates were immunoblotted with the indicated antibodies to assess relative protein levels. Actin was used as loading control.

(**B**) mRNA levels of E2F1 target genes upon PRMT1 and/or PRMT5 depletion. SAOS2 cells were treated under the same conditions as in (A) and the corresponding RNA levels were assessed by reverse transcription PCR. 18S rRNA and GAPDH mRNA were used as control.

(**C**) mRNA levels of E2F1 target genes quantified by real-time PCR. The results were normalised to GAPDH signals. 18S rRNA was used as control. Data shown are means of 3 independent experiments with error bars representing standard deviation.

(**D**) Percentage change in RNA levels relative to non-targeting siRNA control treatment. 18S rRNA was used as control.

4.4 Arginine methylation regulates E2F1 promoter binding and activity

Chromatin immunoprecipitation (ChIP) was used to assess the binding affinity of E2F1 to its target gene promoters. It was observed that PRMT1 depletion led to a slight decrease in E2F1 binding to the promoters of Apaf-1, E2F1, p73, cyclin E, CDC6 and DHFR, whereas PRMT5 depletion led to a visible increase in E2F1 binding to all six promoters (Fig 4.5A). Co-depletion of both PRMTs led to a phenotype similar to PRMT5 depletion alone. The negative control albumin was not an E2F1 target and showed no changes to E2F1 binding. Immunoblotting was used to visualise the efficiency of siRNA-mediated depletion (Fig 4.5B). However, due to the effects of arginine methylation on E2F1 degradation, the changes in E2F1 promoter binding may be complicated by differences in endogenous E2F1 protein levels.

To address this shortcoming, ChIP experiments were performed using transfected E2F1 mutants. Since the mutant proteins show different stabilities in cells, they were expressed at equivalent levels by carefully adjusting the amount of plasmids transfected. It was observed that the R109K mutant had a lower binding affinity to all six E2F1 target gene promoters compared to wild-type E2F1, whereas R111K, R113K, R111/113K and KKK mutants all showed increased binding. The double and triple arginine-to-lysine substitutions appeared to cause the greatest increase in E2F1 binding affinity, implying that arginine methylation of the E2F1 RG-rich motif may directly decrease promoter binding.

To determine how differences in promoter binding affected E2F1 transcription, reporter assays were performed in cells transfected with plasmids expressing E2F1-responsive promoters fused with luciferase genes. It was found that PRMT1 depletion caused a slight decrease in the promoter activities of Apaf-1, E2F1, p73, cyclin E, CDC6 and DHFR, whereas PRMT5 or co-depletion of both PRMTs led to at least twice the transcriptional activities (Fig. 4.7A). Similarly, expression of R109K resulted in a slight decrease in reporter activities in all six E2F1 target promoters compared to WT E2F1, whereas expression of R111K, R113K, R111/113K and KKK were associated with higher levels of reporter activities (Fig 4.8). The trends shown in the reporter assays closely followed that of the ChIP assays in Fig 4.5 and Fig 4.6.

Together, these results indicate that asymmetric dimethylation of R109 by PRMT1 upregulates transcription of E2F1 target genes by increasing its affinity to their promoters and enhancing their activities. Symmetric dimethylation of R111 and R113 by PRMT5 downregulates transcription of E2F1 target genes by decreasing its affinity to their promoters and inhibiting their activities. A complete absence of methylation at the E2F1 RG-rich motif led to a transcriptional activation similar to SDMA depletion, implying that the effects were mediated through SDMA rather than ADMA.

Figure 4.5 Promoter binding upon PRMT depletion

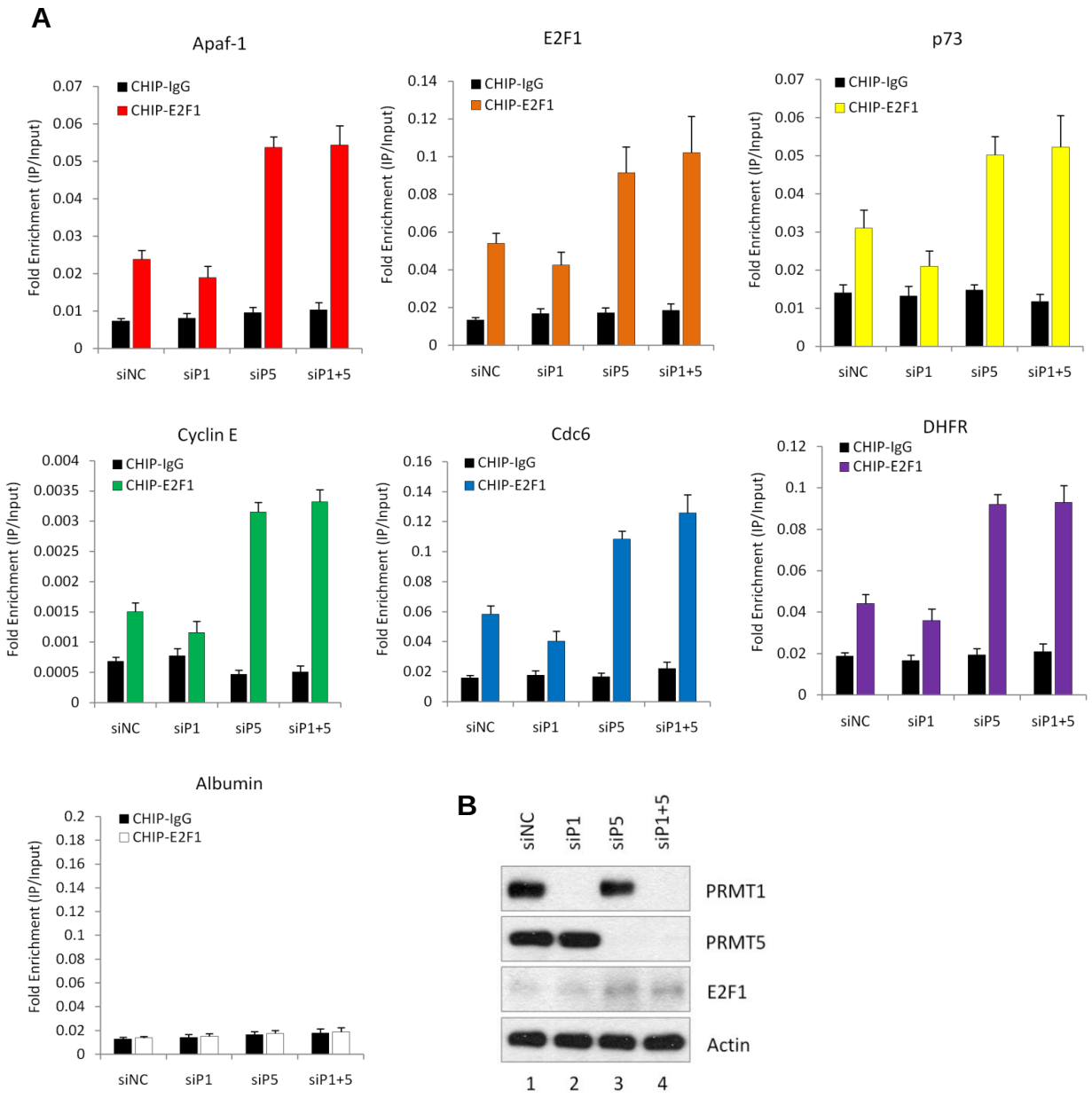

(**A**) E2F1 binding to target promoters assessed by ChIP. SAOS2 cells were treated with siRNA for 48 hours as previously described and immunoprecipitated with control IgG or E2F1 antibodies. The amount of bound chromatin was quantified by real-time PCR and normalised against their input levels. Albumin was used as ChIP negative control. Data shown are means of 3 independent experiments with error bars representing standard deviation.

(**B**) Cell lysates reserved for immunoblotting were probed with the indicated antibodies to assess relative protein levels. Actin was used as loading control.

Figure 4.6 Promoter binding of E2F1 mutants

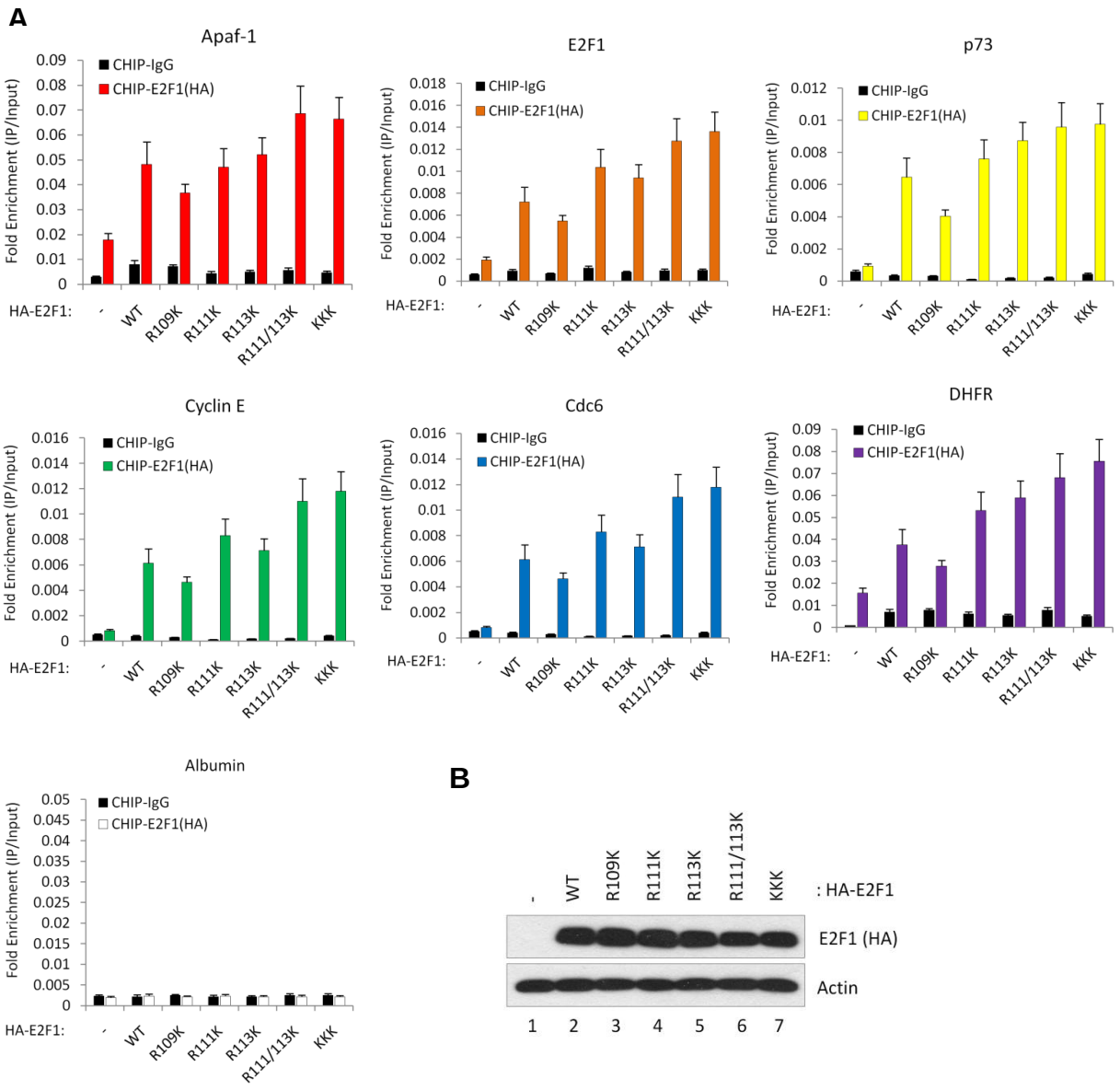

(**A**) E2F1 binding to target promoters assessed by ChIP. SAOS2 cells were transfected with ~1 µg empty vector control (–) or HA-E2F1 plasmids as previously described and immunoprecipitated with control IgG or E2F1 antibodies. The amount of bound chromatin was quantified by real-time PCR and normalised against their input levels. Albumin was used as ChIP negative control. Data shown are means of 3 independent experiments with error bars representing standard deviation.

(**B**) Cell lysates reserved for immunoblotting were probed with HA antibody to assess transfected E2F1 protein levels. Actin was used as loading control.

Figure 4.7 Promoter activities of E2F1 target genes upon PRMT depletion

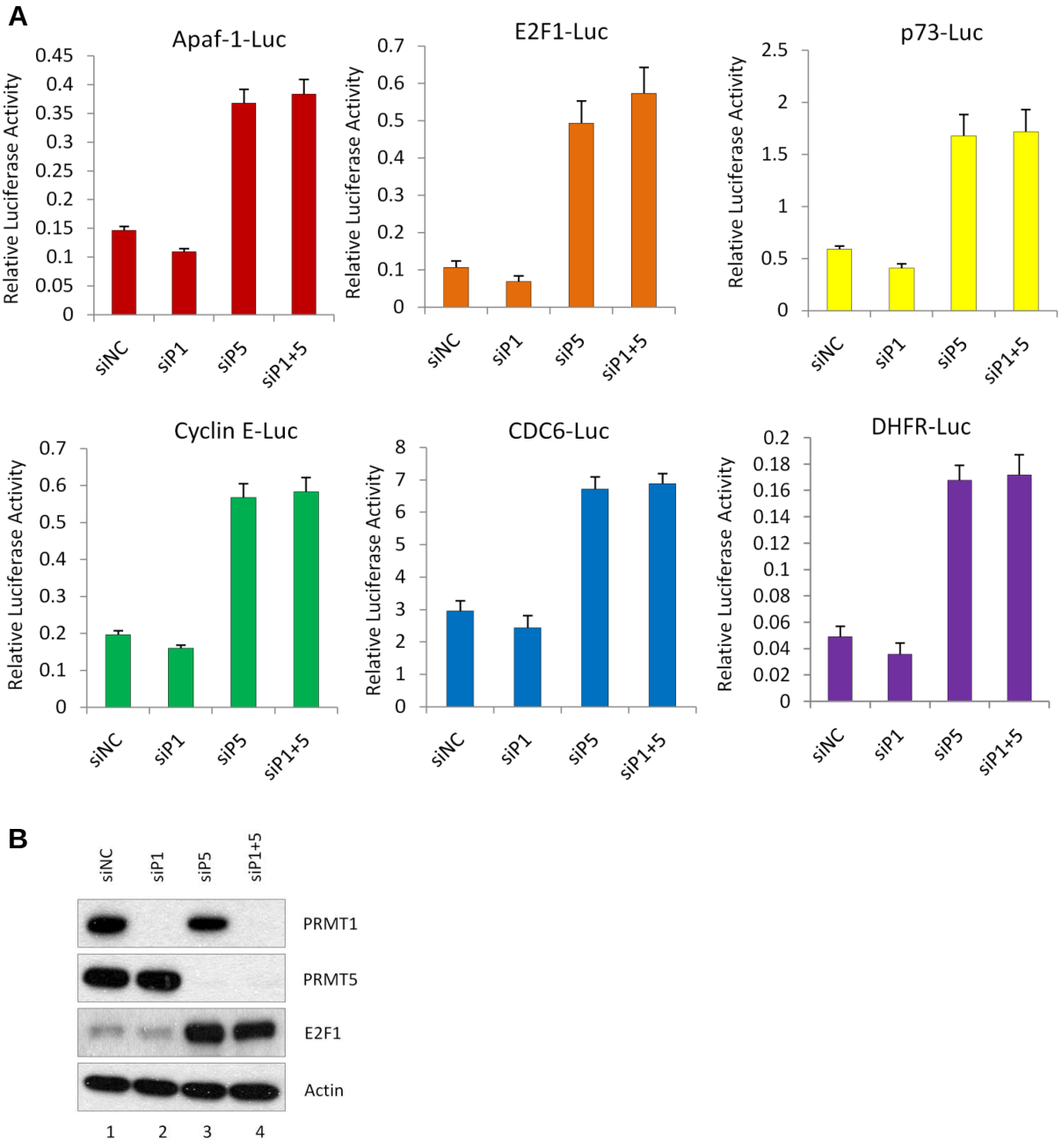

(**A**) SAOS2 cells were treated with siRNA as previously described and co-transfected with β-gal and the indicated promoter luciferase plasmids. The cells were harvested after 48 hours and the reporter activity was measured and normalised against β-gal. Data shown are means of 3 independent experiments with error bars representing standard deviation.

(**B**) Cell lysates reserved for immunoblotting were probed with the indicated antibodies to assess relative protein levels. Actin was used as loading control.

Figure 4.8 Promoter activities of E2F1 mutants

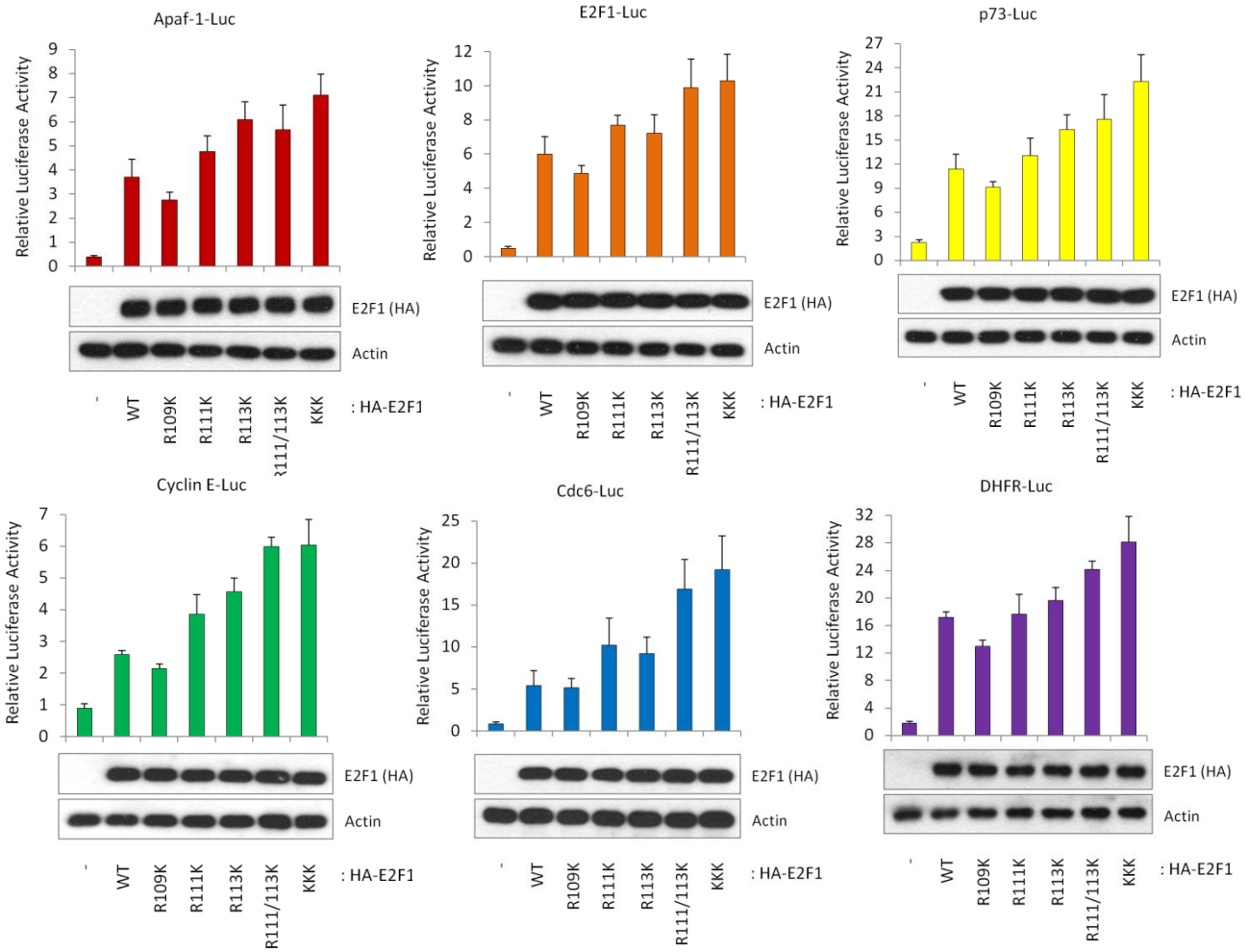

SAOS2 cells were transfected with ~1 µg empty vector control (–) or HA-E2F1 plasmids and co-transfected with β-gal and the indicated promoter luciferase plasmids. The cells were harvested after 48 hours and the reporter activity was measured and normalised against β-gal. Data shown are means of 3 independent experiments with error bars representing standard deviation. Cell lysates reserved for immunoblotting were probed with HA antibody to assess transfected E2F1 protein levels. Actin was used as loading control.

4.5 Chapter summary

After establishing PRMT1 and PRMT5 as the enzymes responsible for E2F1 methylation, it was observed that PRMT5 depletion caused an upregulation of E2F1. Stability assays involving the protein synthesis inhibitor cycloheximide revealed that SDMA marks on R111 and R113 decreases E2F1 half-life. This may be attributed to an increased interaction with Skp2, the substrate recognition component of the E3 ubiquitin ligase complex, which in turn caused ubiquitination and degradation of E2F1. In addition, the SDMA marks also enhance E2F1 binding to its target gene promoters, increasing their transcriptional activity, mRNA and protein levels. Inhibition of SDMAs on R111 and R113 can reverse these effects. This may be achieved partially by the steric hindrance of ADMA on R109, or completely by PRMT5 depletion. Experiments using E2F1 arginine-to-lysine point mutants suggest that the differences in E2F1 transcriptional activity is not entirely due to changes in E2F1 levels alone, since expression of equivalent levels of mutant E2F1 resulted in differences in promoter binding. Together, the results in this chapter show that type and position of arginine dimethylation on E2F1 modulates gene transcription by influencing its protein stability and DNA affinity (Fig 4.9).

Figure 4.9 Arginine dimethylation affects molecular properties of E2F1

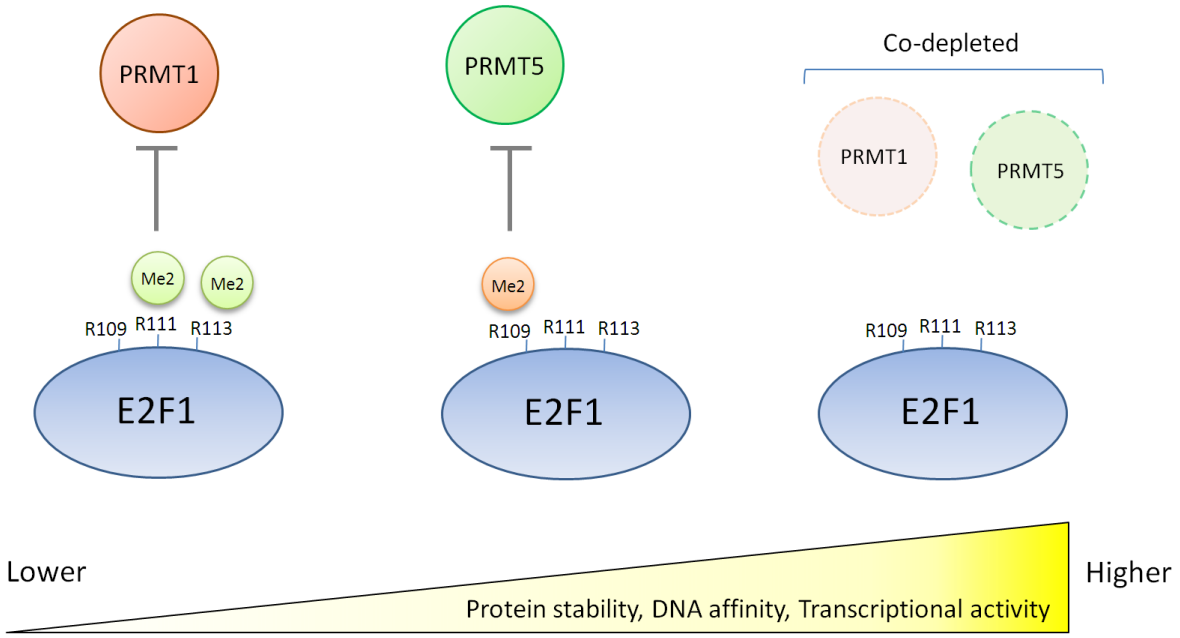

The type and position of arginine dimethylation on E2F1 modulates gene transcription by influencing its protein stability and DNA affinity. Symmetric dimethylation of R111 and R113 on E2F1 inhibits PRMT1 binding and recruits Skp2, which increases ubiquitination and degradation. Asymmetric dimethylation of R109 partially inhibits SDMA marks on R111 and R113 by sterically blocking PRMT5, which reduces Skp2 binding and increases protein stability. The abolishment of methylation on all three arginine residues, which may be achieved by siRNA-mediated depletion of PRMT1 and PRMT5, results in the greatest increase in stability. Experiments using E2F1 R-to-K mutants show that even under equivalent protein expression levels, arginine methylation can still affect transcriptional activity in a similar manner by modulating E2F1 binding affinity to its target gene promoters.

5. Phenotypic effects of E2F1 arginine methylation

In the previous chapter, I established that arginine dimethylation could affect transcription of E2F1 target genes through the modulation of E2F1 protein stability, promoter binding affinity and transcriptional activity. These E2F1 target genes are involved in a range of cellular processes such as cell cycle progression, DNA synthesis, differentiation, signal transduction and apoptosis. This chapter investigates how transcriptional changes caused by E2F1 arginine dimethylation translate to phenotypic responses such as cell proliferation rate and apoptosis.

5.1 E2F1 arginine methylation regulates cell growth

To test this idea, a colony formation assay experiment was performed on cells treated with PRMT1 and/or PRMT5 siRNA to visualize the effects of PRMT depletion on cell growth. After staining with crystal violet dye (Fig 5.1A), colony densities were quantified (Fig 5.1B) and relative percentage changes to control treatment were calculated and plotted (Fig 5.1C). It was observed that PRMT1 depletion led to an increase in cell growth relative to non-targeting control, whereas PRMT5 depletion or co-depletion of both PRMTs resulted in a 40-50% decrease compared to control. Co-depletion of E2F1 under the same conditions provided phenotypic rescue, implying that these changes were likely to be E2F1 dependent. As the colony assays only provided a snapshot of cell growth, adenosine triphosphate (ATP) assays, which measured metabolism activity in cells, were

used to determine the proliferation rates following PRMT depletion. The readings, measured in relative luminescence units, were plotted against time (Fig 5.2A), which allowed the doubling times (Fig 5.2B) and proliferation rates to be determined (Fig 5.2C). The relative protein levels of each condition are shown (Fig 5.2D). Again, these results indicate that PRMT1 depletion caused a slight increase in proliferation rate, whereas PRMT5 depletion led to a visible decrease, and the effect of co-depleting both PRMTs was similar to PRMT5 depletion alone. It appeared that the proliferation rate was negatively correlated to E2F1 levels and co-depletion of E2F1 resulted in reversal of the phenotypic changes, implying that the effects of PRMT depletion were E2F1 dependent. It is worth noting that the primary drawback of the ATP assay is that it measures overall metabolic rate and is thus unable to differentiate between increased cell number and increased metabolism in each individual cell. Nevertheless, the results in Fig 5.1 and Fig 5.2 both show similar trends which mutually support each other.

To map the specific E2F1 arginine residues responsible for the changes in cell growth, the colony assay experiment was repeated upon expression of different E2F1 mutants (Fig 5.3A). The colony densities were quantified (Fig 5.3B) and relative percentage changes to control treatment were calculated and plotted (Fig 5.3C) as before. In parallel, an ATP assay experiment was performed and the relative luminescence units were charted over time (Fig 5.4A). The doubling times (Fig 5.4B) and proliferate rates (Fig 5.4C) were calculated. The protein levels of the expressed E2F1 mutant derivatives in these experiments are shown (Fig 5.4D). When the ectopic E2F1 proteins were expressed at equivalent levels, the R109K

mutant had positive impact on cell density and overall metabolism as compared to WT E2F1. Expression of R111K and R113K had negative impacts on cell growth compared to WT E2F1, while R111/113K and KKK mutants resulted in the greatest decline in proliferation. These indicated that asymmetric dimethylation of E2F1 at R109 may limit proliferation, whereas symmetric dimethylation of E2F1 at R111 and R113 may increase cell growth. The observation that the KKK mutant resulted in the greatest decline in cell growth implied that the complete lack of methylation on the E2F1 RG-rich motif was strongly anti-proliferative.

Together with the results from the previous chapter, it appeared that removal of SDMAs from R111 and R113 caused an increase in E2F1 stability and transcriptional activity. The upregulation of pro-apoptotic genes Apaf-1 and p73 was observed to be greater than the activation of proliferative genes cyclin E, CDC6 and DHFR. The differential upregulation of these E2F1 target genes could attribute to the net inhibitory effect on cell growth. The role of ADMA in antagonizing SDMA was also witnessed and supported the hypothesis that it acted as a steric inhibitor of SDMAs.

Figure 5.1 PRMT depletion on cell growth

A

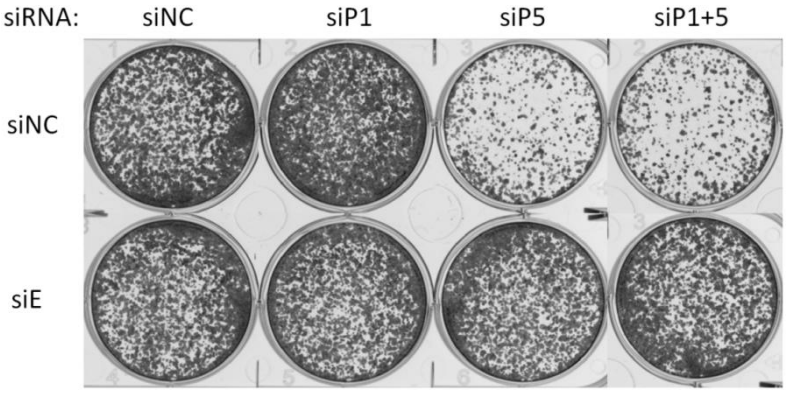

B

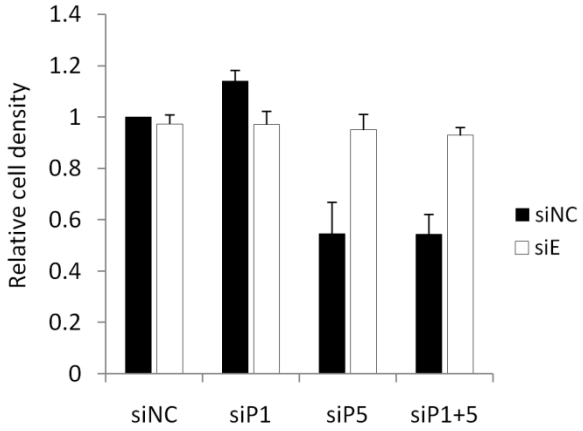

C

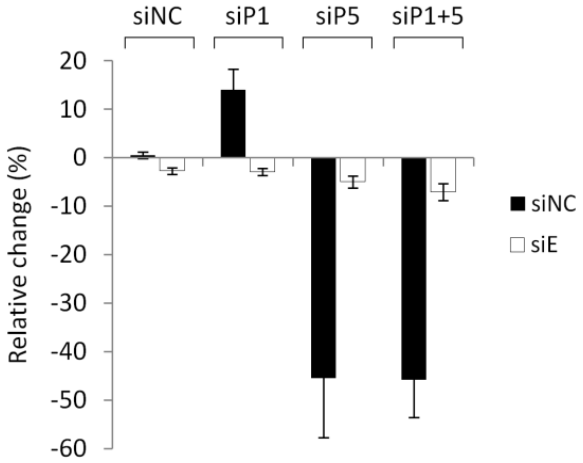

(**A**) SAOS2 cells were seeded at low density in 6-well plates (1000 cells per well) and treated with the indicated siRNA as previously described. The cells were harvested after 10 days and stained with crystal violet dye.

(**B**) Cell density of the above images relative to non-targeting siRNA control treatment. Quantitation was performed by Image J (National Institutes of Health). Non-targeting control (siNC) are represented by black bars and E2F1 depletion (siE) represented by white bars. Data shown are means of 3 independent experiments with error bars representing standard deviation.

(**C**) Percentage change in cell density relative to mock control treatment.

Figure 5.2 PRMT depletion on cell proliferation rates

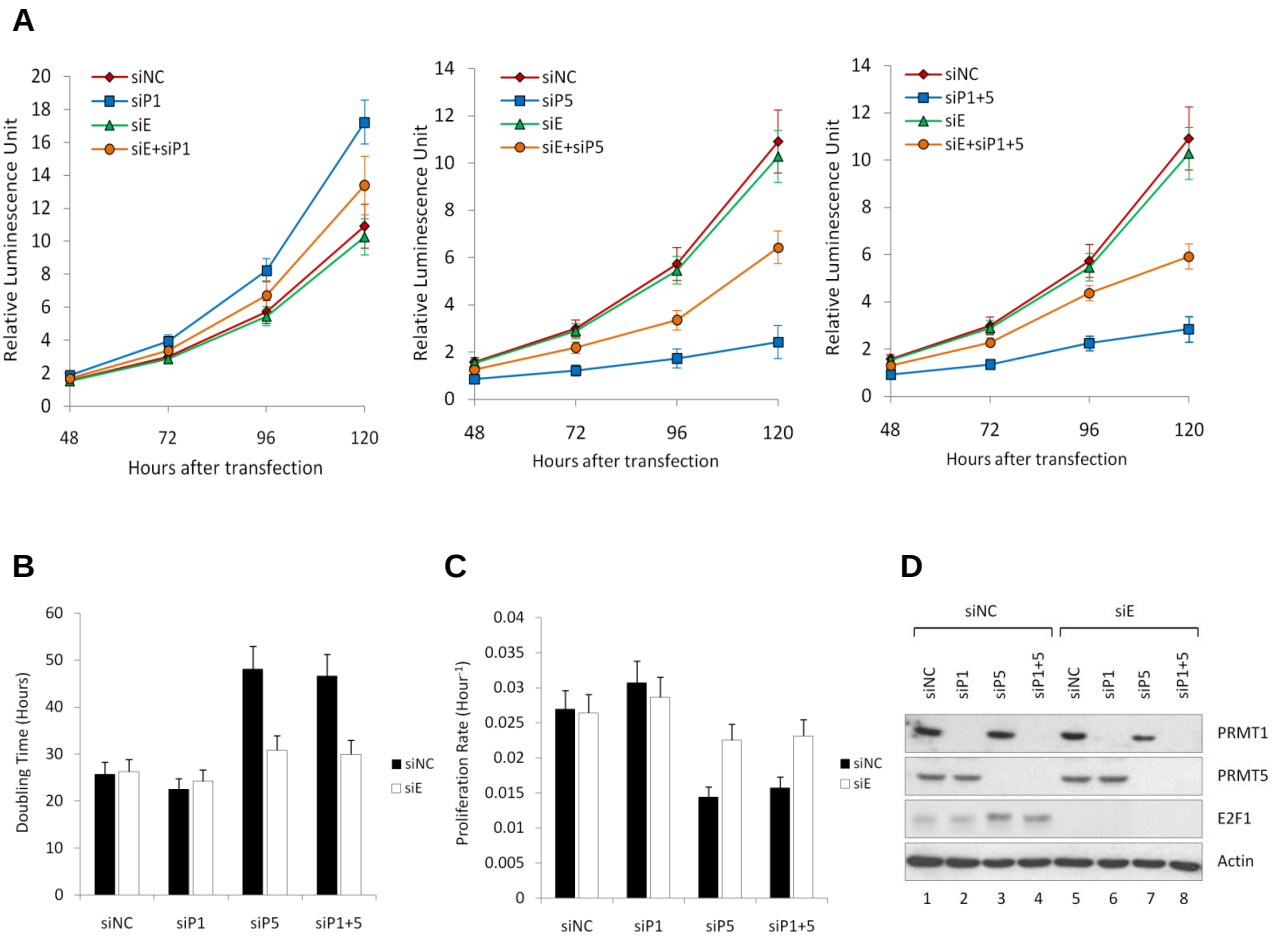

(**A**) ATP assay showing cell metabolism upon PRMT1 and/or PRMT5 depletion. SAOS2 cells were treated with the indicated siRNA as previously described and subjected to fluorometric ATP assay at 48, 72, 96 and 120 hours post-treatment time points. Data shown are means of 3 independent experiments with error bars representing standard deviation.

(**B**) Doubling time of cells calculated from the above data. Non-targeting control (siNC) are represented by black bars and E2F1 depletion (siE) represented by white bars.

(**C**) Proliferation rate calculated from the above data.

(**D**) Cell lysates reserved for immunoblotting were probed with the indicated antibodies to assess relative protein levels. Actin was used as loading control.

Figure 5.3 E2F1 mutants on cell growth

A

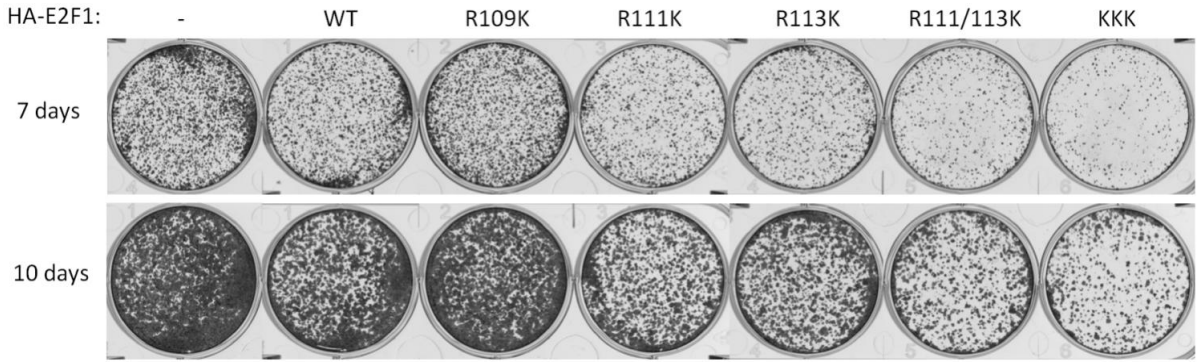

B

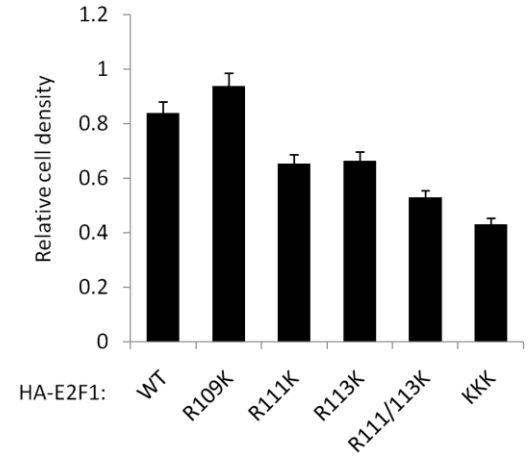

C

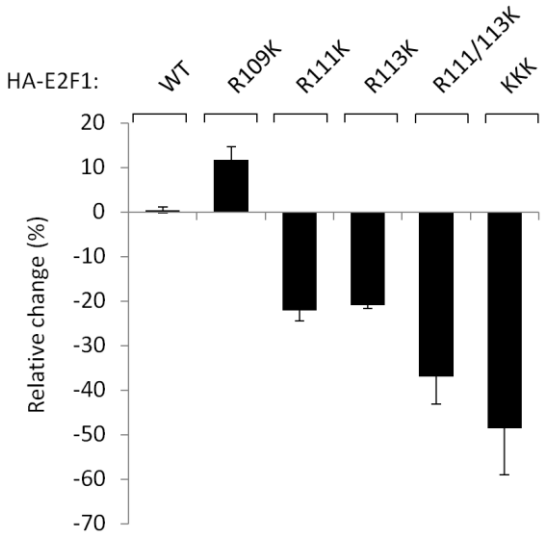

(**A**) SAOS2 cells were seeded at low density in 6-well plates (2000 cells per well) and transfected with ~1 µg empty vector control (–) or HA-E2F1 plasmids as previously described. The cells were harvested after 7 or 10 days post-transfection and stained with crystal violet dye.

(**B**) Cell density of the above images relative to empty vector control treatment. Quantitation was performed by Image J (National Institutes of Health). Data shown are means of 3 independent experiments with error bars representing standard deviation.

(**C**) Percentage change in cell density relative to wild type E2F1 treatment.

Figure 5.4 E2F1 mutants on cell proliferation rates

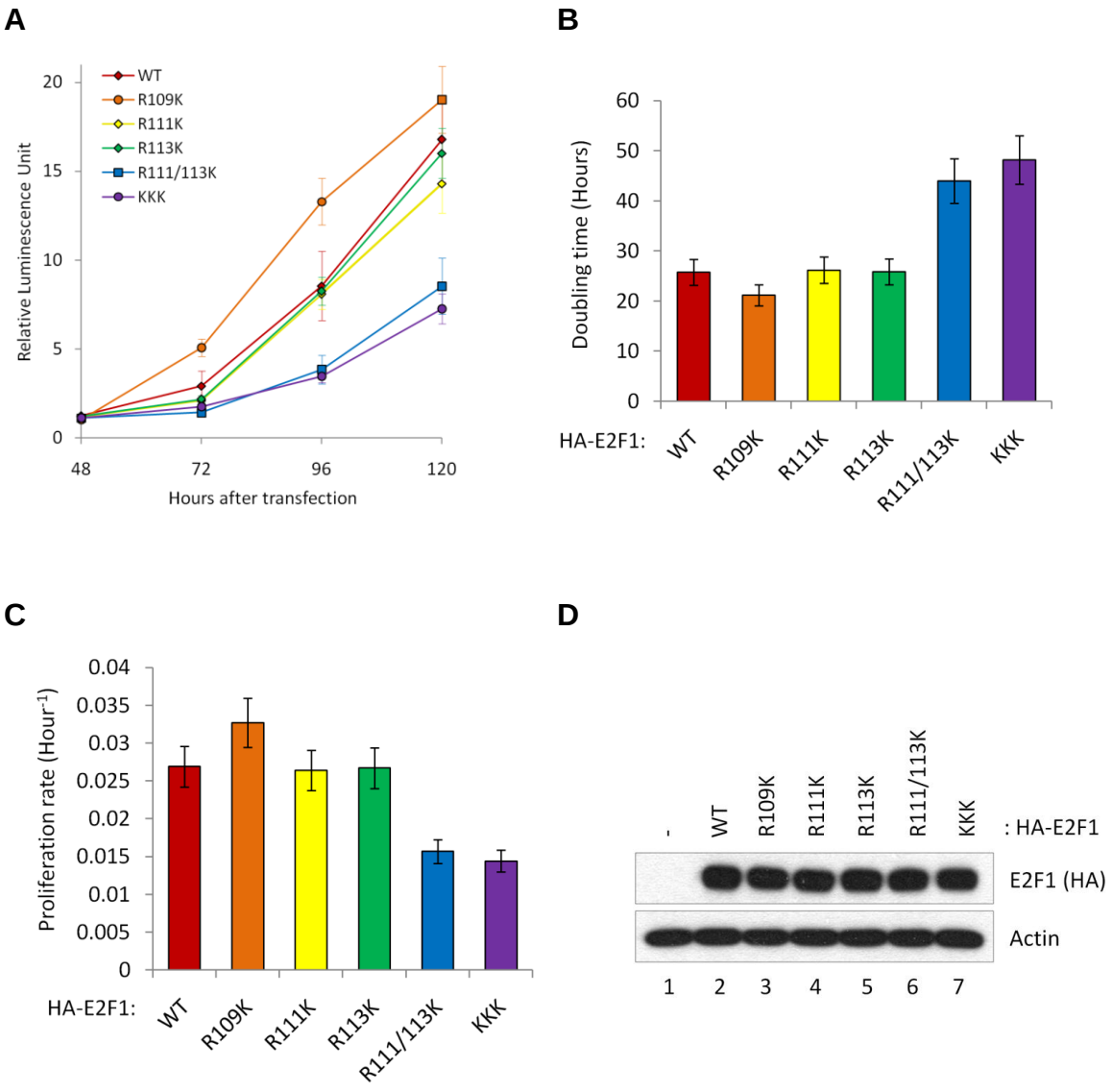

(**A**) ATP assay showing cell metabolism upon expression of E2F1 mutant derivatives. SAOS2 cells were transfected with the indicated HA-E2F1 plasmids as previously described and subjected to fluorometric ATP assay at 48, 72, 96 and 120 hours post-treatment time points. Data shown are means of 3 independent experiments with error bars representing standard deviation.

(**B**) Doubling time of cells calculated from the above data.

(**C**) Proliferation rate calculated from the above data.

(**D**) Cell lysates reserved for immunoblotting were probed with HA antibody to assess transfected E2F1 protein levels. Actin was used as loading control.

5.2 E2F1 arginine methylation during the cell cycle

It is known that the E2F1 transcriptional activity fluctuates throughout the cell cycle and our current findings suggest that changes in E2F1 activity may be influenced by arginine methylation. Since PRMT1 and PRMT5 have been discovered as the enzymes responsible for the asymmetric and symmetric dimethylation of E2F1 respectively, it was important to see how their levels vary during the cell cycle. To study the protein levels at different stages of the cell cycle, cells will first have to be synchronised at the G0/G1 phase. Serum starvation was chosen as the method of choice as it is a well-established strategy and did not involve addition of other drugs which may introduce artifacts.

As we follow through the cell cycle profile of SAOS2 cells after serum starvation release (Fig 5.5A, top 3 panels), it was observed that the degree of synchronisation was limited. This might be attributed to osteosarcoma cell lines having self-sufficiency in growth signals and insensitivity to anti-growth signals (Lundberg and Weinberg, 1998; Hanahan and Weinberg, 2011). The percentage of cells in G1 showed a modest decrease from 76.44% to 69.72%, while the percentage of cells in other phases increased slightly, signalling re-entry of a fraction of cells into the cell cycle. Upon closer observation, it was noticed that the percentage of cells in sub-G1 increased from 1.02% to 2.44% after re-entry into the cell cycle (Fig 5.5B). As DNA fragmentation is a marker of apoptosis, this observation suggests that re-entry into the cell cycle might be intricately linked to apoptotic activation as a result of increased E2F1 activity, although the effects may

be subtle. An immunoblot showing cleaved PARP, another marker of apoptosis, provided substantiation to this hypothesis (Fig 5.5C).

As the E2F1 level increases during cell cycle progression, transcriptional activation of both proliferative and apoptotic genes may occur, though at different magnitudes. In the absence of other factors, this resulted in a net effect of cell growth rather than death.

From the immunoblot, one could see an increase in PRMT1 and decrease in PRMT5 during progression of the cell cycle, and these correlated with increased E2F1 (Fig 5.5C, lanes 1, 4 and 7). This was consistent with previous results showing that asymmetric methylation by PRMT1 enhanced E2F1 stability whereas symmetric methylation by PRMT5 promoted E2F1 degradation. To substantiate, siRNA-mediated depletions of PRMT1 and PRMT5 were performed in parallel and the results led to the same conclusion (Fig 5.5C).

Figure 5.5 PRMT depletion in synchronised cells

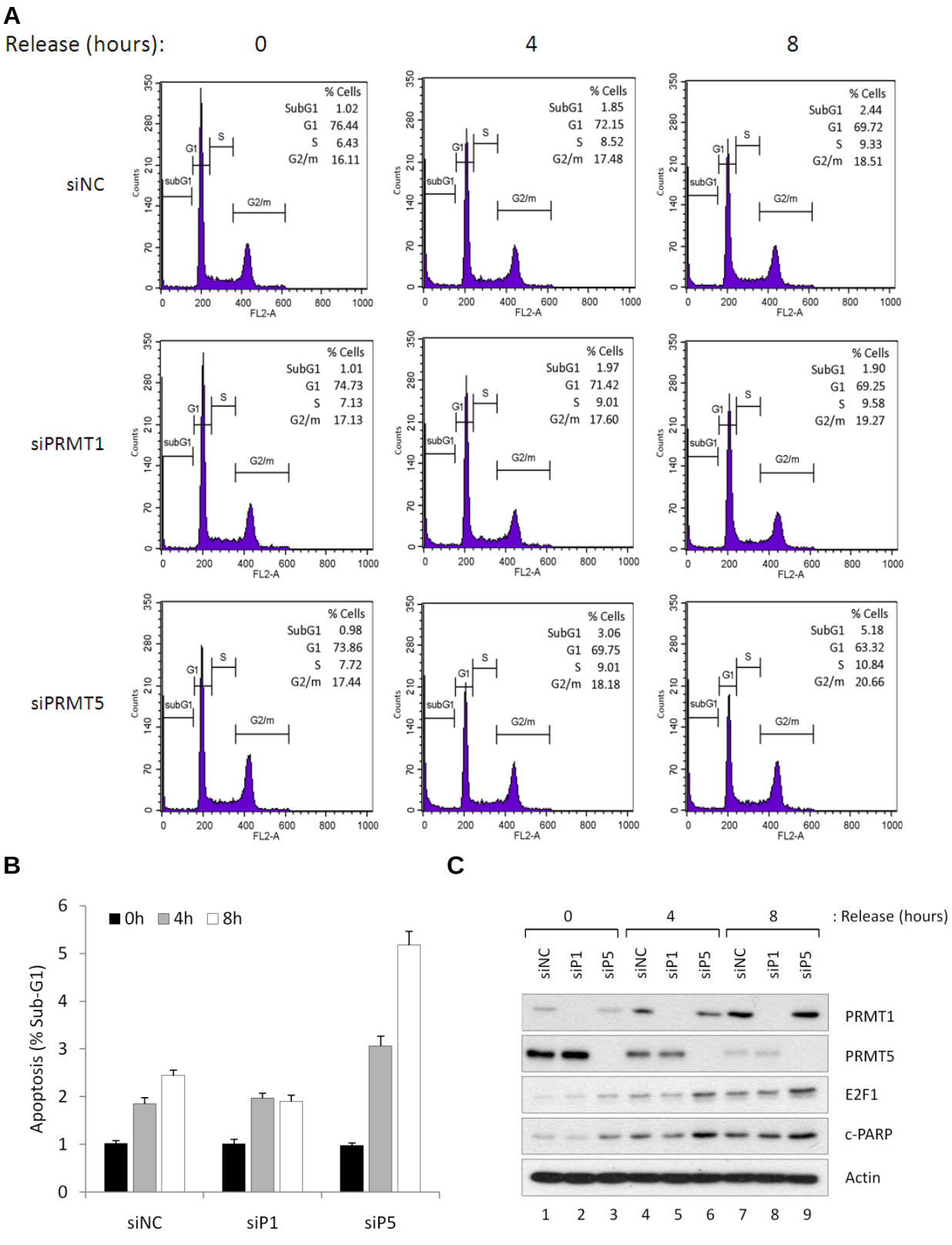

(**A**) Cell cycle profiles of cells synchronised through serum starvation under PRMT1 or PRMT5 depleted conditions. SAOS2 cells were treated with the indicated siRNA as previously described and incubated in DMEM without serum for 72 hours to synchronize them at G0/G1. Thereafter, 10% fetal bovine serum was introduced to re-stimulate the cell cycle. The cells were harvested at 0, 4 and 8 hour post-release time points and analysed by flow cytometry.

(**B**) Level of apoptosis as percentage of cells in sub-G1. Results were plotted using the above data. The 0, 4 and 8 hours post-serum release time points are represented in black, grey and white respectively. Data shown are means of 3 independent experiments with error bars representing standard deviation.

(**C**) Cell lysates reserved for immunoblotting were probed with the indicated antibodies to assess relative protein levels. Actin was used as loading control.

5.3 Depletion of PRMTs affects E2F1-dependent apoptosis

To determine how depletion of PRMTs affects E2F1-dependent apoptosis, siRNA-treated cells were subjected to flow cytometry and immunoblotting. The results showed a 50% apoptotic reduction in PRMT1-depleted cells, while PRMT5-depleted cells showed at least a two-fold increase (Fig 5.6A). Co-depletion of both PRMTs led to a phenotype similar to that of PRMT5 depletion alone. The co-depletion of E2F1 abolished these apoptotic changes, implying that the phenotypic effects were E2F1 dependent.

A portion of cells used in the flow cytometry was lysed and probed for apoptotic markers such as cleaved PARP and p73. Similarly, the level of cleaved PARP was visibly reduced in PRMT1-depleted cells (Fig 5.6B, lane 3), but was markedly elevated in PRMT5-depleted cells (Fig 5.6B, lane 5). Co-depletion of both PRMTs also led to upregulation of cleaved PARP (Fig 5.6B, lane 7). The E2F1 apoptotic target p73 was detectable only under greater levels of apoptosis, which occurred when PRMT5 or both PRMTs were depleted (Fig 5.6B, lanes 5 and 7). Co-depletion of E2F1 abolished these apoptotic changes (Fig 5.6B, lanes 2, 4, 6 and 8) and hence the results were consistent with the rest of the experiment.

As an extension to the previous experiment, an inducible ER-E2F1 system was used to overexpress E2F1 activity under PRMT-depleted conditions. This system is composed of plasmids expressing a modified form of the estrogen receptor ligand-binding domain (ER) fused to E2F1 and stably expressed in cell lines (Littlewood et al., 1995). The ER modification greatly increases its affinity to

4-hydroxytamoxifen (OHT) while at the same time reducing its affinity to endogenous estrogen (Lazzerini Denchi and Helin, 2005). Upon addition of OHT, ER-E2F1 translocates from the cytoplasm to the nucleus, where it can bind to E2F1 promoters and activate gene targets (Fig 5.7A).

In the experiment, the SAOS2 ER-E2F1 cell lines were treated with siRNAs against PRMT1 and/or PRMT5 and induced with OHT 24 hours later. The cells were harvested for flow cytometry and immunoblotting. The results show that OHT induction caused an overall apoptotic increase (Fig 5.7B) which correlated with translocation of ER-E2F1 from cytoplasm to the nucleus (Fig 5.7C).

Despite having markedly increased levels of apoptosis upon OHT induction, the phenotypic differences under PRMT depletion was still discernible. In the backdrop of OHT induction, PRMT1 depletion led to a 20% decrease in apoptosis while PRMT5 depletion led to a 20% increase. Depletion of both PRMTs resulted in a phenotype similar to PRMT5 depletion (Fig 5.7B). These results are substantiated by immunoblots indicating levels of other apoptotic markers such as p73 and cleaved PARP (Fig 5.7C). Together, the experimental results tell us that E2F1 activation is a key driver of apoptosis and its activity can be modulated through PRMTs.

Figure 5.6 PRMT depletion in E2F1-dependent apoptosis

A

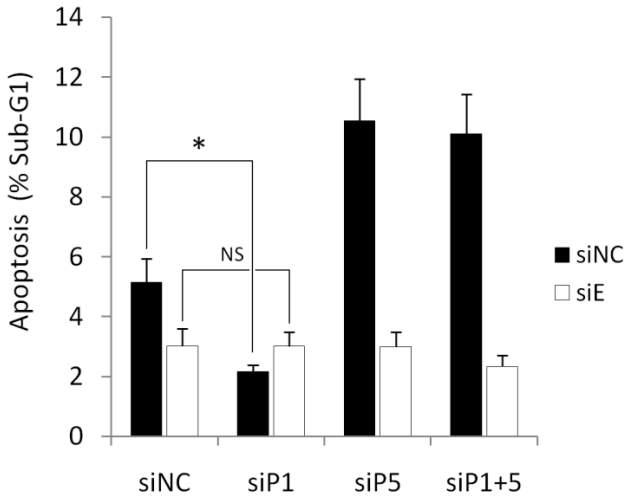

B

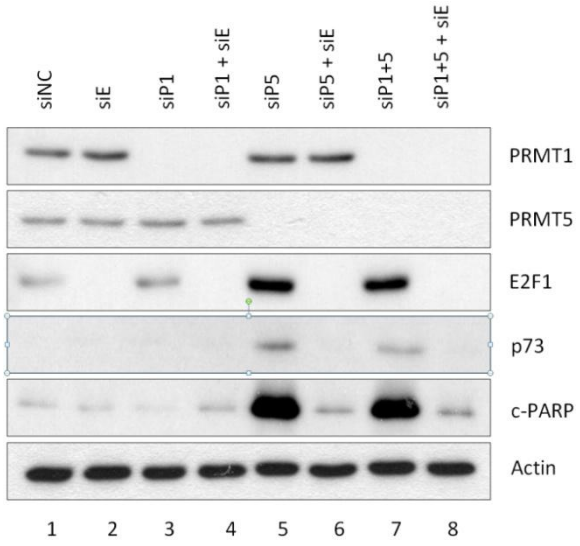

(**A**) Level of apoptosis as percentage of cells in sub-G1. SAOS2 cells were treated with the indicated siRNA as previously described and harvested at 72 hours post-transfection for FACS analysis. Non-targeting control (siNC) are represented by black bars and E2F1 depletion (siE) represented by white bars. Data shown are means of 3 independent experiments with error bars representing standard deviation; * $p < 0.05$; NS – no statistically significant difference.

(**B**) Cell lysates reserved for immunoblotting were probed with the indicated antibodies to assess relative protein levels. Actin was used as loading control.

Figure 5.7 PRMT depletion in E2F1-triggered apoptosis

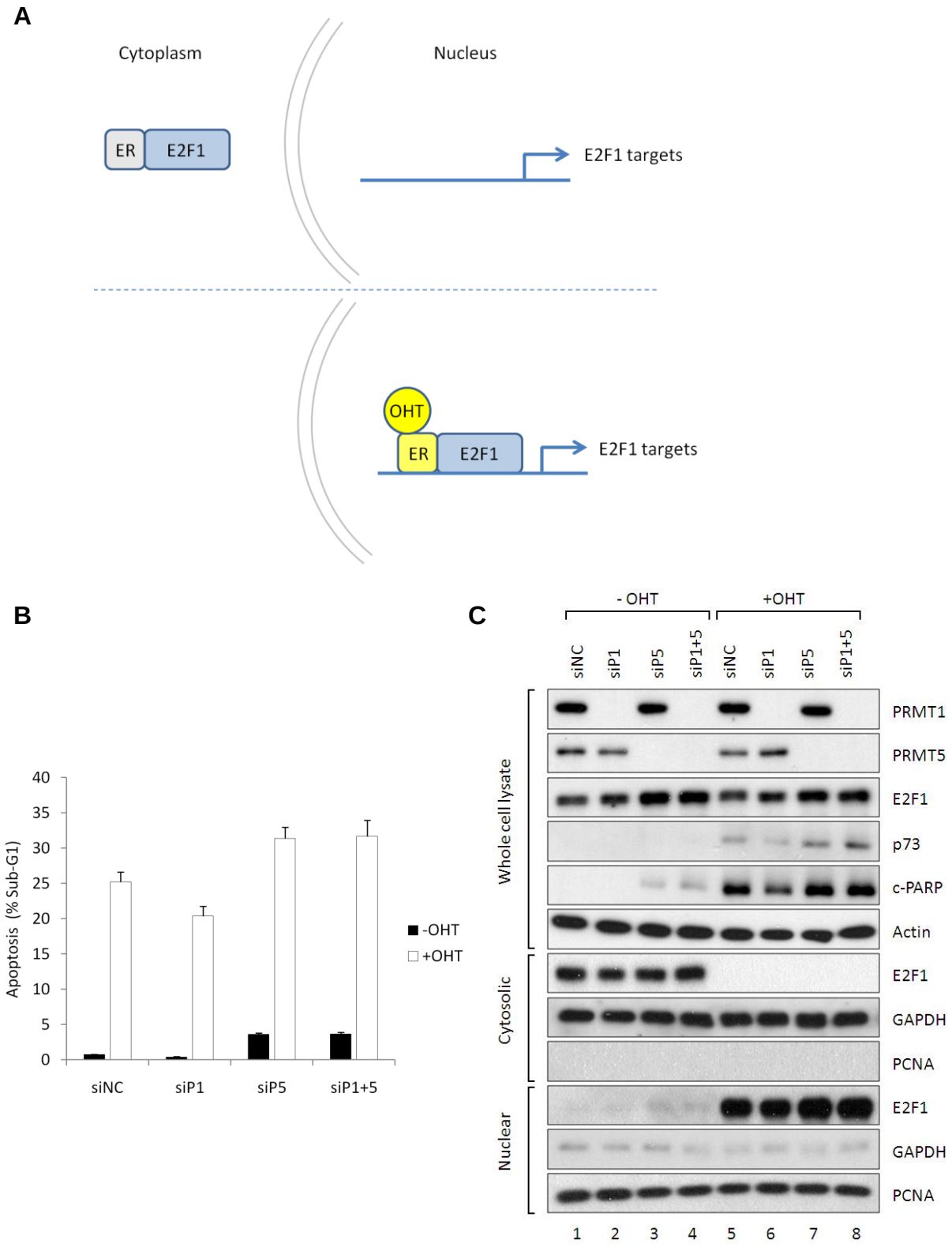

(**A**) In the absence of 4-hydroxytamoxifen (OHT), the ER-E2F1 fusion protein is localised in the cytoplasm and is unable to activate E2F1 target genes. Upon addition of OHT, the activated ligand binding domain of the estrogen receptor translocates ER-E2F1 into the nucleus, allowing it to bind to the promoters of E2F1 target genes, such as p73.

(**B**) Level of apoptosis as percentage of cells in sub-G1. SAOS2 cells containing inducible ER-E2F1 plasmids were treated with the indicated siRNA as previously described and 300nM OHT was added 24 hours post-transfection. The cells were harvested 48 hours later and analysed by FACS. Data shown are means of 3 independent experiments with error bars representing standard deviation; * $p < 0.05$; NS – no statistically significant difference.

(**C**) Some cells were reserved for fractionation and the corresponding lysates were immunoblotted with the indicated antibodies to assess relative protein levels. Actin, GAPDH and PCNA was used as loading controls for whole cell lysate, cytosolic, and nuclear fraction respectively.

5.4 Apoptotic response of cells expressing different E2F1 mutants

To study the importance of each arginine residue of the E2F1 RG-rich motif in apoptosis, equivalent levels of E2F1 mutants were expressed in cells and after 72 hours, harvested for flow cytometry and immunoblotting. Expression of the R109K mutant caused a lower level of apoptosis compared to wild-type E2F1, whereas expression of R111K, R113K, R111/113K and KKK resulted in higher apoptosis (Fig 5.8A). The relative expression levels of each E2F1 mutant are shown (Fig 5.8B). From these results it can be deduced that the SDMA marks on R111 and R113 protect cells from apoptosis, since prevention of these marks enhanced cell death. The ADMA mark on R109 promotes apoptosis by inhibiting symmetric dimethylation on R111 and R113. It is also clear that hypomethylation of the E2F1 RG-rich motif sent a strong signal to trigger cell death.

If the hypothesis is true that PRMT1 methylates R109 and PRMT5 methylates R111 and R113 on E2F1, then depletion of these enzymes should not produce any apoptotic difference in cells transfected with certain E2F1 mutants. To test, E2F1 mutants were expressed in PRMT1 or PRMT5-depleted cells and subjected to flow cytometry and immunoblotting. The results indicate under wild-type E2F1 expression, PRMT1 depletion led to a decrease in apoptosis whereas PRMT5-depletion led to an increase (Fig 5.9A). This was correlated to E2F1 and cleaved PARP levels (Fig 5.9B). The observations were consistent with previous results and acted as the experimental control.

While the expression of R109K led to a decrease in apoptosis compared to wild-type E2F1, the concurrent depletion of PRMT1 did not cause any further changes to cell death. This implies that the R109K mutant could not be methylated by PRMT1, thus PRMT1 depletion did not result in any further apoptotic effect. On the contrary, concurrent depletion of PRMT5 in R109K-expressed cells did cause an apoptotic increase, implying that the removal of methyl groups from R111 and R113 was responsible for the phenotypic change.

The expression of R111/113K led to an overall increase in apoptosis compared to wild-type E2F1. However, concurrent depletion of PRMT1 or PRMT5 resulted in no further changes to apoptosis. Since R109 is the only arginine residue that can be methylated in this mutant, it shows that removal of ADMA alone did not cause any significant changes to apoptosis. This is consistent with the hypothesis that the ADMA mark on R109 acted through competition with SDMAs on R111 and R113.

Figure 5.8 E2F1 mutants on apoptosis

A

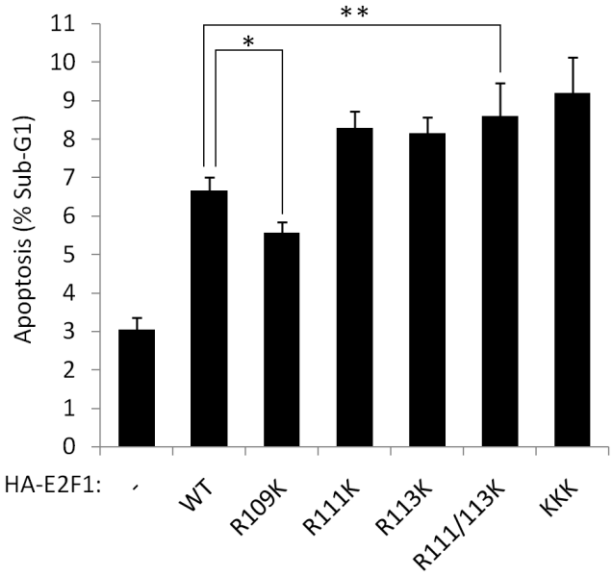

B

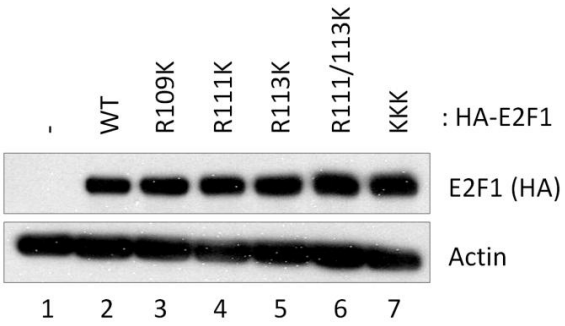

(**A**) Level of apoptosis as percentage of cells in sub-G1. SAOS2 cells were transfected with ~1 µg empty vector control (–) or HA-E2F1 plasmids as previously described. The cells were harvested 72 hours later and analysed by FACS. Data shown are means of 3 independent experiments with error bars representing standard deviation; * $p < 0.05$; ** $p < 0.01$.

(**B**) Cell lysates reserved for immunoblotting were probed with HA antibody to assess transfected E2F1 protein levels. Actin was used as loading control.

Figure 5.9 PRMT depletion and E2F1 mutants on apoptosis

A

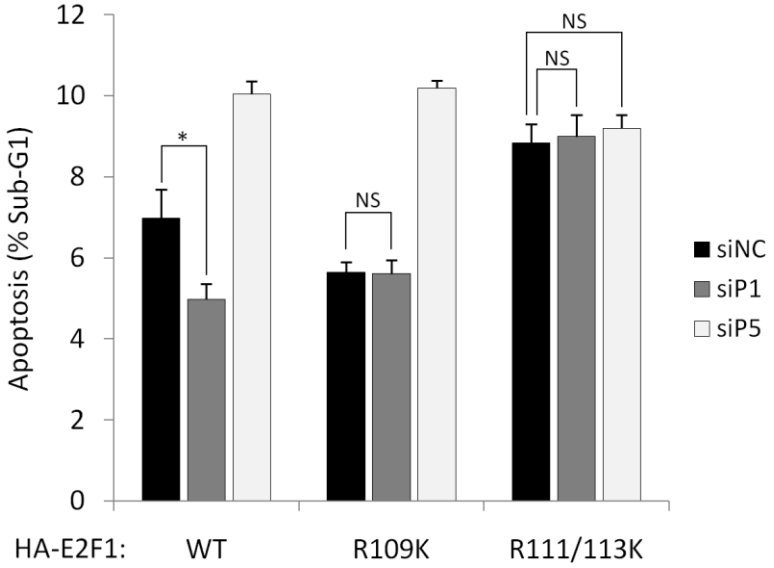

B

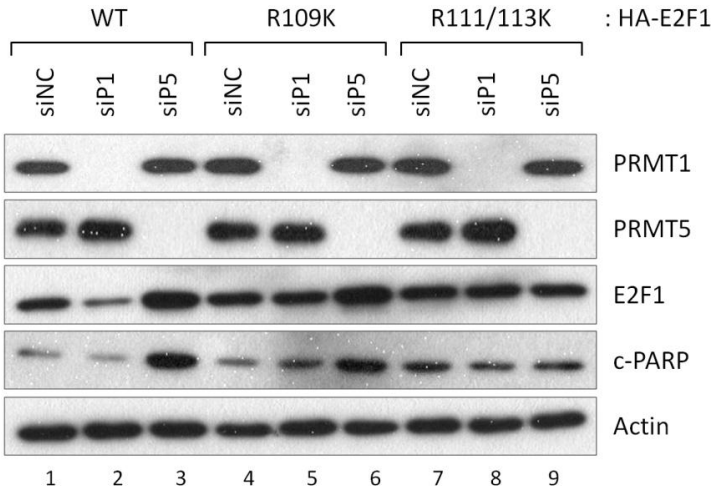

(**A**) Level of apoptosis as percentage of cells in sub-G1. SAOS2 cells were treated with the indicated siRNA as previously described and re-seeded at 24 hours post-transfection. They were then transfected with the indicated HA-E2F1 plasmids and harvested at 48 hours post-transfection for FACS analysis. Data shown are means of 3 independent experiments with error bars representing standard deviation; * $p < 0.05$; NS – no statistically significant difference.

(**B**) Cell lysates reserved for immunoblotting were probed with the indicated antibodies to assess relative protein levels. Actin was used as loading control.

5.5 PRMT5 induction reduces E2F1-triggered apoptosis

To confirm that E2F1 arginine methylation by PRMT5 could modulate apoptosis, inducible cell lines were created in which the expression of PRMT5 or enzymatically inactive ΔPRMT5 could be induced by doxycycline.

Under wild-type E2F1 overexpression conditions, PRMT5 induction caused a decrease in apoptosis (Fig 5.10, lanes 3 and 4), implying that additional SDMAs on E2F1 protected cells from death. On the contrary, induction of ΔPRMT5 caused an increase in apoptosis (Fig 5.10, lanes 9 and 10), suggesting competition with endogenous PRMT5 in a dominant negative fashion, which suppressed SDMA marks on E2F1.

Expression of the KKK mutant at equivalent levels of wild-type E2F1 generally led to higher levels of apoptosis (Fig 5.10, lanes 5 and 11). However, unlike wild-type E2F1, induction of either PRMT5 or ΔPRMT5 did not cause any further changes to cell death (Fig 5.10, lanes 6 and 12). This underscores the importance of symmetric dimethylation in the E2F1 RG-rich motif in regulating cell apoptosis.

Figure 5.10 PRMT5 induction on apoptosis

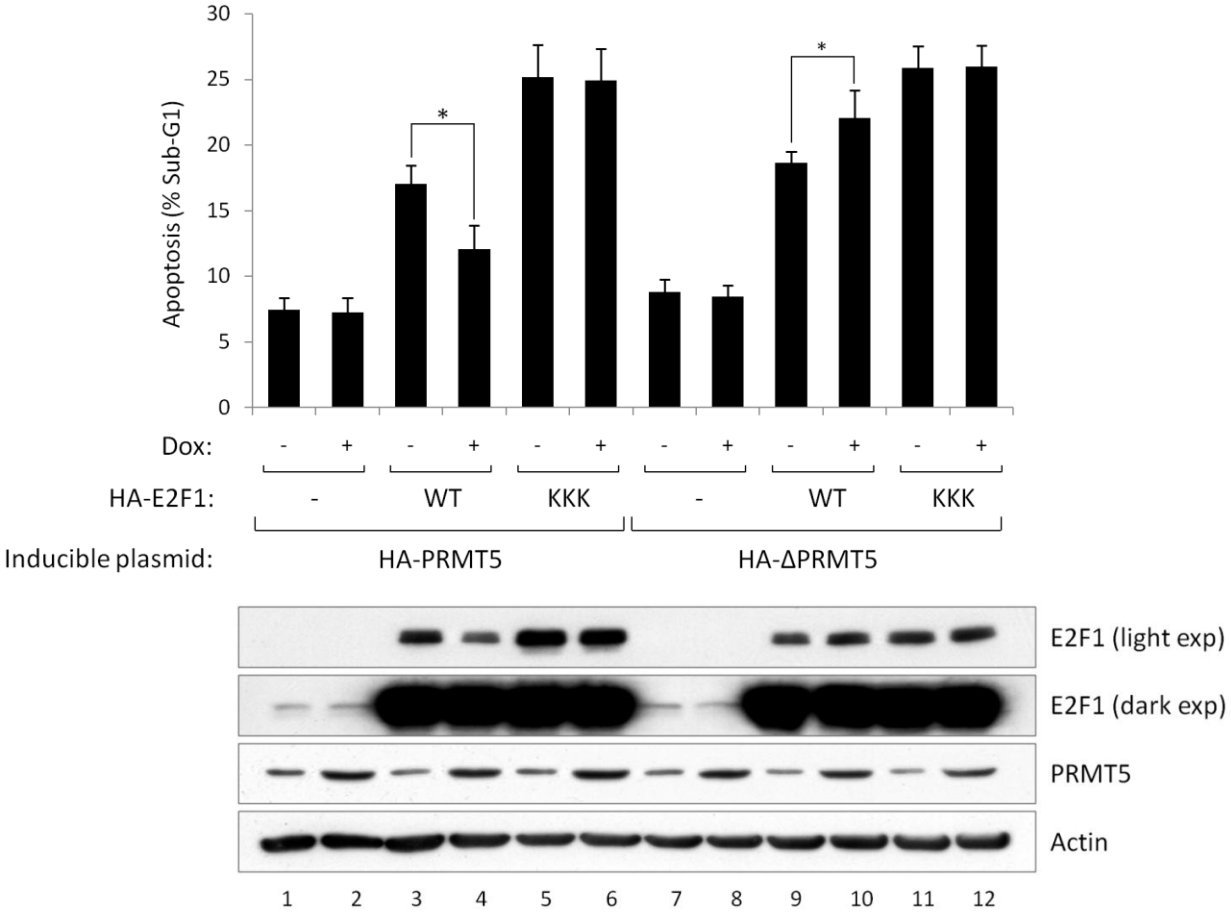

Level of apoptosis as percentage of cells in sub-G1. SAOS2 stable Tet-On cells expressing either wild type HA-PRMT5 or catalytically inactive HA-ΔPRMT5 were transfected with ~1 µg empty vector control (–) or HA-E2F1 plasmids as previously described. After 24 hours post-transfection, the cells were treated with 1 µg/ml doxycycline and harvested 48 hours later for FACS analysis. Data shown are means of 3 independent experiments with error bars representing standard deviation; * $p < 0.05$. Cell lysates reserved for immunoblotting were probed with the indicated antibodies to assess relative protein levels. Actin was used as loading control.

5.6 Chapter summary

The results in this chapter imply that symmetric dimethylation of E2F1 residues R111 and R113 by PRMT5 protect cells from apoptosis and enhances proliferation. Asymmetric dimethylation of R109 by PRMT1 promotes apoptosis and inhibits proliferation by suppressing SDMA marks on the adjacent arginine residues.

The influence of arginine methylation on E2F1-dependent phenotypes is twofold. The first involves modulating overall E2F1 levels through changes in protein stability; the second involves altering target gene promoter affinity. Both factors work together to mediate E2F1 target gene transcription, but a slight difference exists. Whilst changes in protein stability affect overall E2F1 activity, changes to promoter binding affinity can be selective towards certain groups of genes. In this case, it is evident that SDMA marks on E2F1 have the potential to downregulate apoptotic genes and reduce cell death.

As this new phenomenon is uncovered, it is tempting to ask whether changes in E2F1 arginine methylation could be triggered through external means. Hence in the next chapter, we will investigate how DNA damage agents could affect E2F1 arginine methylation and explain how it may work through cyclin A binding.

6. Regulators of E2F1 arginine methylation

In the previous chapters, I described the enzymes responsible for E2F1 arginine methylation, the positions of the methylated residues and the effects of methylation on E2F1 protein stability, promoter binding, transcriptional activity and cell phenotype. That prompted me to ask the question of what causes the methylation status of E2F1 to change. DNA damage has been reported to induce E2F1 protein levels (Blattner et al., 1999) and from our studies we observed that PRMT5 depletion could do the same. By deduction, it was possible that these two could be correlated.

6.1 Impact of DNA damage on E2F1 arginine methylation

To test the hypothesis, immunoprecipitation of E2F1 was performed under DNA damaging conditions using two standard chemotherapy drugs, doxorubicin and etoposide. The results show that cells treated with the DNA damaging agents displayed enhanced interaction between PRMT1 and E2F1, resulting in an increase in ADMA signals (Fig 6.1, lanes 8 and 9). This coincided with the disruption of PRMT5 and E2F1 interaction, together with a decrease in SDMA signals.

An immunoblot was performed to compare the effects of PRMT depletion and DNA damage on E2F1 and its target proteins. The results showed that DNA

damaging agents did not produce significant changes to PRMT1 or PRMT5 levels (Fig 6.2, lanes 1, 5 and 9), but had caused an increase in E2F1 and its target proteins. This was in line with earlier studies on E2F1 and DNA damage (Meng et al., 1999), which implies that DNA damage affects E2F1 arginine methylation not by altering the overall levels of PRMTs, but by disrupting their interactions.

Importantly, it was observed that combination of PRMT5 depletion and DNA damage had additive effects on E2F1 overexpression (Fig 6.2, lanes 7 and 11), suggesting that DNA damage can upregulate E2F1 through more than one mechanism, such as phosphorylation of S31 by ATM/ATR kinase (Lin et al., 2001) or S364 by Chk2 kinase (Stevens et al., 2003).

Figure 6.1 DNA damage on E2F1 arginine dimethylation

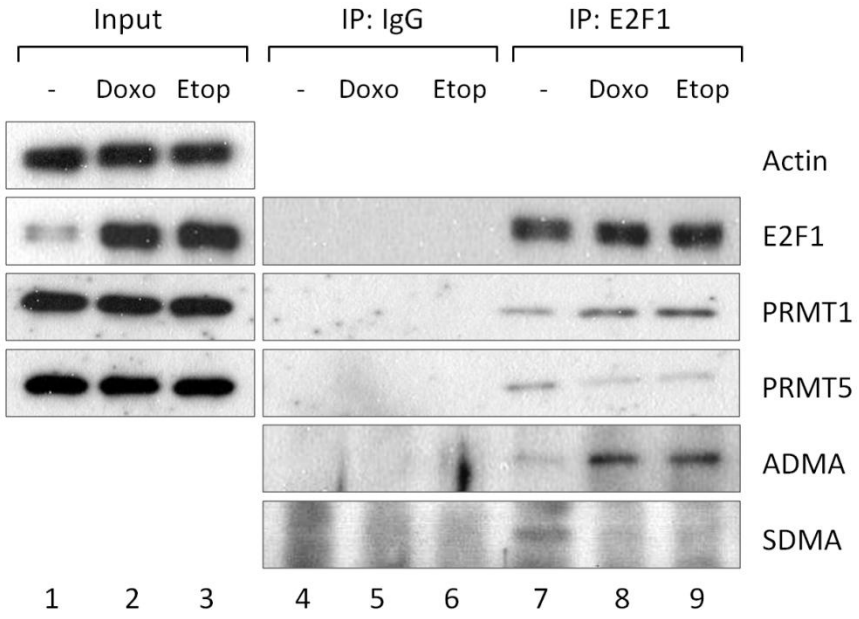

SAOS2 cells were treated with 2 μM doxorubicin, 10 μM etoposide, or an equivalent volume of DMSO solvent (–) for 48 hours. The corresponding cell lysates were immunoprecipitated with control IgG or E2F1 antibodies, and subsequently immunoblotted with the indicated antibodies. Input levels of the respective proteins are shown.

Figure 6.2 PRMT depletion on E2F1 targets upon DNA damage

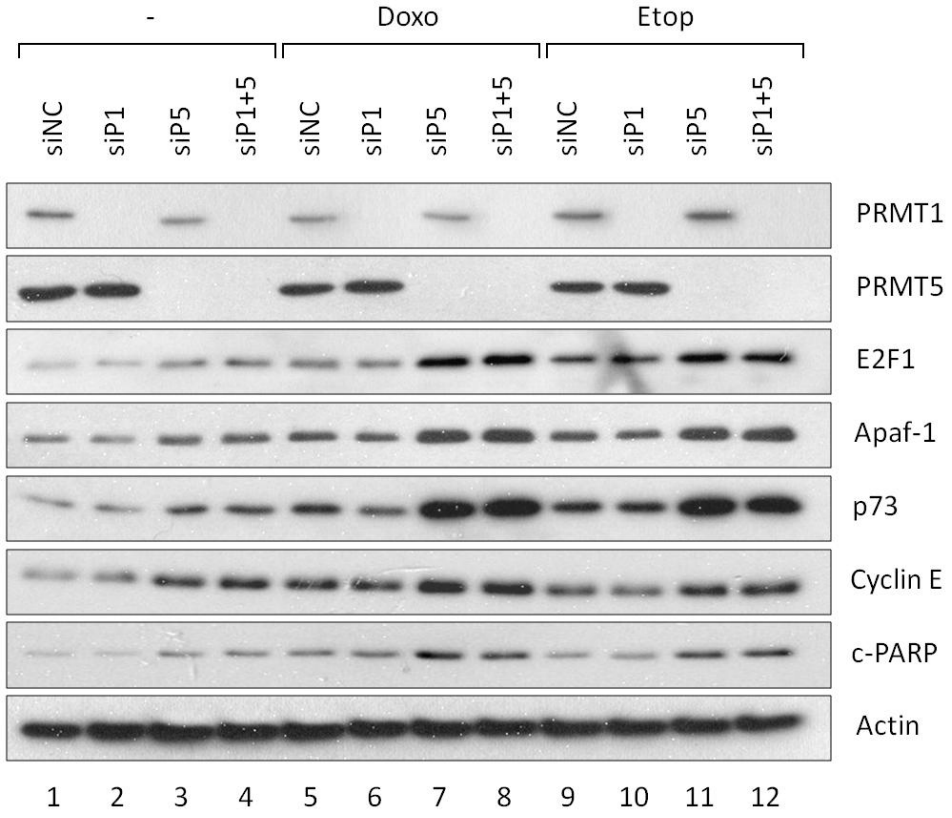

SAOS2 cells were treated with the indicated siRNA as previously described. After 48 hours post-transfection, the cells were treated with 2 μM doxorubicin, 10 μM etoposide, or an equivalent volume of 1.0 μl DMSO (–), which was used as drug solvent. The cells were harvested 48 hours later and immunoblotted with the indicated antibodies to assess relative protein levels. Actin was used as loading control.

6.2 Impact of DNA damage on E2F1-dependent cell phenotypes

To investigate how DNA damage affects the cell upon depletion of PRMT1 or 5, a colony assay was performed under siRNA-treatment followed by etoposide treatment. After staining the cells with crystal violet (Fig 6.3A), the cell densities were quantified (Fig 6.3C) and the relative percentage changes were calculated (Fig 6.3D). Immunoblotting was performed to visualise relative protein levels (Fig 6.3B). The results show that DNA damage caused an overall decrease in cell growth but did not alter the effect of PRMT1 depletion which enhanced growth while PRMT5 depletion inhibited growth. In particular, even upon DNA damage, the relative enhancement of cell growth persisted under PRMT1 depletion, suggesting that the increase in SDMA marks as a result of lack of competition from ADMA had protected the cells from growth inhibition.

A flow cytometry experiment was performed on cells treated with siRNA against PRMT1 and PRMT5, followed by addition of etoposide in a similar fashion. The results showed that DNA damage led to an overall increase in apoptosis, but also did not affect the trend that PRMT1 depletion inhibited apoptosis while PRMT5 depletion enhanced cell death (Fig 6.4A). Nonetheless, the overall increase in apoptosis allowed greater visual distinction to be made when comparing sub-G1 levels between PRMT1 depletion and control treatment. An immunoblot of these cells showed that E2F1, p73 and cleaved PARP levels were consistent with the observations seen in the flow cytometry, providing further substantiation (Fig 6.4B).

The DNA damage experiments were expanded to include cells expressing E2F1 mutants. Colony assays (Fig 6.5A, B and C), flow cytometry (Fig 6.5D) and immunoblotting (Fig 6.5E) were performed in a similar manner as before. Cells expressing the R109K mutant had higher growth and decreased apoptosis compared to WT E2F1, while those expressing R111K, R113K, R111/113K and KKK had a lower growth and increased apoptosis. Under etoposide treatment, there was an overall inhibition of growth and induction of apoptosis, but it did not alter the trend.

Although DNA damage was shown to disrupt E2F1 and PRMT5 interaction (Fig 6.1), resulting in upregulation of E2F1 target genes (Fig 6.2), it is unlikely that its effects on cells acted solely through E2F1. For example, if DNA damage had caused an increase in apoptosis through inhibiting PRMT5 alone, then additional PRMT5 depletion would not have caused further apoptosis. This was not the case in Fig 6.4. As such, the influence of DNA damage on E2F1-dependent phenotypes is only partially, rather than completely, attributed to changes in E2F1 arginine methylation.

Figure 6.3 PRMT depletion on cell growth upon DNA damage

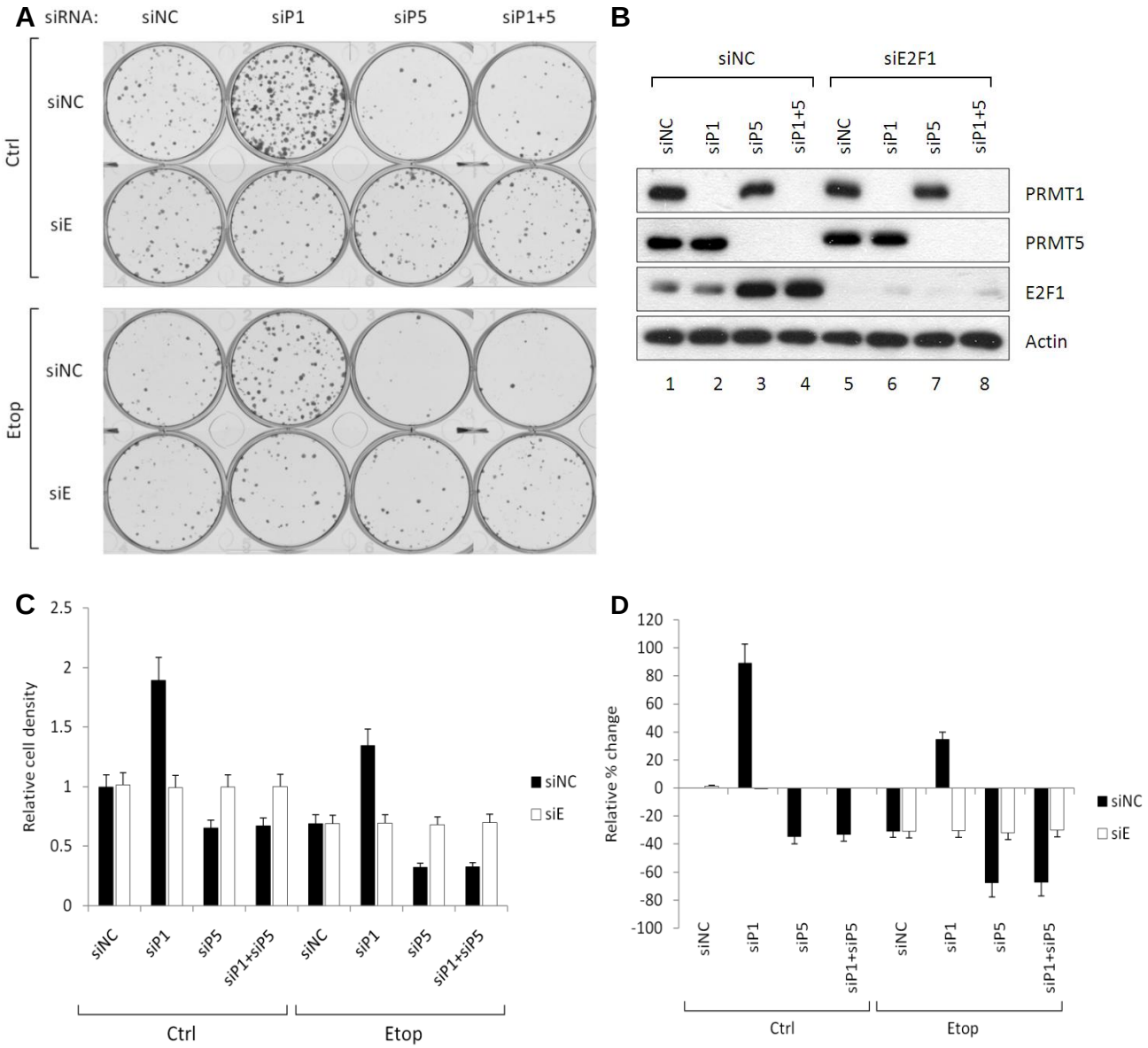

(**A**) SAOS2 cells were seeded at low density in 6-well plates (1000 cells per well) and treated with the indicated siRNA as previously described. At 24 hours post-transfection, the cells were treated with 10μM etoposide (Etop) or an equivalent volume of DMSO solvent (Ctrl). After 10 days, the cells were harvested and stained with crystal violet dye.

(**B**) Cell lysates reserved for immunoblotting were probed with the indicated antibodies to assess relative protein levels. Actin was used as loading control.

(**C**) Cell density of the above images relative to non-targeting siRNA control treatment. Treatments with non-targeting siRNA (siNC) are represented by black bars and E2F1 siRNA (siE2F1) represented by white bars. Data shown are means of 3 independent experiments with error bars representing standard deviation.

(**D**) Percentage change in cell density relative to non-targeting siRNA control treatment.

Figure 6.4 PRMT depletion on apoptosis upon DNA damage

A

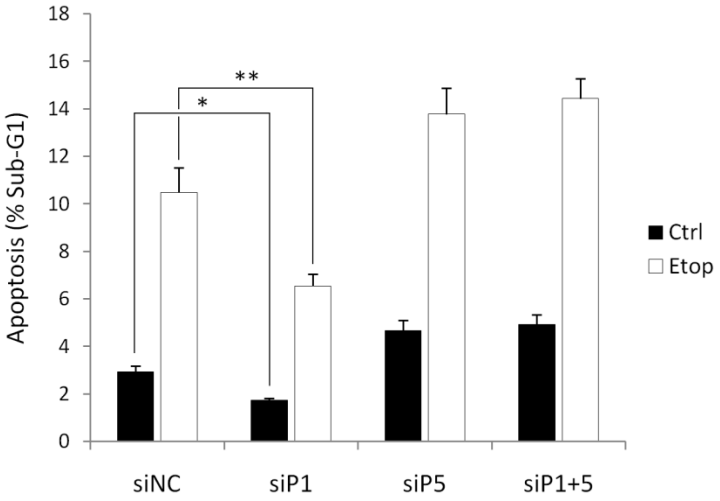

B

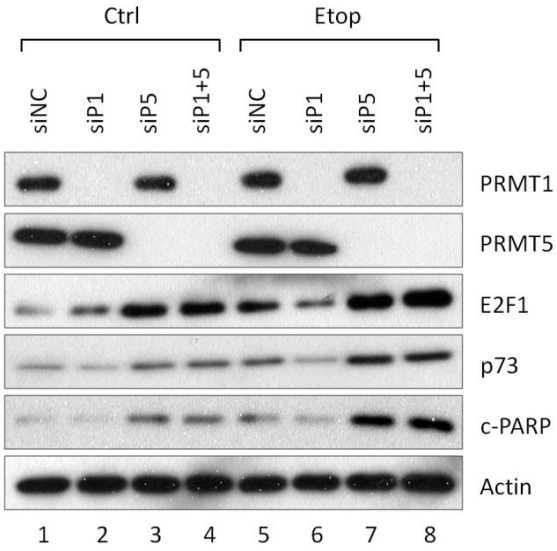

(**A**) Level of apoptosis as percentage of cells in sub-G1. SAOS2 cells were treated with the indicated siRNA as previously described. At 24 hours post-transfection, the cells were treated with 10μM etoposide or an equivalent volume of DMSO solvent, and harvested 48 later for FACS analysis. DMSO control treatment (Ctrl) are represented by black bars and etoposide treatment (Etop) represented by white bars. Data shown are means of 3 independent experiments with error bars representing standard deviation; * $p < 0.05$; ** $p < 0.01$

(**B**) Cell lysates reserved for immunoblotting were probed with the indicated antibodies to assess relative protein levels. Actin was used as loading control.

Figure 6.5 E2F1 mutants and cell phenotypes upon DNA damage

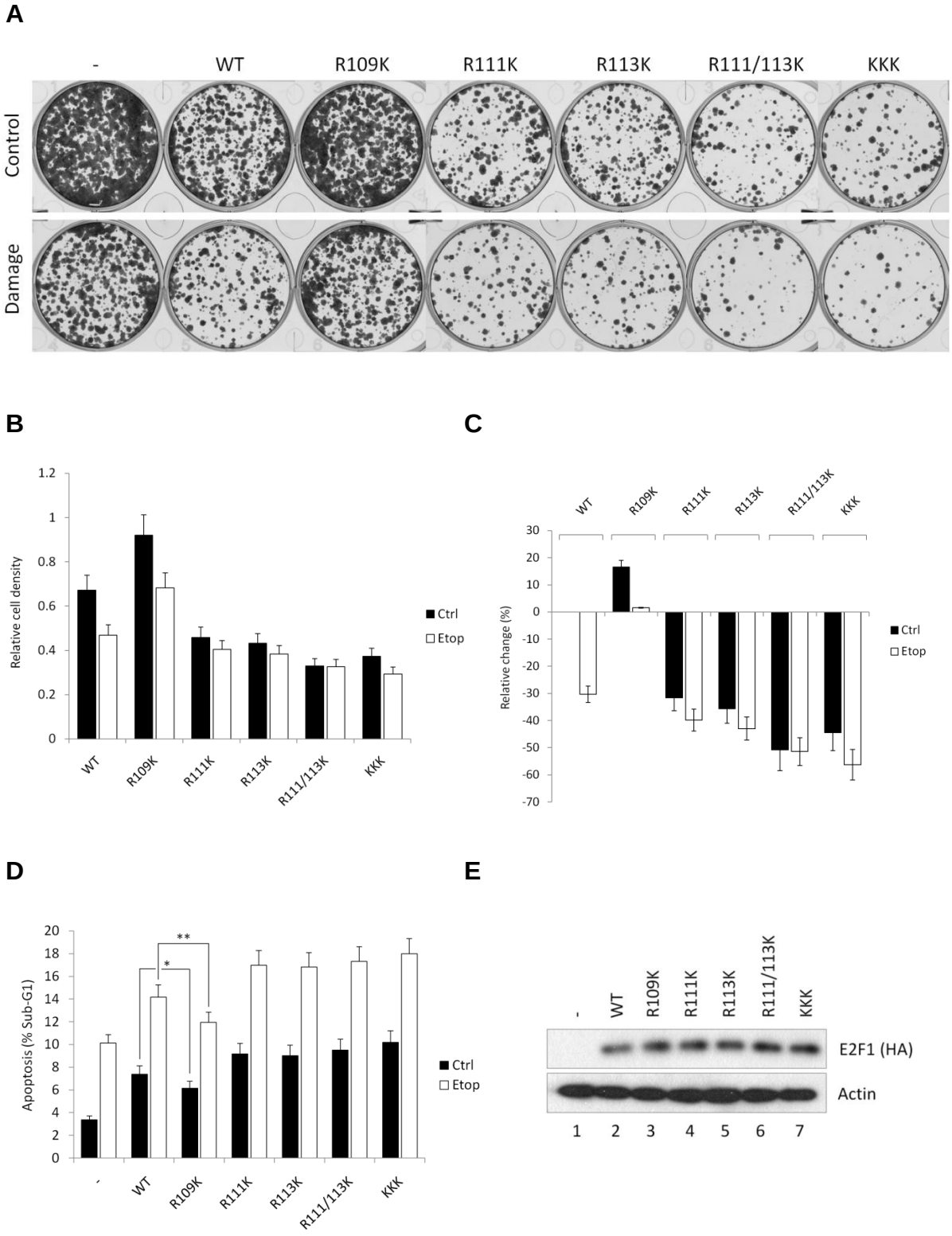

(**A**) SAOS2 cells were seeded at low density in 6-well plates (2000 cells per well) and transfected with ~1 µg empty vector control (–) or HA-E2F1 plasmids as previously described. At 24 hours post-transfection, the cells were treated with 10µM etoposide (Etop) or an equivalent volume of DMSO solvent (Ctrl). After 10 days, the cells were harvested and stained with crystal violet dye.

(**B**) Cell density of the above images relative to empty vector control treatment. DMSO control treatment (Ctrl) are represented by black bars and etoposide treatment (Etop) represented by white bars. Data shown are means of 3 independent experiments with error bars representing standard deviation.

(**C**) Percentage change in cell density relative to wild type E2F1 treatment.

(**D**) Level of apoptosis as percentage of cells in sub-G1. SAOS2 cells were transfected with ~1 µg empty vector control (–) or HA-E2F1 plasmids as previously described. At 24 hours post-transfection, the cells were treated with 10µM etoposide or an equivalent volume of DMSO solvent, and harvested 48 later for FACS analysis. DMSO control treatment (Ctrl) are represented by black bars and etoposide treatment (Etop) represented by white bars. Data shown are means of 3 independent experiments with error bars representing standard deviation; * $p < 0.05$; ** $p < 0.01$

(**E**) Cell lysates reserved for immunoblotting were probed with HA antibody to assess transfected E2F1 protein levels. Actin was used as loading control.

6.3 DNA damage mediates E2F1 methylation through cyclin A

Cyclin A, the first cyclin ever cloned, is an essential component of the cell cycle (Swenson et al., 1986). Two types of cyclin A have been discovered in mammals (Nieduszynski et al., 2002). Cyclin A1 is expressed exclusively in male germ cells (Sweeney et al., 1996), while cyclin A2 is expressed in all proliferating cell types (Hochegger et al., 2008). Cyclin A2 is induced during the S-phase, where it interacts with and activates kinases Cdk1 and Cdk2 (Yam et al., 2002). Depletion of cyclin A2 in mice was shown to be embryonic lethal (Murphy et al., 1997), highlighting its importance in cell survival.

Previous studies have shown that binding to cyclin A prevents E2F1 from interacting with p53 to induce apoptosis. Under DNA damage conditions, cyclin A levels were reported to decrease, with a concurrent increase in E2F1-p53 complex formation (Hsieh et al., 2002). The cyclin A binding domain of E2F1 sits in the region between P87 to E95 (Krek et al., 1994) which lies adjacent to the putative arginine methylation motif (Fig 6.6A). This leads us to speculate whether there could be steric competition between cyclin A binding and PRMT methylation. After treating cells with the DNA damaging agents doxorubicin and etoposide, the levels of cyclin A fell as previously reported (Fig 6.6B, lanes 2 and 3). This drop in cyclin A levels coincided with an increased interaction between E2F1 and PRMT1, and a concomitant decrease in PRMT5 binding. Correspondingly, this was correlated with increased ADMA and decreased SDMA signals.

Figure 6.6 E2F1/Cyclin A interaction upon DNA damage

A

```
        10         20         30         40         50         60
MALAGAPAGG PCAPALEALL GAGALRLLDS SQIVIISAAQ DASAPPAPTG PAAPAAGPCD

        70         80         90        100        110        120
PDLLLFATPQ APRPTPSAPR PALGRPPVKR RLDLETDHQY LAESSGPARG RGRHPGKGVK

       130        140        150        160        170        180
SPGEKSRYET SLNLTTKRFL ELLSHSADGV VDLNWAAEVL KVQKRRIYDI TNVLEGIQLI

       190        200        210        220        230        240
AKKSKNHIQW LGSHTTVGVG GRLEGLTQDL RQLQESEQQL DHLMNICTTQ LRLLSEDTDS

       250        260        270        280        290        300
QRLAYVTCQD LRSIADPAEQ MVMVIKAPPE TQLQAVDSSE NFQISLKSKQ GPIDVFLCPE

       310        320        330        340        350        360
ETVGGISPGK TPSQEVTSEE ENRATDSATI VSPPPSSPPS SLTTDPSQSL LSLEQEPLLS

       370        380        390        400        410        420
RMGSLRAPVD EDRLSPLVAA DSLLEHVRED FSGLLPEEFI SLSPPHEALD YHFGLEEGEG

       430
IRDLFDCDFG DLTPLDF
```

B

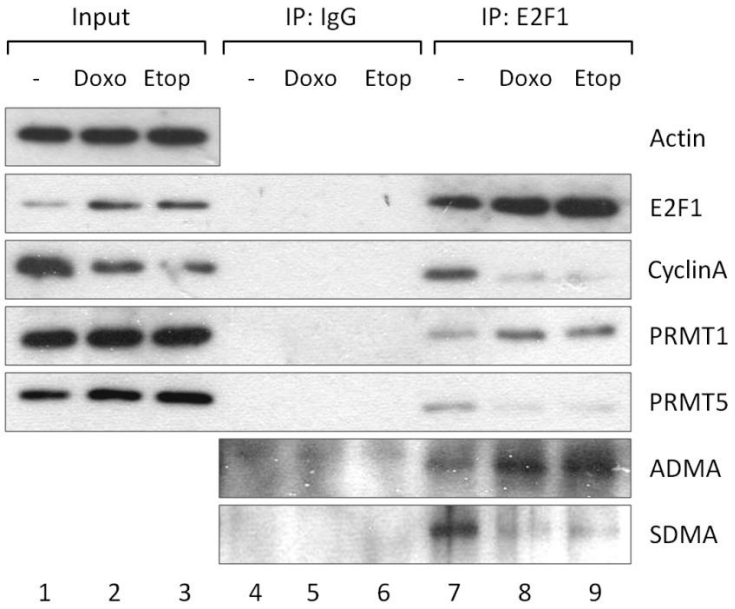

(**A**) E2F1 sequence with the cyclin A binding domain highlighted in yellow.

(**B**) SAOS2 cells were treated with 2 µM doxorubicin, 10 µM etoposide, or an equivalent volume of DMSO solvent (–) for 48 hours. The corresponding cell lysates were immunoprecipitated with control IgG or E2F1 antibodies, and subsequently immunoblotted with the indicated antibodies. Input levels of the respective proteins are shown.

6.4 Interplay between cyclin A and PRMTs on E2F1

To determine whether the DNA damage induced changes in E2F1 arginine methylation was effected through cyclin A, an immunoprecipitation of endogenous E2F1 was performed under siRNA-mediated depletion of cyclin A (Fig 6.7A). It was observed that upon cyclin A depletion, there was an upregulation of endogenous E2F1 (Fig 6.7A, lane 2), which may account for its increased immunoprecipitation Fig 6.7A, lane 6). This coincided with a decrease in complex formation between E2F1 and PRMT5, as well as a corresponding decrease in SDMA signals. While enhanced PRMT1 and ADMA signals were also detected, they might be attributed to the increased E2F1 immunoprecipitation, which makes it difficult to assess their interaction changes. Nevertheless, it can be seen that the pattern of PRMT binding and arginine dimethylation upon cyclin A depletion closely follows that resulting from DNA damage (Fig 6.6B).

A major drawback of this experiment is that the endogenous E2F1 level changes upon DNA damage and cyclin A depletion, making it difficult for equivalent comparison. To get a clearer picture, an immunoprecipitation of cyclin A was performed in the absence or presence of siRNA against E2F1 (Fig 6.7B). From the results, we deduced that cyclin A formed a complex with PRMT5, but only through E2F1, as depletion of E2F1 abolishes PRMT5 binding. The results also suggest that PRMT1 binding is either weak or non-existent in an E2F1 complex formed with cyclin A and PRMT5. The depletion of PRMT1 and PRMT5 may affect E2F1-cyclin A interaction as well. Depletion of PRMT1 results in

increased cyclin A binding, while PRMT5 depletion had an opposite effect (Fig 6.8).

To ensure that these effects were truly dependent on E2F1, an E2F1 mutant containing a deletion Δ87-95 which disrupted cyclin A binding was immunoprecipitated and probed for the interacting proteins (Fig 6.9). The R109K and R111/113K mutants were included as controls. The results supported the model of steric inhibition between the three players. The Δ87-95 E2F1 mutant, which abolished cyclin A binding, had visibly enhanced PRMT1 binding coupled with a decreased PRMT5 binding (Fig 6.9, lane 10). The R109K mutant had an increased cyclin A binding while the R111/113K mutant had a decreased cyclin A binding (Fig 6.9, lanes 11 and 12). The ADMA and SDMA signals were consistent with their respective PRMT binding.

Together, these results suggest that interplay of cyclin A and PRMTs exists on a closely situated region of E2F1. Since both PRMT1 and PRMT5 levels appear constant under DNA damage conditions, the decrease in cyclin A levels may provide an explanation of how increased PRMT1 and decreased PRMT5 interaction occurs on E2F1 and how the changes in methylation status can occur.

Figure 6.7 Cyclin A depletion on E2F1 arginine dimethylation

A

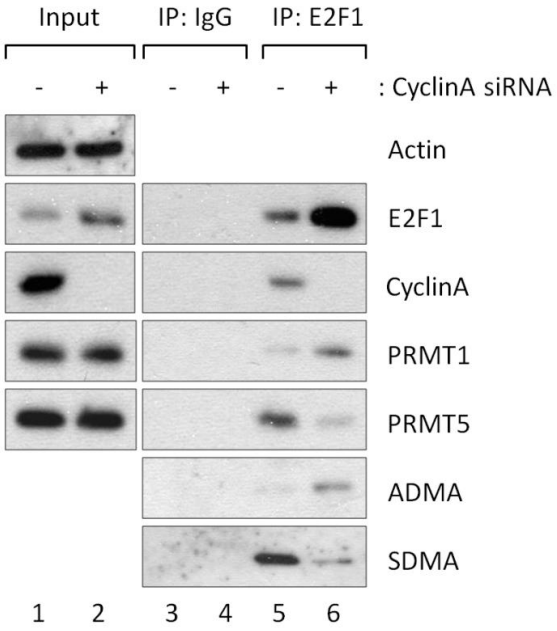

B

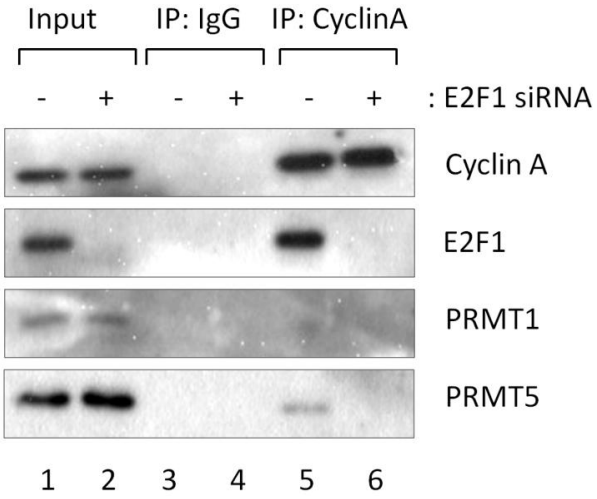

(**A**) Cyclin A depletion promotes ADMA but not SDMA. SAOS2 cells were transfected with 50nM non-targeting control or cyclin A siRNA. The corresponding cell lysates were subjected to immunoprecipitation with control IgG or E2F1 antibodies, and immunoblotted with the indicated antibodies. Input levels of the respective proteins are shown and actin served as the loading control.

(**B**) SAOS2 cells were transfected with 50nM non-targeting control or cyclin A siRNA. The corresponding cell lysates were subjected to immunoprecipitation with control IgG or cyclin A antibodies, and immunoblotted with the indicated antibodies. Input levels of the respective proteins are shown.

Figure 6.8 PRMT depletion on E2F1/cyclin A interaction

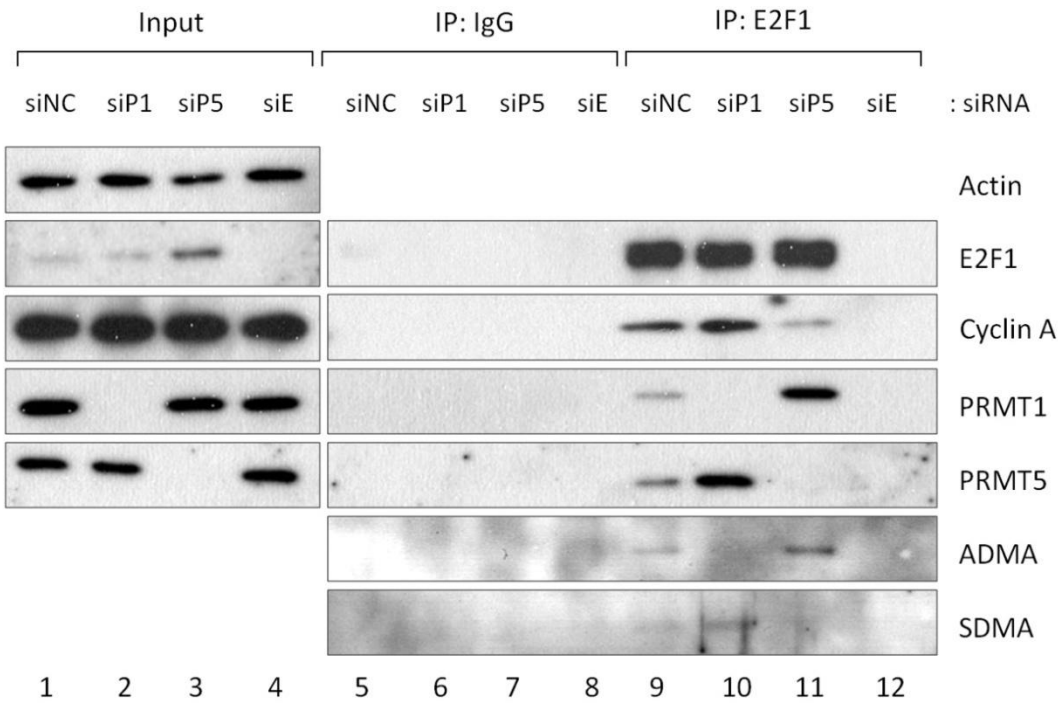

SAOS2 cells were transfected with 50nM non-targeting control (siNC), PRMT1 (siP1), PRMT5 (siP5) or E2F1 (siE) siRNA. The corresponding cell lysates were immunoprecipitated with control IgG or E2F1 antibodies, and subsequently immunoblotted with the indicated antibodies. Input levels of the respective proteins are shown and actin served as the loading control.

Figure 6.9 E2F1 mutants on cyclin A interaction

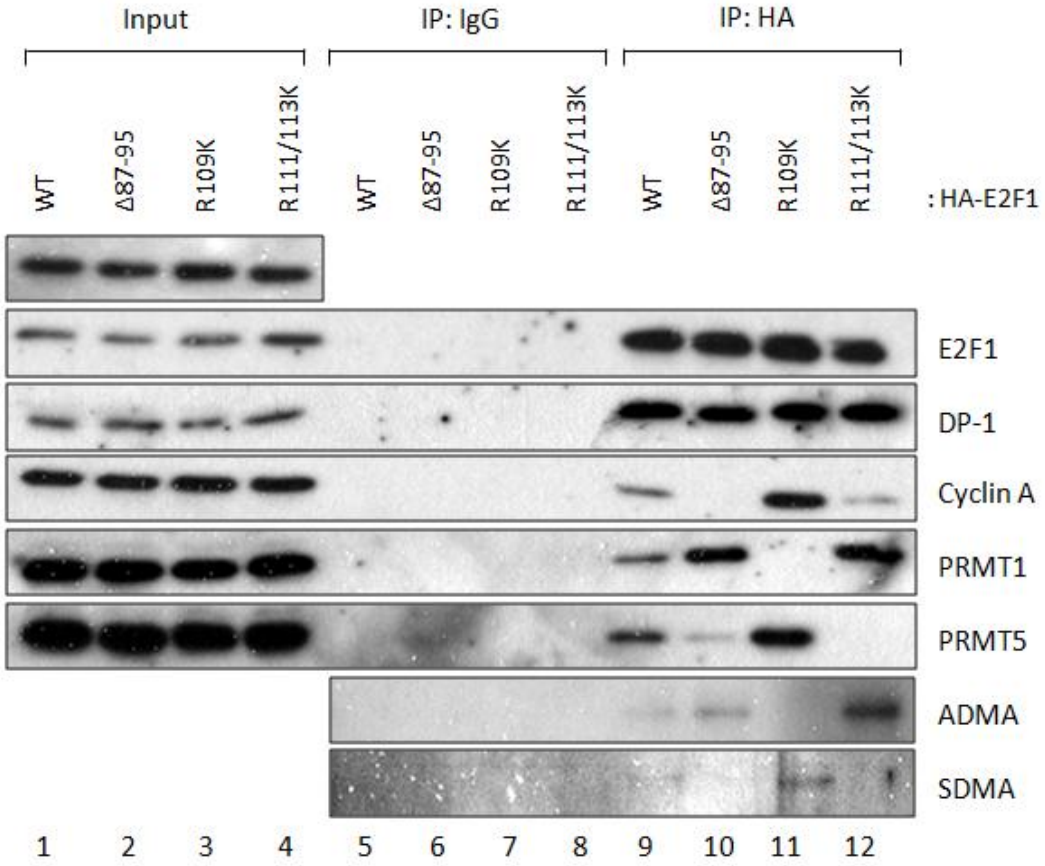

SAOS2 cells were transfected with ~1 µg empty vector control (–) or the indicated HA-E2F1 plasmids and the corresponding lysates were subjected to immunoprecipitation using control IgG or HA antibodies, followed by immunoblotting with the indicated antibodies. Input levels of the respective proteins are shown. Actin was used as loading control.

6.5 Disruption of cyclin A binding alters the influence of E2F1

As an extension to the previous experiment, colony assays (Fig 6.10A to C) and flow cytometry (Fig 6.10D) of cells transfected with E2F1 Δ87-95 mutant were performed to assess the phenotypic consequences arising from lack of cyclin A binding. The relative level of each E2F1 mutant protein is shown (Fig 6.10E). Expression of the Δ87-95 mutant led to a decreased cell growth and increased apoptosis compared to WT E2F1, in a manner similar to R111/113K mutant expression, implying that lack of cyclin A binding site can result in a similar phenotype as the loss of SDMA marks on R111 and R113. This is in contrast with expression of R109K, which saw an increased cell growth and decreased apoptosis compared to WT E2F1 expression. When cells expressing Δ87-95 mutant were treated with etoposide, there was a further reduction in proliferation and increase in apoptosis, suggesting that the effects on cells could be additive. This is unsurprising, as DNA damage has the ability to trigger apoptosis through a wide array of mechanisms.

Figure 6.10 Phenotypes of E2F1 mutant with cyclin A binding site deletion

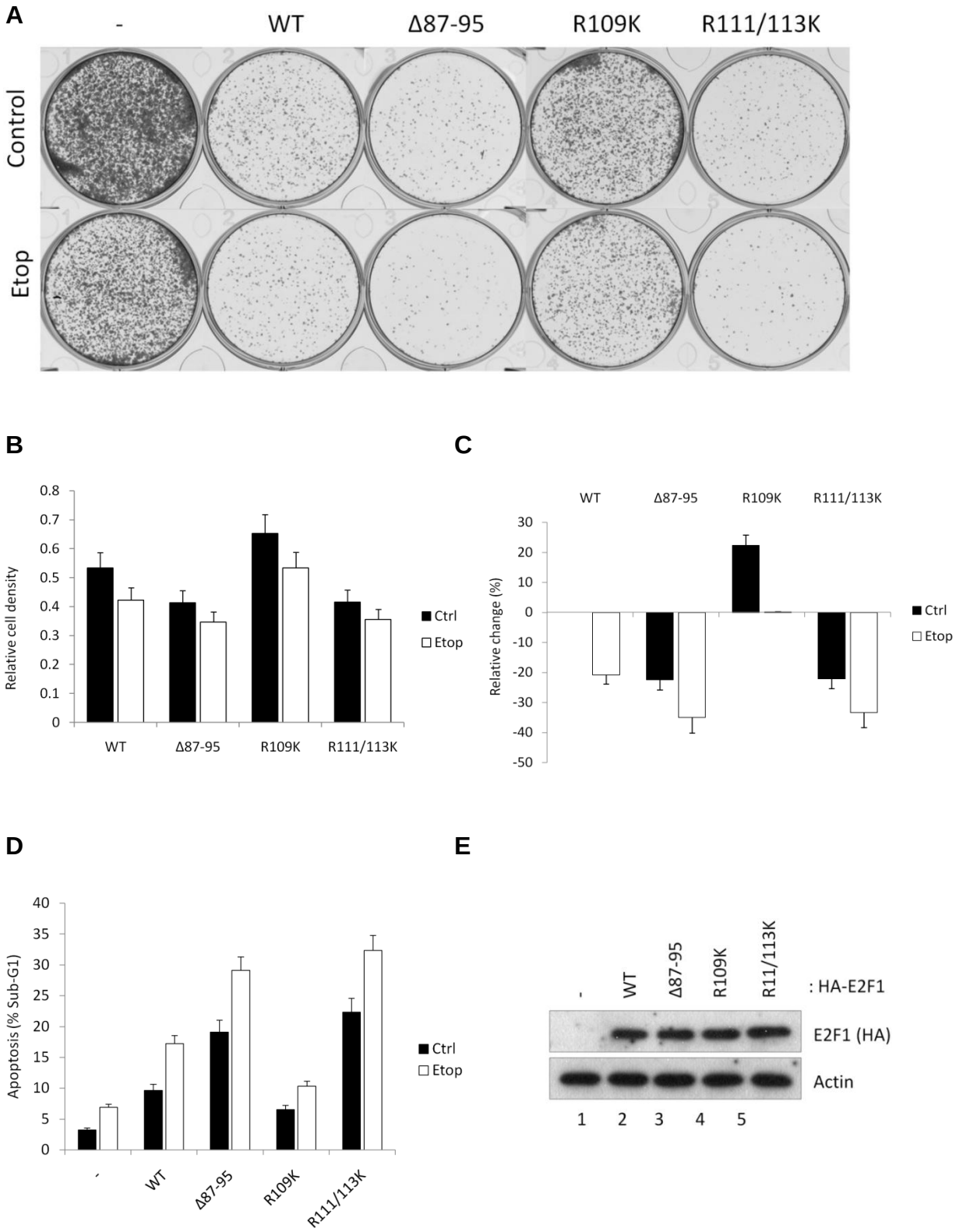

(**A**) SAOS2 cells were seeded at low density in 6-well plates (2000 cells per well) and transfected with ~1 µg empty vector control (–) or HA-E2F1 plasmids as previously described. At 24 hours post-transfection, the cells were treated with 10µM etoposide (Etop) or an equivalent volume of DMSO solvent (Ctrl). After 10 days, the cells were harvested and stained with crystal violet dye.

(**B**) Cell density of the above images relative to empty vector control treatment. DMSO control treatment (Ctrl) are represented by black bars and etoposide treatment (Etop) represented by white bars. Data shown are means of 3 independent experiments with error bars representing standard deviation.

(**C**) Percentage change in cell density relative to wild type E2F1 treatment.

(**D**) Level of apoptosis as percentage of cells in sub-G1. SAOS2 cells were transfected with ~1 µg empty vector control (–) or HA-E2F1 plasmids as previously described. At 24 hours post-transfection, the cells were treated with 10µM etoposide or an equivalent volume of DMSO solvent, and harvested 48 later for FACS analysis. DMSO control treatment (Ctrl) are represented by black bars and etoposide treatment (Etop) represented by white bars. Data shown are means of 3 independent experiments with error bars representing standard deviation; * $p < 0.05$; ** $p < 0.01$

(**E**) Cell lysates reserved for immunoblotting were probed with HA antibody to assess transfected E2F1 protein levels. Actin was used as loading control.

6.6 Chapter summary

From the information gathered, we can conclude that DNA damage causes disruption to the interaction between PRMT5 and E2F1, leading to a decrease in SDMA signals and cell growth. This is achieved not by an overall decrease in PRMT5, but rather, a downregulation of cyclin A level. Since the cyclin A binding site on E2F1 is adjacent to R109, a decrease in cyclin A binding could remove steric hindrance to PRMT1, allowing it to asymmetrically dimethylate R109, which in turn prevents PRMT5 from binding and symmetrically dimethylating R111 and R113. Furthermore, changes to the level of any one of these E2F1 interacting proteins can influence the binding and activity of the other two, thus supporting a model of dynamic interplay between cyclin A, PRMT1 and PRMT5 on E2F1 (Fig 6.11). In this chapter, I have shown how modulation of E2F1 methylation may be achieved through DNA damage by depletion of cyclin A. However, this does not preclude the possibility of modulating E2F1 arginine methylation through other mechanisms.

Figure 6.11 Dynamic interplay between cyclin A, PRMT1 and PRMT5

A No damage

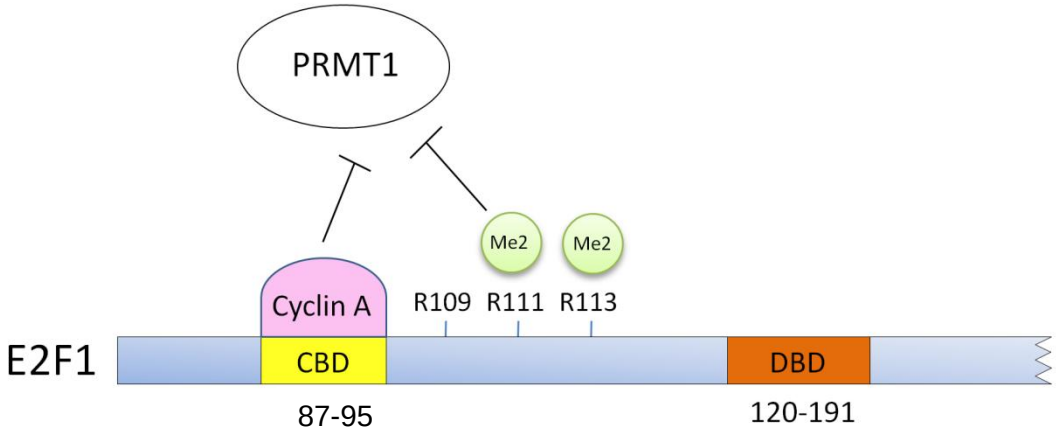

B DNA damage

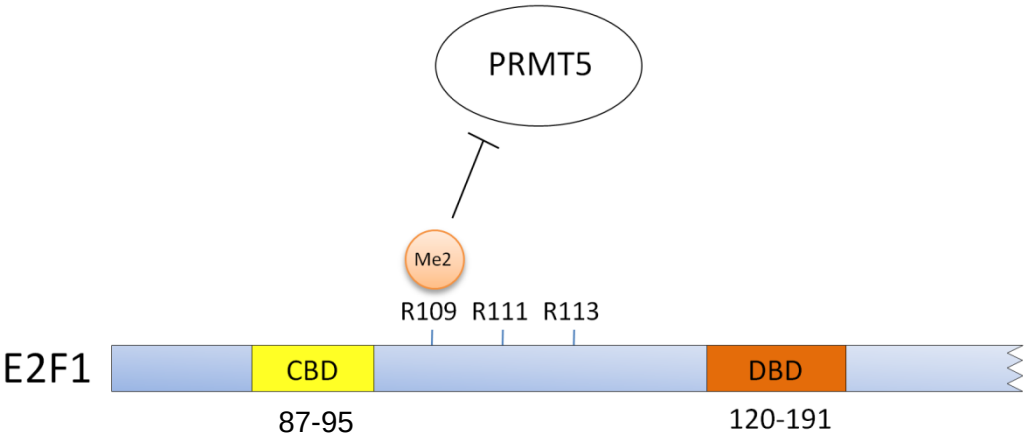

The cyclin A binding site on E2F1 lies in the region between residues 87 to 95 and PRMT1 methylates the adjacent R109. If symmetric dimethylation on R111 and R113 could sterically block PRMT1 and prevent asymmetric dimethylation of R109, it is possible that cyclin A binding also does. The binding competition between these three players is dynamic; removal of one will affect the other two. DNA damage causes an overall decrease in cyclin A, which relieves the block on PRMT1, allowing R109 to be asymmetrically dimethylated. The ADMA in turn prevents PRMT5 binding and symmetric dimethylation of R111 and R113. CBD – Cyclin A binding domain; DBD – DNA binding domain.

Chapter 7 Discussion

7.1 Insights from this study

E2F1 is a transcription factor that can activate a diverse set of genes, including those that govern cell proliferation, apoptosis and DNA damage response. The activity of this master regulator itself is carefully controlled via multiple layers of regulation, including but not limited to post-translational modifications (PTMs).

In this study, two new PTMs were discovered on E2F1. PRMT1 was found to asymmetrically dimethylate R109 on E2F1, whereas PRMT5 symmetrically dimethylates R111 and R113. These PRMTs compete for binding and methylation of adjacent residues on an RG-rich motif. The ADMA and SDMA marks have opposing effects on the molecular properties of E2F1 and the phenotypes they induce. The ADMA mark on R109 increases E2F1 protein stability, promotes transcription, inhibits proliferation and enhances cell death, while the SDMA marks on R111 and R113 give the opposite effect. As co-depletion of both PRMTs always led to responses similar to that of PRMT5 depletion alone, it is likely that the changes caused by ADMA signals was mediated through the antagonism of SDMAs.

The SDMA marks on E2F1 are essential for the recruitment of Skp2, which forms part of an ubiquitin ligase complex. It is likely that the polyubiquitination of E2F1 and its subsequent degradation by the proteasome complex is one of the

many ways in which E2F1 activity can be regulated. Removal of the SDMA marks not only enhances E2F1 protein stability, but also increases its affinity to target gene promoters. This is particularly significant for the activation of apoptotic gene targets which, compared to proliferative targets, are reported to have lower affinities for E2F1 (Pediconi et al., 2003). The ability to transcriptionally activate apoptotic gene targets sets E2F1 apart from other members of the E2F family (DeGregori et al., 1997; Hallstrom and Nevins, 2003; Lazzerini Denchi and Helin, 2005). Hence, it provides an explanation of how PRMT5 depletion reduces cell proliferation through the enhancement of E2F1-dependent apoptosis.

Cells inflicted with DNA damage usually undergo cell cycle arrest or apoptosis. The associated DNA damage response is governed centrally by transcription factors such as p53 or E2F1. Due to the close proximity of the E2F1 cyclin A binding site and the RG-rich motif, a DNA damage-triggered reduction in cyclin A may remove steric hindrance to PRMT1, promoting ADMA marks on R109, and concomitantly reducing SDMA marks on R111 and R113. The interplay between cyclin A, PRMT1 and PRMT5 appears to be dynamic, as removal of any component can affect binding of the other two.

Together, these findings allow us to understand how two different forms of arginine dimethylation may compete against each other to bring about changes to gene transcription and cell growth.

7.2 Effects of DNA damage on E2F1 PTM status

In this study, it was shown that DNA damage impacts on E2F1 arginine methylation status. However, it should be noted that other post-translational modifications are also affected under DNA damage. These PTMs may also contribute to changes in E2F1 protein stability, promoter affinity, transcriptional activity and protein/DNA interactions.

Activation of ATM/ATR is a well-established indicator of DNA damage which leads to the phosphorylation of E2F1 at serine 31 (Lin et al., 2001). CHK2, a downstream target of ATM, is also activated upon DNA damage and phosphorylates E2F1 at serine 364 (Stevens et al., 2003). These phosphorylation events trigger the recruitment of p300/CBP-associated factor (PCAF) or p300, which acetylates E2F1 on lysines K117, K120 and K125 (Ianari et al., 2004). As these lysines are juxtaposed to the E2F1 RG-rich motif, it is possible that their acetylation may also sterically affect arginine methylation.

We should also consider the impact of DNA damage on CDK2 activity. In normal cell cycle progression, activation of CDK2 by cyclin A binding allows E2F1 phosphorylation at serine 375 (Xu et al., 1994). This phosphorylation leads to reduced DNA binding and it is possible that the decrease in cyclin A seen under DNA damage may result in the opposite. This could be clarified through further experimentation. It is also plausible that crosstalk between E2F1 methylation and phosphorylation exists and further investigation is needed to explore their relationship.

PTMs have the potential to alter the properties of proteins but they are unlikely to occur in isolation. In reality, it is likely that a certain pattern of PTMs ensure that E2F1 drives growth under normal conditions, while another pattern of PTMs results in cell cycle arrest or apoptosis during DNA damage. Therefore, arginine methylation should not be pictured as the sole contributing factor in E2F1 regulation, but its importance should nevertheless be recognised within the context of other important PTMs.

7.3 E2F1 PTMs as cancer biomarkers

Clinical evaluations of tumour samples have indicated that E2F1 (Verhaegen et al., 2012), PRMT1 (Mathioudaki et al., 2011) and PRMT5 (Wei et al., 2012) were individually elevated in melanomas, breast and lung cancers. An online database search of gene expression levels in clinical samples revealed that in cancers with elevated PRMT5, the expression of PRMT1 or E2F1 was downregulated, whereas in cancers with elevated E2F1 or PRMT1, the expression of PRMT5 was lower than normal (Fig 7.1). This, in part, verifies our model of PRMTs regulation of E2F1. However, more work needs to be done to determine how these expression combinations correlate with tumour progression and patient survival.

In addition, results from this study suggest that the absolute levels of PRMT1 or PRMT5 may not be as important as their interactions with E2F1, and the types of methylation marks they put on it. It may be useful to consider using arginine methylation status as a biomarker of cancer progression. In broader context, it is now clear that E2F1 shows different PTM patterns under different conditions. By using cutting-edge custom antibody technologies, it may be possible to map out linkages between overall PTM status of E2F1 and disease progression, thereby creating more accurate cancer biomarkers.

Figure 7.1 Correlation between E2F1 and PRMTs in human cancers

A

Gene Expression across Normal and Tumour tissue (GENT)

U133A Database — No. of Tissue Samples

PRMT5 High	PRMT1 Low	E2F1 Low	Cancer	Normal
Bladder		Bladder	87	15
Breast		Breast	2635	91
Kidney		Kidney	366	66
Pancreas	Pancreas	Pancreas	13	8
Prostate		Prostate	244	83
Testis		Testis	184	13
PRMT5 Low	**PRMT1 High**	**E2F1 High**		
Cervix	Cervix (NS)	Cervix	64	34
Head_Neck	Head_Neck	Head_Neck	21	2
Skin	Skin	Skin	499	59
Thyroid	Thyroid (NS)	Thyroid	44	25

B

Comparison of E2F1, PRMT1 and PRMT5 in Badea Pancreas

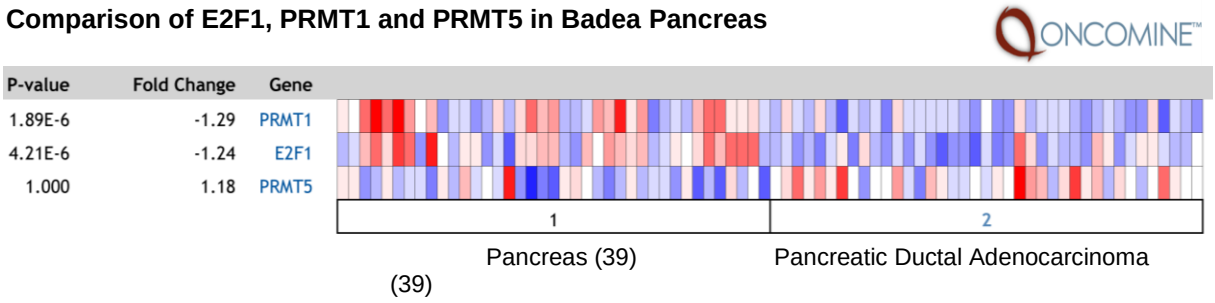

(**A**) A bioinformatics search in the public database GENT revealed a list of cancers that display positive correlation between E2F1 and PRMT1, as well as inverse correlation between E2F1 and PRMT5. The data was published in the journal Cancer Informatics (Shin et al., 2011).

(**B**) A human genome array was used to compare the expression levels of E2F1, PRMT1 and PRMT5 in normal pancreas and pancreatic cancer. The data was published in the journal Hepatogastroenterology (Badea et al., 2008). Oncomine™ (Compendia Bioscience, Ann Arbor, MI) was used for analysis and visualization.

7.4 Harnessing the power of E2F1 apoptosis in cancer

Recent reviews by David Engelmann and Brigitte M. Pützer propose that E2F1 may trigger tumour invasion and metastasis, arguing that at a certain point in cancer progression, E2F1 can flip from a tumour suppressor back into an oncogene (Engelmann and Putzer, 2012; Putzer and Engelmann, 2013). This usually occurs in late stage cancers when aberrations of other molecular pathways are implicated and the tumour cells have gained chemoresistance.

Although elevated E2F1 expression is associated with a large number of cancers, a sizable body of evidence over the past two decades have confirmed the fact that overexpression of E2F1 in human cancer cells can lead to enhanced apoptosis (Lazzerini Denchi and Helin, 2005). Increased transcription of pro-apoptotic gene targets such as *TP73* (Lissy et al., 2000) and *APAF1* (Moroni et al., 2001) caused by overexpression of E2F1 amounted to significant increases in apoptosis. A concurrent depletion of p73 (Stiewe and Putzer, 2000) and Apaf-1 rescued cell death (Furukawa et al., 2002), providing mechanistic examples of how overexpression of E2F1 may induce apoptosis. In that case, the overarching question in E2F1 biology is why in the context of cellular microevolution would it be advantageous for cancer cells to be selected for E2F1 overexpression?

The working theory in the field suggests that a certain threshold of E2F activity needs to be reached before apoptotic targets can be turned on (Trimarchi and Lees, 2002). Below this threshold, any increase in E2F1 activity serves only to activate its proliferative functions, such as cell cycle progression and DNA

replication (Fig 7.2). The threshold may be reached by increasing total E2F1 protein levels or its affinity to pro-apoptotic genes, both which can be achieved by inhibiting PRMT5. The potential risk of increasing E2F1 expression in patients is that if the threshold is not reached, the elevated E2F1 may promote cancer progression. While it is possible to use inducible plasmid expression systems or viral transfection in cell or animal models, such delivery systems are not currently suitable for use in humans. A feasible alternative strategy would be to design inhibitory drugs against modulators of E2F1 activity, such as PRMT5.

Figure 7.2 Relationship between E2F1 activity and tumour growth

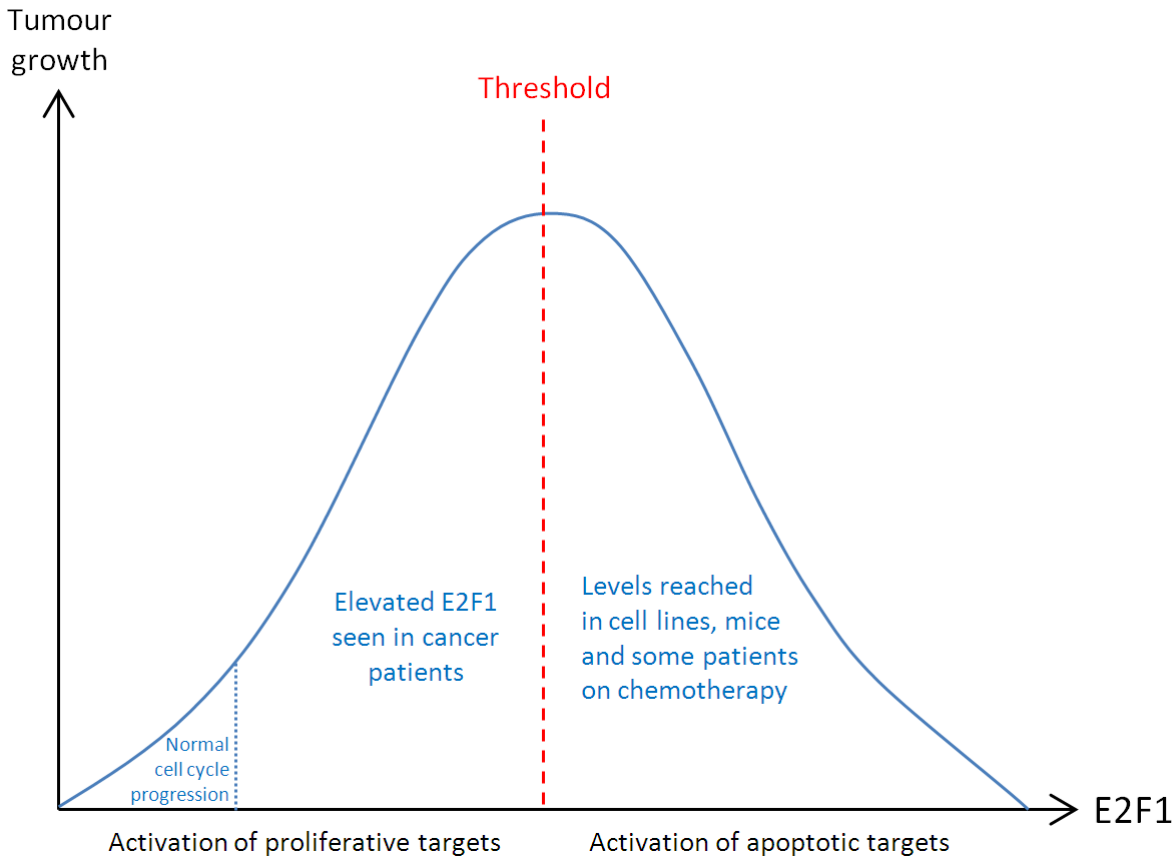

Accumulated results from previous studies in cell lines, animals and humans all point to the presence of a threshold level which E2F1 switches from growth promotion to inhibition (red dashed line). In normal cells, E2F1 activity is regulated by the cell cycle but the levels are kept low. In tumour cells of cancer patients, deregulation of the E2F1 pathway results in activation of proliferative genes, resulting in enhanced growth. Tumour growth in this phase is proportional to E2F1 levels. Artificial overexpression of E2F1 through plasmid/ viral transfection or chemotherapeutic drugs allows cells to cross the threshold and activate apoptotic genes. Tumour growth in this phase is inversely correlated with E2F1 levels.

7.5 PRMT5 as a drug target

Despite the upregulation of both PRMT1 and PRMT5 in cancers, the use of PRMT1 as a chemotherapeutic target may be fraught with difficulties as inhibition of its activity promotes E2F1 symmetric dimethylation at R111 and R113, resulting in enhanced cell growth. On the contrary, removal of SDMA marks from R111 and R113 has been shown to trigger E2F1-dependent apoptosis. Hence, the development of inhibitors that disrupt PRMT5 catalytic activity may work as an effective anti-cancer strategy. PRMT inhibitors that are available on the market to date, such as AMI-1, work by competition with the cofactor SAM/AdoMet, the common methyl-group donor to all PRMTs. Clearly, such a mode of action would not be specific for PRMT5 inhibition. A better strategy would be to synthesize an inhibitor that competes with the E2F1 RG-rich motif, preventing its symmetric dimethylation. Alternatively, the activity of PRMT5 in cells could be specifically attenuated by disrupting its interaction with MEP50. However, it is worth noting that this strategy would result in PRMT5 substrates other than E2F1 to become unmethylated, such as p53 and histones H3R8 and H4R3. Nevertheless, since PRMT5 is markedly elevated in cancer versus normal tissue, it is possible that treatment with PRMT5 inhibitors may selectively kill cancer cells while minimizing the negative effects on normal tissue by exploiting this expressional difference. This study also provides a proof of concept that PRMT5 inhibition could sensitize cancer cells to treatment with chemotherapy drugs. The development of specific PRMT5 inhibitors would make it easier to investigate drug synergy.

7.6 Readers of E2F1 arginine methylation

From the results obtained, it can be deduced that the two symmetric dimethyl groups on R111 and R113 are primarily responsible for the changes in E2F1 molecular properties and the resulting phenotypes, while PRMT1 and cyclin A function as modulators of SDMA marks on E2F1. Although the interplay between cyclin A, PRMT1 and PRMT5 on E2F1 has been established, the mechanism through which they exert their effects remains unclear. In addition to exerting steric effects, it may be possible that the SDMAs on E2F1 serve as recognition sites for effector proteins. The “readers” of these SDMA marks may be from the Tudor domain-containing protein (TDRD) family, the only identified group of proteins that contain methylarginine-binding structures (Chen et al., 2011). A binding assay utilizing methylated E2F1 peptides may reveal the identity of these effector proteins and allows us to have a finer picture of how these methylation “readers” and “writers” work together to regulate E2F1.

7.7 Conclusion

Over the past century, research carried out by cancer scientists, drug developers and medical doctors have steadily improved people's chances of survival from cancer. By understanding the science behind cellular biochemistry and the deregulation that happens in cancer, it has made possible for the development of cancer vaccines and chemotherapy drugs, saving millions of lives worldwide. As the life expectancy of the world population increases, so will the cancer incidences, and more people will stand to benefit from new discoveries in cancer biology.

E2F1, a master regulator of cell growth, is deregulated in a great majority of cancers, which makes it an attractive anti-cancer target. This study reveals how E2F1 activity can be modulated by PRMT1 and PRMT5, the representative type I and II arginine methyltransferases. Symmetric dimethylation of R111 and R113 by PRMT5 helps recruit Skp2, part of the ubiquitin ligase complex, to E2F1 and promotes its degradation. The SDMA marks also decreases DNA binding affinity of E2F1 to its target gene promoters, attenuating its transcriptional activity. Asymmetric dimethylation of R109 by PRMT1 reverses these trends by sterically hindering the SDMA marks. The ADMA marks are in turn negatively regulated by interaction between cyclin A and E2F1. The dynamic interplay between cyclin A, PRMT1 and PRMT5 can be modulated by external stimuli such as the addition of DNA damaging agents, which decreases cyclin A level, resulting in decreased cell growth and increased apoptosis. It is hypothesized that the SDMA marks on E2F1

are crucial for the recognition and binding by effector proteins such as those that contain Tudor domains.

Given that E2F1 is responsible for regulating the transcription of a wide spectrum of genes, it is unsurprising to find that its activity is regulated by a large number of post-translational modifications. The discovery of arginine methylation adds a piece of the puzzle to the overall picture of E2F1 regulation, allowing us to have a better understanding of how cell growth and death may be modulated. The knowledge generated in this study provides a reference for researchers working on the Rb/E2F1 pathway, arginine methylation of non-histone proteins, competition between type I and II PRMTs, and many more. In time, the accumulated knowledge stemming from this research may find its way into useful medical applications and bring about benefit to society.

References

1. (1984). IUPAC-IUB Joint Commission on Biochemical Nomenclature (JCBN). Nomenclature and symbolism for amino acids and peptides. Recommendations 1983. Biochem J *219*, 345-373.
2. Adams, P.D., and Kaelin, W.G., Jr. (1995). Transcriptional control by E2F. Semin. Cancer Biol. 6, 99-108.
3. Aggarwal, P., Vaites, L. P., Kim, J. K., Mellert, H., Gurung, B., Nakagawa, H., Herlyn, M., Hua, X., Rustgi, A. K., McMahon, S. B., and Diehl, J. A. (2010). Nuclear cyclin D1/CDK4 kinase regulates CUL4 expression and triggers neoplastic growth via activation of the PRMT5 methyltransferase. Cancer cell *18*, 329-340.
4. Andreu-Perez, P., Esteve-Puig, R., de Torre-Minguela, C., Lopez-Fauqued, M., Bech-Serra, J. J., Tenbaum, S., Garcia-Trevijano, E. R., Canals, F., Merlino, G., Avila, M. A., and Recio, J. A. (2011). Protein arginine methyltransferase 5 regulates ERK1/2 signal transduction amplitude and cell fate through CRAF. Science signaling *4*, ra58.
5. Antman, K., and Chang, Y. (2000). Kaposi's sarcoma. The New England journal of medicine *342*, 1027-1038.
6. Antonysamy, S., Bonday, Z., Campbell, R. M., Doyle, B., Druzina, Z., Gheyi, T., Han, B., Jungheim, L. N., Qian, Y., Rauch, C*., et al.* (2012). Crystal structure of the human PRMT5:MEP50 complex. Proceedings of the National Academy of Sciences of the United States of America *109*, 17960-17965.
7. Badea, L., Herlea, V., Dima, S. O., Dumitrascu, T., and Popescu, I. (2008). Combined gene expression analysis of whole-tissue and microdissected pancreatic ductal adenocarcinoma identifies genes specifically overexpressed in tumor epithelia. Hepato-gastroenterology *55*, 2016-2027.
8. Bandara, L. R., and La Thangue, N. B. (1991). Adenovirus E1a prevents the retinoblastoma gene product from complexing with a cellular transcription factor. Nature *351*, 494-497.
9. Bandara, L. R., Lam, E. W., Sorensen, T. S., Zamanian, M., Girling, R., and La Thangue, N. B. (1994). DP-1: a cell cycle-regulated and phosphorylated component of transcription factor DRTF1/E2F which is functionally important for recognition by pRb and the adenovirus E4 orf 6/7 protein. The EMBO journal *13*, 3104-3114.
10. Bedford, M. T., and Clarke, S. G. (2009). Protein arginine methylation in mammals: who, what, and why. Molecular cell *33*, 1-13.
11. Bedford, M. T., Frankel, A., Yaffe, M. B., Clarke, S., Leder, P., and Richard, S. (2000). Arginine methylation inhibits the binding of proline-rich ligands to Src homology 3, but not WW, domains. J Biol Chem *275*, 16030-16036.
12. Benassi, M. S., Molendini, L., Gamberi, G., Ragazzini, P., Sollazzo, M. R., Merli, M., Asp, J., Magagnoli, G., Balladelli, A., Bertoni, F., and Picci, P. (1999). Alteration of pRb/p16/cdk4 regulation in human osteosarcoma. International journal of cancer Journal international du cancer *84*, 489-493.
13. Berdasco, M., and Esteller, M. (2010). Aberrant epigenetic landscape in cancer: how cellular identity goes awry. Dev Cell *19*, 698-711.
14. Berkovich, E., and Ginsberg, D. (2003). ATM is a target for positive regulation by E2F-1. Oncogene *22*, 161-167.

15. Blattner, C., Sparks, A., and Lane, D. (1999). Transcription factor E2F-1 is upregulated in response to DNA damage in a manner analogous to that of p53. Molecular and cellular biology *19*, 3704-3713.
16. Boffa, L. C., Karn, J., Vidali, G., and Allfrey, V. G. (1977). Distribution of NG, NG,-dimethylarginine in nuclear protein fractions. Biochem Biophys Res Commun *74*, 969-976.
17. Boisvert, F. M., Rhie, A., Richard, S., and Doherty, A. J. (2005). The GAR motif of 53BP1 is arginine methylated by PRMT1 and is necessary for 53BP1 DNA binding activity. Cell Cycle *4*, 1834-1841.
18. Boulanger, M. C., Miranda, T. B., Clarke, S., Di Fruscio, M., Suter, B., Lasko, P., and Richard, S. (2004). Characterization of the Drosophila protein arginine methyltransferases DART1 and DART4. The Biochemical journal *379*, 283-289.
19. Buendia, M. A. (1992). Hepatitis B viruses and hepatocellular carcinoma. Advances in cancer research *59*, 167-226.
20. Cha, B., Kim, W., Kim, Y. K., Hwang, B. N., Park, S. Y., Yoon, J. W., Park, W. S., Cho, J. W., Bedford, M. T., and Jho, E. H. (2011). Methylation by protein arginine methyltransferase 1 increases stability of Axin, a negative regulator of Wnt signaling. Oncogene *30*, 2379-2389.
21. Chen, C., Nott, T. J., Jin, J., and Pawson, T. (2011). Deciphering arginine methylation: Tudor tells the tale. Nature reviews Molecular cell biology *12*, 629-642.
22. Cheng, D., Cote, J., Shaaban, S., and Bedford, M. T. (2007). The arginine methyltransferase CARM1 regulates the coupling of transcription and mRNA processing. Mol Cell *25*, 71-83.
23. Chern, M. K., Chang, K. N., Liu, L. F., Tam, T. C., Liu, Y. C., Liang, Y. L., and Tam, M. F. (2002). Yeast ribosomal protein L12 is a substrate of protein-arginine methyltransferase 2. The Journal of biological chemistry *277*, 15345-15353.
24. Cheung, N., Chan, L. C., Thompson, A., Cleary, M. L., and So, C. W. (2007). Protein arginine-methyltransferase-dependent oncogenesis. Nat Cell Biol *9*, 1208-1215.
25. Chiang, A. C., and Massague, J. (2008). Molecular basis of metastasis. N Engl J Med *359*, 2814-2823.
26. Cho, E. C., Zheng, S., Munro, S., Liu, G., Carr, S. M., Moehlenbrink, J., Lu, Y. C., Stimson, L., Khan, O., Konietzny, R.*, et al.* (2012). Arginine methylation controls growth regulation by E2F-1. EMBO J *31*, 1785-1797.
27. Connolly, K. M., and Bogdanffy, M. S. (1993). Evaluation of proliferating cell nuclear antigen (PCNA) as an endogenous marker of cell proliferation in rat liver: a dual-stain comparison with 5-bromo-2'-deoxyuridine. The journal of histochemistry and cytochemistry : official journal of the Histochemistry Society *41*, 1-6.
28. Croce, C. M. (2008). Oncogenes and cancer. N Engl J Med *358*, 502-511.
29. de Bruin, A., Maiti, B., Jakoi, L., Timmers, C., Buerki, R., and Leone, G. (2003). Identification and characterization of E2F7, a novel mammalian E2F family member capable of blocking cellular proliferation. The Journal of biological chemistry *278*, 42041-42049.
30. DeGregori, J., and Johnson, D. G. (2006). Distinct and Overlapping Roles for E2F Family Members in Transcription, Proliferation and Apoptosis. Curr Mol Med *6*, 739-748.
31. DeGregori, J., Leone, G., Miron, A., Jakoi, L., and Nevins, J. R. (1997). Distinct roles for E2F proteins in cell growth control and apoptosis. Proceedings of the National Academy of Sciences of the United States of America *94*, 7245-7250.
32. DH (2007). Cancer Reform Strategy. In, (UK Department of Health).
33. Di Stefano, L., Jensen, M. R., and Helin, K. (2003). E2F7, a novel E2F featuring DP-independent repression of a subset of E2F-regulated genes. The EMBO journal *22*, 6289-6298.

34. Dimova, D. K., and Dyson, N. J. (2005). The E2F transcriptional network: old acquaintances with new faces. Oncogene *24*, 2810-2826.
35. Downward, J. (2003). Targeting RAS signalling pathways in cancer therapy. Nat Rev Cancer *3*, 11-22.
36. Dynlacht, B. D., Brook, A., Dembski, M., Yenush, L., and Dyson, N. (1994). DNA-binding and trans-activation properties of Drosophila E2F and DP proteins. Proc Natl Acad Sci U S A *91*, 6359-6363.
37. Emili, A., and Ingles, C. J. (1995). Promoter-dependent photocross-linking of the acidic transcriptional activator E2F-1 to the TATA-binding protein. J Biol Chem *270*, 13674-13680.
38. Engelmann, D., and Putzer, B. M. (2012). The dark side of E2F1: in transit beyond apoptosis. Cancer research *72*, 571-575.
39. Evan, G. I., and Vousden, K. H. (2001). Proliferation, cell cycle and apoptosis in cancer. Nature *411*, 342-348.
40. Fabbrizio, E., El Messaoudi, S., Polanowska, J., Paul, C., Cook, J. R., Lee, J. H., Negre, V., Rousset, M., Pestka, S., Le Cam, A., and Sardet, C. (2002). Negative regulation of transcription by the type II arginine methyltransferase PRMT5. EMBO Rep *3*, 641-645.
41. Farber, E. (1994). Programmed cell death: necrosis versus apoptosis. Mod Pathol *7*, 605-609.
42. Feng, M., and Yu, Q. (2010). miR-449 regulates CDK-Rb-E2F1 through an auto-regulatory feedback circuit. Cell Cycle *9*, 213-214.
43. Field, S. J., Tsai, F. Y., Kuo, F., Zubiaga, A. M., Kaelin, W. G., Jr., Livingston, D. M., Orkin, S. H., and Greenberg, M. E. (1996). E2F-1 functions in mice to promote apoptosis and suppress proliferation. Cell *85*, 549-561.
44. Finzer, P., Krueger, A., Stohr, M., Brenner, D., Soto, U., Kuntzen, C., Krammer, P. H., and Rosl, F. (2004). HDAC inhibitors trigger apoptosis in HPV-positive cells by inducing the E2F-p73 pathway. Oncogene *23*, 4807-4817.
45. Friedberg, E. C., Aguilera, A., Gellert, M., Hanawalt, P. C., Hays, J. B., Lehmann, A. R., Lindahl, T., Lowndes, N., Sarasin, A., and Wood, R. D. (2006). DNA repair: from molecular mechanism to human disease. DNA Repair (Amst) *5*, 986-996.
46. Friend, S. H., Bernards, R., Rogelj, S., Weinberg, R. A., Rapaport, J. M., Albert, D. M., and Dryja, T. P. (1986). A human DNA segment with properties of the gene that predisposes to retinoblastoma and osteosarcoma. Nature *323*, 643-646.
47. Frolov, M. V., Huen, D. S., Stevaux, O., Dimova, D., Balczarek-Strang, K., Elsdon, M., and Dyson, N. J. (2001). Functional antagonism between E2F family members. Genes Dev *15*, 2146-2160.
48. Furukawa, Y., Nishimura, N., Satoh, M., Endo, H., Iwase, S., Yamada, H., Matsuda, M., Kano, Y., and Nakamura, M. (2002). Apaf-1 is a mediator of E2F-1-induced apoptosis. The Journal of biological chemistry *277*, 39760-39768.
49. Gary, J. D., and Clarke, S. (1998). RNA and protein interactions modulated by protein arginine methylation. Progress in nucleic acid research and molecular biology *61*, 65-131.
50. Gaubatz, S., Lees, J. A., Lindeman, G. J., and Livingston, D. M. (2001). E2F4 is exported from the nucleus in a CRM1-dependent manner. Molecular and cellular biology *21*, 1384-1392.
51. Gaubatz, S., Wood, J. G., and Livingston, D. M. (1998). Unusual proliferation arrest and transcriptional control properties of a newly discovered E2F family member, E2F-6. Proceedings of the National Academy of Sciences of the United States of America *95*, 9190-9195.
52. Girling, R., Partridge, J. F., Bandara, L. R., Burden, N., Totty, N. F., Hsuan, J. J., and La Thangue, N. B. (1993). A new component of the transcription factor DRTF1/E2F. Nature *365*, 468.

53. Goulet, I., Gauvin, G., Boisvenue, S., and Cote, J. (2007). Alternative splicing yields protein arginine methyltransferase 1 isoforms with distinct activity, substrate specificity, and subcellular localization. J Biol Chem *282*, 33009-33021.
54. Grivennikov, S. I., Greten, F. R., and Karin, M. (2010). Immunity, inflammation, and cancer. Cell *140*, 883-899.
55. Gunawardena, R. W., Siddiqui, H., Solomon, D. A., Mayhew, C. N., Held, J., Angus, S. P., and Knudsen, E. S. (2004). Hierarchical requirement of SWI/SNF in retinoblastoma tumor suppressor-mediated repression of Plk1. J Biol Chem *279*, 29278-29285.
56. Guo, A., Salomoni, P., Luo, J., Shih, A., Zhong, S., Gu, W., and Pandolfi, P. P. (2000). The function of PML in p53-dependent apoptosis. Nat Cell Biol *2*, 730-736.
57. Hallstrom, T. C., and Nevins, J. R. (2003). Specificity in the activation and control of transcription factor E2F-dependent apoptosis. Proceedings of the National Academy of Sciences of the United States of America *100*, 10848-10853.
58. Hanahan, D., and Weinberg, R. A. (2011). Hallmarks of cancer: the next generation. Cell *144*, 646-674.
59. Harbour, J. W., Luo, R. X., Dei Santi, A., Postigo, A. A., and Dean, D. C. (1999). Cdk phosphorylation triggers sequential intramolecular interactions that progressively block Rb functions as cells move through G1. Cell *98*, 859-869.
60. Hatakeyama, M., and Weinberg, R. A. (1995). The role of RB in cell cycle control. Progress in cell cycle research *1*, 9-19.
61. Helin, K., Kees, J.A., Vidal, M., Dyson, N., Harlow, E., and Fattaey, A. (1992). A cDNA encoding a pRB-binding protein with properties of the transcription factor E2F. Cell 70, 337-350.
62. Helin, K., Wu, C. L., Fattaey, A. R., Lees, J. A., Dynlacht, B. D., Ngwu, C., and Harlow, E. (1993). Heterodimerization of the transcription factors E2F-1 and DP-1 leads to cooperative trans-activation. Genes Dev *7*, 1850-1861.
63. Hershko, T., Chaussepied, M., Oren, M., and Ginsberg, D. (2005). Novel link between E2F and p53: proapoptotic cofactors of p53 are transcriptionally upregulated by E2F. Cell Death Differ *12*, 377-383.
64. Higashimoto, K., Kuhn, P., Desai, D., Cheng, X., and Xu, W. (2007). Phosphorylation-mediated inactivation of coactivator-associated arginine methyltransferase 1. Proceedings of the National Academy of Sciences of the United States of America *104*, 12318-12323.
65. Hochegger, H., Takeda, S., and Hunt, T. (2008). Cyclin-dependent kinases and cell-cycle transitions: does one fit all? Nat Rev Mol Cell Biol *9*, 910-916.
66. Hollstein, M., Sidransky, D., Vogelstein, B., and Harris, C. C. (1991). p53 mutations in human cancers. Science *253*, 49-53.
67. Hou, Z., Peng, H., Ayyanathan, K., Yan, K. P., Langer, E. M., Longmore, G. D., and Rauscher, F. J., 3rd (2008). The LIM protein AJUBA recruits protein arginine methyltransferase 5 to mediate SNAIL-dependent transcriptional repression. Mol Cell Biol *28*, 3198-3207.
68. Hsieh, J. K., Fredersdorf, S., Kouzarides, T., Martin, K., and Lu, X. (1997). E2F1-induced apoptosis requires DNA binding but not transactivation and is inhibited by the retinoblastoma protein through direct interaction. Genes Dev *11*, 1840-1852.
69. Hsieh, J. K., Yap, D., O'Connor, D. J., Fogal, V., Fallis, L., Chan, F., Zhong, S., and Lu, X. (2002). Novel function of the cyclin A binding site of E2F in regulating p53-induced apoptosis in response to DNA damage. Mol Cell Biol *22*, 78-93.
70. Hughes, R. M., and Waters, M. L. (2006). Arginine methylation in a beta-hairpin peptide: implications for Arg-pi interactions, DeltaCp(o), and the cold denatured state. J Am Chem Soc *128*, 12735-12742.

71. Hung, C. M., and Li, C. (2004). Identification and phylogenetic analyses of the protein arginine methyltransferase gene family in fish and ascidians. Gene *340*, 179-187.
72. Ianari, A., Gallo, R., Palma, M., Alesse, E., and Gulino, A. (2004). Specific role for p300/CREB-binding protein-associated factor activity in E2F1 stabilization in response to DNA damage. The Journal of biological chemistry *279*, 30830-30835.
73. Iavarone, A., and Massague, J. (1999). E2F and histone deacetylase mediate transforming growth factor beta repression of cdc25A during keratinocyte cell cycle arrest. Molecular and cellular biology *19*, 916-922.
74. Ikeda, M. A., Jakoi, L., and Nevins, J. R. (1996). A unique role for the Rb protein in controlling E2F accumulation during cell growth and differentiation. Proceedings of the National Academy of Sciences of the United States of America *93*, 3215-3220.
75. Irwin, M., Marin, M. C., Phillips, A. C., Seelan, R. S., Smith, D. I., Liu, W., Flores, E. R., Tsai, K. Y., Jacks, T., Vousden, K. H., and Kaelin, W. G., Jr. (2000). Role for the p53 homologue p73 in E2F-1-induced apoptosis. Nature *407*, 645-648.
76. Ivanova, I. A., Nakrieko, K. A., and Dagnino, L. (2009). Phosphorylation by p38 MAP kinase is required for E2F1 degradation and keratinocyte differentiation. Oncogene *28*, 52-62.
77. Ivanova, I. A., Vespa, A., and Dagnino, L. (2007). A novel mechanism of E2F1 regulation via nucleocytoplasmic shuttling: determinants of nuclear import and export. Cell Cycle *6*, 2186-2195.
78. Jansson, M., Durant, S. T., Cho, E. C., Sheahan, S., Edelmann, M., Kessler, B., and La Thangue, N. B. (2008). Arginine methylation regulates the p53 response. Nature cell biology *10*, 1431-1439.
79. Jemal, A., Bray, F., Center, M. M., Ferlay, J., Ward, E., and Forman, D. (2011). Global cancer statistics. CA Cancer J Clin *61*, 69-90.
80. Ji, J. Y., Miles, W. O., Korenjak, M., Zheng, Y., and Dyson, N. J. (2012). In Vivo Regulation of E2F1 by Polycomb Group Genes in Drosophila. G3 (Bethesda) *2*, 1651-1660.
81. Kachhap, S. K., Rosmus, N., Collis, S. J., Kortenhorst, M. S., Wissing, M. D., Hedayati, M., Shabbeer, S., Mendonca, J., Deangelis, J., Marchionni, L.*, et al.* (2010). Downregulation of homologous recombination DNA repair genes by HDAC inhibition in prostate cancer is mediated through the E2F1 transcription factor. PLoS One *5*, e11208.
82. Kaelin, W.G., Jr., Krek, W., Sellers, W.R., DeCaprio, J.A., Ajchenbaum, F., Fuchs, C.S., Chittenden, T., Li, Y., Farnham, P.J., Blanar, M.A., et. (1992). Expression cloning of a cDNA encoding a retinoblastoma-binding protein with E2F-like properties. Cell 70, 351-364.
83. Kasahara, M., Takahashi, Y., Nagata, T., Asai, S., Eguchi, T., Ishii, Y., Fujii, M., and Ishikawa, K. (2000). Thymidylate synthase expression correlates closely with E2F1 expression in colon cancer. Clin Cancer Res *6*, 2707-2711.
84. Kastan, M. B., and Bartek, J. (2004). Cell-cycle checkpoints and cancer. Nature *432*, 316-323.
85. Kato, J., Matsushime, H., Hiebert, S. W., Ewen, M. E., and Sherr, C. J. (1993). Direct binding of cyclin D to the retinoblastoma gene product (pRb) and pRb phosphorylation by the cyclin D-dependent kinase CDK4. Genes & development *7*, 331-342.
86. Kim, J. M., Sohn, H. Y., Yoon, S. Y., Oh, J. H., Yang, J. O., Kim, J. H., Song, K. S., Rho, S. M., Yoo, H. S., Kim, Y. S.*, et al.* (2005). Identification of gastric cancer-related genes using a cDNA microarray containing novel expressed sequence tags expressed in gastric cancer cells. Clin Cancer Res *11*, 473-482.
87. Knudson, A. G., Jr. (1971). Mutation and cancer: statistical study of retinoblastoma. Proc Natl Acad Sci U S A *68*, 820-823.
88. Kohn, M. J., Bronson, R. T., Harlow, E., Dyson, N. J., and Yamasaki, L. (2003). Dp1 is required for extra-embryonic development. Development *130*, 1295-1305.

89. Kontaki, H., and Talianidis, I. (2010). Lysine methylation regulates E2F1-induced cell death. Molecular cell *39*, 152-160.
90. Kovesdi, I., Reichel, R., and Nevins, J. R. (1986). Identification of a cellular transcription factor involved in E1A trans-activation. Cell *45*, 219-228.
91. Krek, W., Ewen, M. E., Shirodkar, S., Arany, Z., Kaelin, W. G., Jr., and Livingston, D. M. (1994). Negative regulation of the growth-promoting transcription factor E2F-1 by a stably bound cyclin A-dependent protein kinase. Cell *78*, 161-172.
92. Krek, W., Xu, G., and Livingston, D. M. (1995). Cyclin A-kinase regulation of E2F-1 DNA binding function underlies suppression of an S phase checkpoint. Cell *83*, 1149-1158.
93. La Thangue, N. B. (1994). DP and E2F proteins: components of a heterodimeric transcription factor implicated in cell cycle control. Curr Opin Cell Biol *6*, 443-450.
94. La Thangue, N.B. (1994). DRTF1/E2F: an expanding family of heterodimeric transcription factors implicated in cell-cycle control. Trends Biochem. Sci. 19, 108-114.
95. La Thangue, N. B., and Rigby, P. W. (1987). An adenovirus E1A-like transcription factor is regulated during the differentiation of murine embryonal carcinoma stem cells. Cell *49*, 507-513.
96. Lacroix, M., El Messaoudi, S., Rodier, G., Le Cam, A., Sardet, C., and Fabbrizio, E. (2008). The histone-binding protein COPR5 is required for nuclear functions of the protein arginine methyltransferase PRMT5. EMBO reports *9*, 452-458.
97. Lazzerini Denchi, E., and Helin, K. (2005). E2F1 is crucial for E2F-dependent apoptosis. EMBO reports *6*, 661-668.
98. Lee, D. Y., Ianculescu, I., Purcell, D., Zhang, X., Cheng, X., and Stallcup, M. R. (2007). Surface-scanning mutational analysis of protein arginine methyltransferase 1: roles of specific amino acids in methyltransferase substrate specificity, oligomerization, and coactivator function. Mol Endocrinol *21*, 1381-1393.
99. Lee, T. I., and Young, R. A. (2000). Transcription of eukaryotic protein-coding genes. Annu Rev Genet *34*, 77-137.
100. Lees, J. A., Saito, M., Vidal, M., Valentine, M., Look, T., Harlow, E., Dyson, N., and Helin, K. (1993). The retinoblastoma protein binds to a family of E2F transcription factors. Mol Cell Biol *13*, 7813-7825.
101. Lei, N. Z., Zhang, X. Y., Chen, H. Z., Wang, Y., Zhan, Y. Y., Zheng, Z. H., Shen, Y. M., and Wu, Q. (2009). A feedback regulatory loop between methyltransferase PRMT1 and orphan receptor TR3. Nucleic acids research *37*, 832-848.
102. Li, J., Ran, C., Li, E., Gordon, F., Comstock, G., Siddiqui, H., Cleghorn, W., Chen, H. Z., Kornacker, K., Liu, C. G*., et al.* (2008). Synergistic function of E2F7 and E2F8 is essential for cell survival and embryonic development. Developmental cell *14*, 62-75.
103. Li, P., Nijhawan, D., Budihardjo, I., Srinivasula, S. M., Ahmad, M., Alnemri, E. S., and Wang, X. (1997). Cytochrome c and dATP-dependent formation of Apaf-1/caspase-9 complex initiates an apoptotic protease cascade. Cell *91*, 479-489.
104. Lin, W. C., Lin, F. T., and Nevins, J. R. (2001). Selective induction of E2F1 in response to DNA damage, mediated by ATM-dependent phosphorylation. Genes & development *15*, 1833-1844.
105. Lin, W. J., Gary, J. D., Yang, M. C., Clarke, S., and Herschman, H. R. (1996). The mammalian immediate-early TIS21 protein and the leukemia-associated BTG1 protein interact with a protein-arginine N-methyltransferase. The Journal of biological chemistry *271*, 15034-15044.
106. Lissy, N. A., Davis, P. K., Irwin, M., Kaelin, W. G., and Dowdy, S. F. (2000). A common E2F-1 and p73 pathway mediates cell death induced by TCR activation. Nature *407*, 642-645.

107. Littlewood, T. D., Hancock, D. C., Danielian, P. S., Parker, M. G., and Evan, G. I. (1995). A modified oestrogen receptor ligand-binding domain as an improved switch for the regulation of heterologous proteins. Nucleic Acids Res *23*, 1686-1690.
108. Liu, F., Zhao, X., Perna, F., Wang, L., Koppikar, P., Abdel-Wahab, O., Harr, M. W., Levine, R. L., Xu, H., Tefferi, A*., et al.* (2011). JAK2V617F-mediated phosphorylation of PRMT5 downregulates its methyltransferase activity and promotes myeloproliferation. Cancer cell *19*, 283-294.
109. Liu, K., Lin, F. T., Ruppert, J. M., and Lin, W. C. (2003). Regulation of E2F1 by BRCT domain-containing protein TopBP1. Molecular and cellular biology *23*, 3287-3304.
110. Liu, K., Luo, Y., Lin, F. T., and Lin, W. C. (2004). TopBP1 recruits Brg1/Brm to repress E2F1-induced apoptosis, a novel pRb-independent and E2F1-specific control for cell survival. Genes & development *18*, 673-686.
111. Lize, M., Pilarski, S., and Dobbelstein, M. (2010). E2F1-inducible microRNA 449a/b suppresses cell proliferation and promotes apoptosis. Cell death and differentiation *17*, 452-458.
112. Logan, N., Delavaine, L., Graham, A., Reilly, C., Wilson, J., Brummelkamp, T. R., Hijmans, E. M., Bernards, R., and La Thangue, N. B. (2004). E2F-7: a distinctive E2F family member with an unusual organization of DNA-binding domains. Oncogene *23*, 5138-5150.
113. Logan, N., Graham, A., Zhao, X., Fisher, R., Maiti, B., Leone, G., and La Thangue, N. B. (2005). E2F-8: an E2F family member with a similar organization of DNA-binding domains to E2F-7. Oncogene *24*, 5000-5004.
114. Lundberg, A. S., and Weinberg, R. A. (1998). Functional inactivation of the retinoblastoma protein requires sequential modification by at least two distinct cyclin-cdk complexes. Mol Cell Biol *18*, 753-761.
115. Magae, J., Wu, C. L., Illenye, S., Harlow, E., and Heintz, N. H. (1996). Nuclear localization of DP and E2F transcription factors by heterodimeric partners and retinoblastoma protein family members. J Cell Sci *109 (Pt 7)*, 1717-1726.
116. Maiti, B., Li, J., de Bruin, A., Gordon, F., Timmers, C., Opavsky, R., Patil, K., Tuttle, J., Cleghorn, W., and Leone, G. (2005). Cloning and characterization of mouse E2F8, a novel mammalian E2F family member capable of blocking cellular proliferation. The Journal of biological chemistry *280*, 18211-18220.
117. Malumbres, M., and Barbacid, M. (2003). RAS oncogenes: the first 30 years. Nat Rev Cancer *3*, 459-465.
118. Malumbres, M. & Barbacid, M. (2005). Mammalian cyclin-dependent kinases. Trends Biochem. Sci. 30, 630-641.
119. Malumbres, M., and Barbacid, M. (2009). Cell cycle, CDKs and cancer: a changing paradigm. Nat. Rev. Cancer 9, 153-166
120. Marti, A., Wirbelauer, C., Scheffner, M., and Krek, W. (1999). Interaction between ubiquitin-protein ligase SCFSKP2 and E2F-1 underlies the regulation of E2F-1 degradation. Nature cell biology *1*, 14-19.
121. Martinez-Balbas, M. A., Bauer, U. M., Nielsen, S. J., Brehm, A., and Kouzarides, T. (2000). Regulation of E2F1 activity by acetylation. EMBO J *19*, 662-671.
122. Mathioudaki, K., Papadokostopoulou, A., Scorilas, A., Xynopoulos, D., Agnanti, N., and Talieri, M. (2008). The PRMT1 gene expression pattern in colon cancer. Br J Cancer *99*, 2094-2099.
123. Mathioudaki, K., Scorilas, A., Ardavanis, A., Lymberi, P., Tsiambas, E., Devetzi, M., Apostolaki, A., and Talieri, M. (2011). Clinical evaluation of PRMT1 gene expression in breast cancer.

Tumour biology : the journal of the International Society for Oncodevelopmental Biology and Medicine *32*, 575-582.
124. May, P., and May, E. (1999). Twenty years of p53 research: structural and functional aspects of the p53 protein. Oncogene *18*, 7621-7636.
125. Mazzola, J. L., and Sirover, M. A. (2003). Subcellular localization of human glyceraldehyde-3-phosphate dehydrogenase is independent of its glycolytic function. Biochimica et biophysica acta *1622*, 50-56.
126. McConnell, B. B., Gregory, F. J., Stott, F. J., Hara, E., and Peters, G. (1999). Induced expression of p16(INK4a) inhibits both CDK4- and CDK2-associated kinase activity by reassortment of cyclin-CDK-inhibitor complexes. Molecular and cellular biology *19*, 1981-1989.
127. Meng, R. D., Phillips, P., and El-Deiry, W. S. (1999). p53-independent increase in E2F-1 expression enhances the cytotoxic effects of etoposide and of adriamycin. Int J Oncol *14*, 5-14.
128. Migliori, V., Muller, J., Phalke, S., Low, D., Bezzi, M., Mok, W. C., Sahu, S. K., Gunaratne, J., Capasso, P., Bassi, C.*, et al.* (2012). Symmetric dimethylation of H3R2 is a newly identified histone mark that supports euchromatin maintenance. Nature structural & molecular biology *19*, 136-144.
129. Mittnacht, S. (1998). Control of pRB phosphorylation. Curr Opin Genet Dev *8*, 21-27.
130. Moberg, K., Starz, M. A., and Lees, J. A. (1996). E2F-4 switches from p130 to p107 and pRB in response to cell cycle reentry. Molecular and cellular biology *16*, 1436-1449.
131. Moroni, M. C., Hickman, E. S., Lazzerini Denchi, E., Caprara, G., Colli, E., Cecconi, F., Muller, H., and Helin, K. (2001). Apaf-1 is a transcriptional target for E2F and p53. Nature cell biology *3*, 552-558.
132. Mulligan, G., and Jacks, T. (1998). The retinoblastoma gene family: cousins with overlapping interests. Trends Genet *14*, 223-229.
133. Murphy, M., Stinnakre, M. G., Senamaud-Beaufort, C., Winston, N. J., Sweeney, C., Kubelka, M., Carrington, M., Brechot, C., and Sobczak-Thepot, J. (1997). Delayed early embryonic lethality following disruption of the murine cyclin A2 gene. Nat Genet *15*, 83-86.
134. Nagahata, T., Onda, M., Emi, M., Nagai, H., Tsumagari, K., Fujimoto, T., Hirano, A., Sato, T., Nishikawa, K., Akiyama, F.*, et al.* (2004). Expression profiling to predict postoperative prognosis for estrogen receptor-negative breast cancers by analysis of 25,344 genes on a cDNA microarray. Cancer Sci *95*, 218-225.
135. Nahle, Z., Polakoff, J., Davuluri, R. V., McCurrach, M. E., Jacobson, M. D., Narita, M., Zhang, M. Q., Lazebnik, Y., Bar-Sagi, D., and Lowe, S. W. (2002). Direct coupling of the cell cycle and cell death machinery by E2F. Nature cell biology *4*, 859-864.
136. Neault, M., Mallette, F. A., Vogel, G., Michaud-Levesque, J., and Richard, S. (2012). Ablation of PRMT6 reveals a role as a negative transcriptional regulator of the p53 tumor suppressor. Nucleic acids research *40*, 9513-9521.
137. Nevins, J. R. (1992). E2F: a link between the Rb tumor suppressor protein and viral oncoproteins. Science *258*, 424-429.
138. Nieduszynski, C. A., Murray, J., and Carrington, M. (2002). Whole-genome analysis of animal A- and B-type cyclins. Genome Biol *3*, RESEARCH0070.
139. Nordling, C, (1953). A new theory on cancer-inducing mechanism. British Journal of Cancer 7 (1): 68-72.
140. O'Brien, K. B., Alberich-Jorda, M., Yadav, N., Kocher, O., Diruscio, A., Ebralidze, A., Levantini, E., Sng, N. J., Bhasin, M., Caron, T.*, et al.* (2010). CARM1 is required for proper control of proliferation and differentiation of pulmonary epithelial cells. Development *137*, 2147-2156.

141. Pak, M. L., Lakowski, T. M., Thomas, D., Vhuiyan, M. I., Husecken, K., and Frankel, A. (2011). A protein arginine N-methyltransferase 1 (PRMT1) and 2 heteromeric interaction increases PRMT1 enzymatic activity. Biochemistry *50*, 8226-8240.
142. Pal, S., Baiocchi, R. A., Byrd, J. C., Grever, M. R., Jacob, S. T., and Sif, S. (2007). Low levels of miR-92b/96 induce PRMT5 translation and H3R8/H4R3 methylation in mantle cell lymphoma. The EMBO journal *26*, 3558-3569.
143. Pal, S., Vishwanath, S. N., Erdjument-Bromage, H., Tempst, P., and Sif, S. (2004). Human SWI/SNF-associated PRMT5 methylates histone H3 arginine 8 and negatively regulates expression of ST7 and NM23 tumor suppressor genes. Molecular and cellular biology *24*, 9630-9645.
144. Pawlak, M. R., Scherer, C. A., Chen, J., Roshon, M. J., and Ruley, H. E. (2000). Arginine N-methyltransferase 1 is required for early postimplantation mouse development, but cells deficient in the enzyme are viable. Mol Cell Biol *20*, 4859-4869.
145. Pediconi, N., Ianari, A., Costanzo, A., Belloni, L., Gallo, R., Cimino, L., Porcellini, A., Screpanti, I., Balsano, C., Alesse, E*., et al.* (2003). Differential regulation of E2F1 apoptotic target genes in response to DNA damage. Nature cell biology *5*, 552-558.
146. Peeper, D. S., Keblusek, P., Helin, K., Toebes, M., van der Eb, A. J., and Zantema, A. (1995). Phosphorylation of a specific cdk site in E2F-1 affects its electrophoretic mobility and promotes pRB-binding in vitro. Oncogene *10*, 39-48.
147. Phillips, A. C., Bates, S., Ryan, K. M., Helin, K., and Vousden, K. H. (1997). Induction of DNA synthesis and apoptosis are separable functions of E2F-1. Genes Dev *11*, 1853-1863.
148. Pomerantz, J., Schreiber-Agus, N., Liegeois, N. J., Silverman, A., Alland, L., Chin, L., Potes, J., Chen, K., Orlow, I., Lee, H. W*., et al.* (1998). The Ink4a tumor suppressor gene product, p19Arf, interacts with MDM2 and neutralizes MDM2's inhibition of p53. Cell *92*, 713-723.
149. Putzer, B. M., and Engelmann, D. (2013). E2F1 apoptosis counterattacked: evil strikes back. Trends in molecular medicine *19*, 89-98.
150. Qiao, H., Di Stefano, L., Tian, C., Li, Y. Y., Yin, Y. H., Qian, X. P., Pang, X. W., Li, Y., McNutt, M. A., Helin, K*., et al.* (2007). Human TFDP3, a novel DP protein, inhibits DNA binding and transactivation by E2F. J Biol Chem *282*, 454-466.
151. Raff, M. C. (1992). Social controls on cell survival and cell death. Nature *356*, 397-400.
152. Rijo M. John, H. R. (2012). Global Economic Cost of Cancer. In, (The American Cancer Society).
153. Roberts, J. D., and Kunkel, T. A. (1988). Fidelity of a human cell DNA replication complex. Proc Natl Acad Sci U S A *85*, 7064-7068.
154. Robin-Lespinasse, Y., Sentis, S., Kolytcheff, C., Rostan, M. C., Corbo, L., and Le Romancer, M. (2007). hCAF1, a new regulator of PRMT1-dependent arginine methylation. Journal of cell science *120*, 638-647.
155. Rushlow, D., Piovesan, B., Zhang, K., Prigoda-Lee, N. L., Marchong, M. N., Clark, R. D., and Gallie, B. L. (2009). Detection of mosaic RB1 mutations in families with retinoblastoma. Hum Mutat *30*, 842-851.
156. Sahin, F., and Sladek, T. L. (2010). E2F-1 binding affinity for pRb is not the only determinant of the E2F-1 activity. International journal of biological sciences *6*, 382-395.
157. Sakabe, K., and Hart, G. W. (2010). O-GlcNAc transferase regulates mitotic chromatin dynamics. The Journal of biological chemistry *285*, 34460-34468.
158. Santamaria, D. et al. (2007). Cdk1 is sufficient to drive the mammalian cell cycle. Nature 448, 811-815.

159. Seligson, D. B., Horvath, S., Shi, T., Yu, H., Tze, S., Grunstein, M., and Kurdistani, S. K. (2005). Global histone modification patterns predict risk of prostate cancer recurrence. Nature *435*, 1262-1266.
160. Sherr, C. J. (1996). Cancer cell cycles. Science *274*, 1672-1677.
161. Sherr, C. J. (2004). Principles of tumor suppression. Cell *116*, 235-246.
162. Sherr, C. J., and McCormick, F. (2002). The RB and p53 pathways in cancer. Cancer Cell *2*, 103-112.
163. Sherr, C. J., and Weber, J. D. (2000). The ARF/p53 pathway. Curr Opin Genet Dev *10*, 94-99.
164. Shin, G., Kang, T. W., Yang, S., Baek, S. J., Jeong, Y. S., and Kim, S. Y. (2011). GENT: gene expression database of normal and tumor tissues. Cancer informatics *10*, 149-157.
165. Sprangers, R., Groves, M. R., Sinning, I., and Sattler, M. (2003). High-resolution X-ray and NMR structures of the SMN Tudor domain: conformational variation in the binding site for symmetrically dimethylated arginine residues. J Mol Biol *327*, 507-520.
166. Stevens, C., Smith, L., and La Thangue, N. B. (2003). Chk2 activates E2F-1 in response to DNA damage. Nature cell biology *5*, 401-409.
167. Stiewe, T., and Putzer, B. M. (2000). Role of the p53-homologue p73 in E2F1-induced apoptosis. Nature genetics *26*, 464-469.
168. Sweeney, C., Murphy, M., Kubelka, M., Ravnik, S. E., Hawkins, C. F., Wolgemuth, D. J., and Carrington, M. (1996). A distinct cyclin A is expressed in germ cells in the mouse. Development *122*, 53-64.
169. Swenson, K. I., Farrell, K. M., and Ruderman, J. V. (1986). The clam embryo protein cyclin A induces entry into M phase and the resumption of meiosis in Xenopus oocytes. Cell *47*, 861-870.
170. Swiercz, R., Cheng, D., Kim, D., and Bedford, M. T. (2007). Ribosomal protein rpS2 is hypomethylated in PRMT3-deficient mice. The Journal of biological chemistry *282*, 16917-16923.
171. Tang, J., Frankel, A., Cook, R. J., Kim, S., Paik, W. K., Williams, K. R., Clarke, S., and Herschman, H. R. (2000). PRMT1 is the predominant type I protein arginine methyltransferase in mammalian cells. J Biol Chem *275*, 7723-7730.
172. Tee, W. W., Pardo, M., Theunissen, T. W., Yu, L., Choudhary, J. S., Hajkova, P., and Surani, M. A. (2010). Prmt5 is essential for early mouse development and acts in the cytoplasm to maintain ES cell pluripotency. Genes Dev *24*, 2772-2777.
173. Thompson, C. B. (1995). Apoptosis in the pathogenesis and treatment of disease. Science *267*, 1456-1462.
174. Tophkhane, C., Yang, S. H., Jiang, Y., Ma, Z., Subramaniam, D., Anant, S., Yogosawa, S., Sakai, T., Liu, W. G., Edgerton, S.*, et al.* (2012). p53 inactivation upregulates p73 expression through E2F-1 mediated transcription. PloS one *7*, e43564.
175. Trimarchi, J. M., Fairchild, B., Wen, J., and Lees, J. A. (2001). The E2F6 transcription factor is a component of the mammalian Bmi1-containing polycomb complex. Proceedings of the National Academy of Sciences of the United States of America *98*, 1519-1524.
176. Trimarchi, J. M., and Lees, J. A. (2002). Sibling rivalry in the E2F family. Nature reviews Molecular cell biology *3*, 11-20.
177. Tripsianes, K., Madl, T., Machyna, M., Fessas, D., Englbrecht, C., Fischer, U., Neugebauer, K. M., and Sattler, M. (2011). Structural basis for dimethylarginine recognition by the Tudor domains of human SMN and SPF30 proteins. Nat Struct Mol Biol *18*, 1414-1420.
178. Tsai, K. Y., Hu, Y., Macleod, K. F., Crowley, D., Yamasaki, L., and Jacks, T. (1998). Mutation of E2f-1 suppresses apoptosis and inappropriate S phase entry and extends survival of Rb-deficient mouse embryos. Mol Cell *2*, 293-304.

179. Verhaegen, M., Checinska, A., Riblett, M. B., Wang, S., and Soengas, M. S. (2012). E2F1-dependent oncogenic addiction of melanoma cells to MDM2. Oncogene *31*, 828-841.
180. Vigo, E., Muller, H., Prosperini, E., Hateboer, G., Cartwright, P., Moroni, M. C., and Helin, K. (1999). CDC25A phosphatase is a target of E2F and is required for efficient E2F-induced S phase. Molecular and cellular biology *19*, 6379-6395.
181. Vousden, K. H., and Lu, X. (2002). Live or let die: the cell's response to p53. Nat Rev Cancer *2*, 594-604.
182. Walboomers, J. M., Jacobs, M. V., Manos, M. M., Bosch, F. X., Kummer, J. A., Shah, K. V., Snijders, P. J., Peto, J., Meijer, C. J., and Munoz, N. (1999). Human papillomavirus is a necessary cause of invasive cervical cancer worldwide. The Journal of pathology *189*, 12-19.
183. Wang, B., Liu, K., Lin, F. T., and Lin, W. C. (2004). A role for 14-3-3 tau in E2F1 stabilization and DNA damage-induced apoptosis. The Journal of biological chemistry *279*, 54140-54152.
184. Wang, H., Huang, Z. Q., Xia, L., Feng, Q., Erdjument-Bromage, H., Strahl, B. D., Briggs, S. D., Allis, C. D., Wong, J., Tempst, P., and Zhang, Y. (2001). Methylation of histone H4 at arginine 3 facilitating transcriptional activation by nuclear hormone receptor. Science *293*, 853-857.
185. Wang, J. Y. (1997). Retinoblastoma protein in growth suppression and death protection. Curr Opin Genet Dev *7*, 39-45.
186. Wang, L., Pal, S., and Sif, S. (2008). Protein arginine methyltransferase 5 suppresses the transcription of the RB family of tumor suppressors in leukemia and lymphoma cells. Molecular and cellular biology *28*, 6262-6277.
187. Wei, T. Y., Juan, C. C., Hisa, J. Y., Su, L. J., Lee, Y. C., Chou, H. Y., Chen, J. M., Wu, Y. C., Chiu, S. C., Hsu, C. P.*, et al.* (2012). Protein arginine methyltransferase 5 is a potential oncoprotein that upregulates G1 cyclins/cyclin-dependent kinases and the phosphoinositide 3-kinase/AKT signaling cascade. Cancer Sci *103*, 1640-1650.
188. Weijts, B. G., Bakker, W. J., Cornelissen, P. W., Liang, K. H., Schaftenaar, F. H., Westendorp, B., de Wolf, C. A., Paciejewska, M., Scheele, C. L., Kent, L.*, et al.* (2012). E2F7 and E2F8 promote angiogenesis through transcriptional activation of VEGFA in cooperation with HIF1. The EMBO journal *31*, 3871-3884.
189. Williams, S., and Dale, J. (2006). The effectiveness of treatment for depression/depressive symptoms in adults with cancer: a systematic review. Br J Cancer *94*, 372-390.
190. Wu, L., Timmers, C., Maiti, B., Saavedra, H. I., Sang, L., Chong, G. T., Nuckolls, F., Giangrande, P., Wright, F. A., Field, S. J.*, et al.* (2001). The E2F1-3 transcription factors are essential for cellular proliferation. Nature *414*, 457-462.
191. Xu, G., Livingston, D. M., and Krek, W. (1995). Multiple members of the E2F transcription factor family are the products of oncogenes. Proceedings of the National Academy of Sciences of the United States of America *92*, 1357-1361.
192. Xu, M., Sheppard, K. A., Peng, C. Y., Yee, A. S., and Piwnica-Worms, H. (1994). Cyclin A/CDK2 binds directly to E2F-1 and inhibits the DNA-binding activity of E2F-1/DP-1 by phosphorylation. Molecular and cellular biology *14*, 8420-8431.
193. Yam, C. H., Fung, T. K., and Poon, R. Y. (2002). Cyclin A in cell cycle control and cancer. Cell Mol Life Sci *59*, 1317-1326.
194. Yamagata, K., Daitoku, H., Takahashi, Y., Namiki, K., Hisatake, K., Kako, K., Mukai, H., Kasuya, Y., and Fukamizu, A. (2008). Arginine methylation of FOXO transcription factors inhibits their phosphorylation by Akt. Molecular cell *32*, 221-231.
195. Yamasaki, L., Jacks, T., Bronson, R., Goillot, E., Harlow, E., and Dyson, N. J. (1996). Tumor induction and tissue atrophy in mice lacking E2F-1. Cell *85*, 537-548.
196. Yan, F., Liu, H., Hao, J., and Liu, Z. (2012). Dynamical behaviors of Rb-E2F pathway including negative feedback loops involving miR449. PloS one *7*, e43908.

197. Yang, Y., and Bedford, M. T. (2013). Protein arginine methyltransferases and cancer. Nature reviews Cancer *13*, 37-50.
198. Yoshimatsu, M., Toyokawa, G., Hayami, S., Unoki, M., Tsunoda, T., Field, H. I., Kelly, J. D., Neal, D. E., Maehara, Y., Ponder, B. A.*, et al.* (2011). Dysregulation of PRMT1 and PRMT6, Type I arginine methyltransferases, is involved in various types of human cancers. Int J Cancer *128*, 562-573.
199. Yoshimoto, T., Boehm, M., Olive, M., Crook, M. F., San, H., Langenickel, T., and Nabel, E. G. (2006). The arginine methyltransferase PRMT2 binds RB and regulates E2F function. Experimental cell research *312*, 2040-2053.
200. Yu, W., Chan-On, W., Teo, M., Ong, C. K., Cutcutache, I., Allen, G. E., Wong, B., Myint, S. S., Lim, K. H., Voorhoeve, P. M.*, et al.* (2011). First somatic mutation of E2F1 in a critical DNA binding residue discovered in well-differentiated papillary mesothelioma of the peritoneum. Genome Biol *12*, R96.
201. Yu, Z., Chen, T., Hebert, J., Li, E., and Richard, S. (2009). A mouse PRMT1 null allele defines an essential role for arginine methylation in genome maintenance and cell proliferation. Mol Cell Biol *29*, 2982-2996.
202. Yu, Z., Vogel, G., Coulombe, Y., Dubeau, D., Spehalski, E., Hebert, J., Ferguson, D. O., Masson, J. Y., and Richard, S. (2012). The MRE11 GAR motif regulates DNA double-strand break processing and ATR activation. Cell Res *22*, 305-320.
203. Zalmas, L. P., Zhao, X., Graham, A. L., Fisher, R., Reilly, C., Coutts, A. S., and La Thangue, N. B. (2008). DNA-damage response control of E2F7 and E2F8. EMBO reports *9*, 252-259.
204. Zhang, X., and Cheng, X. (2003). Structure of the predominant protein arginine methyltransferase PRMT1 and analysis of its binding to substrate peptides. Structure *11*, 509-520.
205. Zhang, Y., and Chellappan, S. P. (1995). Cloning and characterization of human DP2, a novel dimerization partner of E2F. Oncogene *10*, 2085-2093.
206. Zou, L., Zhang, H., Du, C., Liu, X., Zhu, S., Zhang, W., Li, Z., Gao, C., Zhao, X., Mei, M.*, et al.* (2012). Correlation of SRSF1 and PRMT1 expression with clinical status of pediatric acute lymphoblastic leukemia. J Hematol Oncol *5*, 42.
207. Zurita-Lopez, C. I., Sandberg, T., Kelly, R., and Clarke, S. G. (2012). Human protein arginine methyltransferase 7 (PRMT7) is a type III enzyme forming omega-NG-monomethylated arginine residues. The Journal of biological chemistry *287*, 7859-7870.